การพัฒนาและตรวจสอบลักษณะของวัสดุโฟมที่มีรูพรุนสูงระดับแมคโครจากท่อคาร์บอนระดับนาโนแมตรด้วยวิธีอบแห้งเยือกแข็ง

นางสาวนภาวรณ ทองประชาญ

วิทยานิพนธ์นี้เป็นส่วนหนึ่งของการศึกษาตามหลักสูตรปริญญาวิศวกรรมศาสตรดุษฎีบัณฑิต
สาขาวิชาวิศวกรรมเคมี ภาควิชาวิศวกรรมเคมี
คณะวิศวกรรมศาสตร์ จุฬาลงกรณ์มหาวิทยาลัย
ปีการศึกษา 2551

DEVELOPMENT AND CHARACTERIZATION OF HIGHLY MACROPOROUS CARBON NANOTUBE FOAMS BY FREEZE-DRYING METHOD

Miss Napawon Thongprachan

A Dissertation Submitted in Partial Fulfillment of the Requirements
for the Degree of Doctor of Engineering Program in Chemical Engineering
Department of Chemical Engineering
Faculty of Engineering
Chulalongkorn University
Academic year 2008

Thesis Title	DEVELOPMENT AND CHARACTERIZATION OF HIGHLY MACROPOROUS CARBON FOAMS BY FREEZE-DRYING METHOD
By	Miss Napawon Thongprachan
Field of study	Chemical Engineering
Advisor	Associate Professor Tawatchai Charinpanitkul, D.Eng.
Co-Advisor	Emeritus Professor Wiwut Tanthapanichakoon, Ph.D.

Accepted by the Faculty of Engineering, Chulalongkorn University in Partial Fulfillment of the Requirements for the Doctoral Degree

..... Dean of the Faculty of Engineering
(Associate Professor Boonsom Lerdhirunwong, Dr.Ing.)

THESIS COMMITTEE

..... Chairman
(Professor Suttichai Assabumrungrat, Ph.D.)

..... Advisor
(Associate Professor Tawatchai Charinpanitkul, D.Eng.)

..... Co-Advisor
(Emeritus Professor Wiwut Tanthapanichakoon, Ph.D.)

..... Examiner
(Assistant Professor Nattaporn Tonanon, D.Eng.)

..... Examiner
(Apinan Soottitantawat, D.Eng.)

..... External Examiner
(Assistant Professor Kyuya Nakagawa, D.Eng.)

นภาวรรณ ทองประชาญ : การพัฒนาและตรวจสอบลักษณะของวัสดุโฟมที่มีรูพรุนสูงระดับแมคโครจากท่อคาร์บอนระดับนาโนเมตรด้วยวิธีอบแห้งเยือกแข็ง. (DEVELOPMENT AND CHARACTERIZATION OF HIGHLY MACROPOROUS CARBON NANOTUBE FOAMS BY FREEZE-DRYING METHOD) อ.ที่ปรึกษาวิทยานิพนธ์หลัก: รศ.ดร.ธวัชชัย ชรินพาณิชกุล, อ.ที่ปรึกษาวิทยานิพนธ์ร่วม: ศ. กิตติคุณ ดร.วิวัฒน์ ตัณฑะพานิชกุล, 127 หน้า.

วัสดุโฟมที่ทำจากท่อคาร์บอนระดับนาโนเมตรซึ่งมีรูพรุนระดับแมคโครสูงถึงร้อยละ 97 ถูกผลิตโดยกระบวนการทำให้แข็งของสารละลายผสมที่ประกอบด้วยการกระจายตัวของท่อคาร์บอนระดับนาโนเมตร และคาร์บอกซีเมทธิลเซลลูโลสโซเดียมซอลต์ (สารลดแรงตึงผิว) แล้วตามด้วยกระบวนการอบแห้งเยือกแข็ง กระบวนการทำให้สารละลายดังกล่าวแข็งตัวมีสองวิธี (การทำให้แข็งโดยการสัมผัสตรงกับแผ่นแลกเปลี่ยนความร้อน กับการทำให้แข็งโดยการจุ่มในอ่างที่มีสารหล่อเย็น) หลังจากนั้นน้ำแข็งจะถูกระเหิดออกในสภาวะสูญญากาศเพื่อให้ได้ตัวอย่างที่แห้ง นอกเหนือจากรูพรุนระดับแมคโครของตัวอย่างที่ถูกผลิตขึ้นแล้ว รูพรุนระดับเมโซก็เกิดขึ้นภายในผนังบาง ๆ ของโฟมด้วย ขนาดเฉลี่ยของรูพรุนระดับแมคโครถูกกำหนดด้วยองค์ประกอบของสารละลายเริ่มต้นและอัตราเร็วในการทำให้แข็งที่ใช้เป็นหลัก เงื่อนไขการทำให้แข็งที่รวดเร็วกว่าจะทำให้ได้เครือข่ายรูพรุนระดับแมคโครที่เล็กกว่าในเมทริกซ์ และจะให้ผลทำนองเดียวกันกับกรณีใช้ความเข้มข้นสูง ๆ ของสารลดแรงตึงผิวในสารละลายเริ่มต้นหรือของท่อคาร์บอนระดับนาโนเมตร อย่างไรก็ตามโครงสร้างสัณฐานของรูพรุนระดับแมคโครจะขึ้นอยู่กับวิธีการทำให้แข็งอย่างมาก โครงสร้างที่มีลักษณะรังผึ้งจะผลิตได้โดยเทคนิคการให้แข็งแบบจุ่ม ในขณะที่การทำให้แข็งแบบสัมผัสตรงจะให้โครงสร้างรูพรุนระดับแมคโครที่มีลักษณะหลากหลายกว่า

สิ่งที่น่าสนใจคือ การพบว่าความต้านทานทางไฟฟ้าของวัสดุโฟมของท่อคาร์บอนระดับนาโนเมตรจะขึ้นกับเงื่อนไขในการเตรียม และยังตอบสนองอย่างรวดเร็วต่อการเปลี่ยนแปลงความดันแก๊ส โครงสร้างสัณฐานของรูพรุนระดับแมคโครมีบทบาทสำคัญในการบ่งชี้ชนิดของแก๊ส รูพรุนระดับแมคโครเฉลี่ยในชิ้นตัวอย่างที่ใหญ่กว่าจะมีความสามารถในการถ่ายเทมวลในระหว่างการใช้งานสูง จึงส่งผลให้การตอบสนองต่อการเปลี่ยนแปลงความต้านทานไฟฟ้าเกิดขึ้นอย่างรวดเร็ว นอกจากนี้รูปแบบของการตอบสนองทางความต้านทานไฟฟ้าในช่วงดูดซับแก๊สแต่ละชนิดจะขึ้นอยู่กับโครงสร้างสัณฐานของรูพรุนระดับแมคโคร รวมทั้งขนาดเฉลี่ยของรูพรุนระดับแมคโครด้วย ปรากฏว่าวัสดุโฟมของท่อคาร์บอนระดับนาโนเมตรที่ผลิตขึ้นจะแสดงลักษณะผสมระหว่างท่อคาร์บอนระดับนาโนเมตรแรกเริ่มและแมทริกซ์ของรูพรุนระดับแมคโครที่ได้ ผลการทดลองเบื้องต้นเสนอแนะว่าวัสดุโฟมของท่อคาร์บอนระดับนาโนเมตรที่ผลิตขึ้นมีศักยภาพที่เหมาะสมในการนำไปใช้เป็นวัสดุบ่งชี้ชนิดของแก๊สได้

ภาควิชา.....วิศวกรรมเคมี.....ลายมือชื่อนิสิต.....นภาวรรณ ทองประชาญ.....

สาขาวิชา.....วิศวกรรมเคมี.....ลายมือชื่ออ.ที่ปรึกษาวิทยานิพนธ์หลัก.....

ปีการศึกษา.....2551.....ลายมือชื่ออ.ที่ปรึกษาวิทยานิพนธ์ร่วม.....

4971815821 : MAJOR CHEMICAL ENGINEERING

KEYWORDS: MULTI-WALLED CARBON NANOTUBE / SOLIDIFICATION / POROUS MATERIAL / ELECTRIC CONDUCTIVITY

NAPAWON THONGPRACHAN: DEVEOPMENT AND CHARACTERIZATION OF HIGHLY MACROPOROUS CARBON NANOTUBE FOAMS BY FREEZE-DRYING METHOD. ADVISOR: ASSOC. PROF. TAWATCHAI CHARINPANITKUL, D.Eng., CO-ADVISOR: EMERITUS PROF. WIWUT TANTHAPANICHAKOON, Ph.D., 127 pp.

Macroporous bulk foams made of multi-walled carbon nanotubes (MWCNTs), and having porosity of up to 97% were produced by freezing aqueous solutions consisting of dispersed MWCNTs and a carboxymethyl cellulose (CMC) sodium salt (surfactant), followed by freeze-drying. The solutions were frozen via two different freezing processes (contact freezing with a plate heat exchanger vs. immersion freezing in a cryo-bath) and then lyophilized to obtain dry specimens. Besides the ordered macropores of the produced CNT foam specimens, mesoporosity also developed inside the thin foam walls. The average macropore size was mainly determined by both the initial formulation and freezing condition. A faster freezing rate led to a smaller macropore network in the bulk matrix, and so did a higher surfactant concentration or a higher MWCNT content. However, the morphology of the macropores was strongly dependent on the freezing method. A rather uniform monolithic honeycomb structure was produced by the immersion freezing technique, whereas the contact freezing method typically gave a rather random macroporous structure.

Interestingly, the electrical resistance of the CNT foams was found to depend on the preparation condition and to rapidly respond to a gas pressure change. The macropore morphology played a critical role in the identification of gas type. A larger average macropore in the bulk specimen led to high mass transfer capability during usage, thereby resulting in a faster response in the electric resistance. Moreover, the pattern of the normalized gas-uptake electric resistance response towards each gas species was affected by the macropore morphology as well as the average macropore size. It was found that the produced CNT foams displayed hybrid characteristics of the original MWCNTs and the resulting macroporous bulk matrix. These preliminary results suggest that the produced CNT foams have reasonable potential as a gas identifier.

Department:.....Chemical Engineering....Student's Signature N. Thongprachan

Field of Study:....Chemical Engineering....Advisor's Signature T. Charinpanitkul

Academic Year:...2008.....Co-advisor's Signature Wiwut T.

ACKNOWLEDGEMENTS

The author would like to sincerely thank Emeritus Prof. Dr. Wiwut Tanthapanichakoon and Assoc. Prof. Dr. Tawatchai Charinpanitkul for their close guidance, deep discussion and continuous advices on many important issues as well as their encouragement to overcome the hurdles throughout this project, including the training for self-learning.

The experiments of this research employed the freeze-drying system and gas detection system developed by Asst. Prof. Dr. Kyuya Nakagawa in the University of Hyogo, Japan. The author would like to sincerely thank Asst. Prof. Dr. Kyuya Nakagawa for his guidance and generosity. He has contributed lots of ideas, efforts and guidance, without which the success of this project would not have been possible.

Meantime, the author would like to acknowledge TGIST (Thailand Graduate Institute of Science and Technology) of NSTDA (National Science and Technology Development Agency) and HUMAP (Hyogo University Mobility in Asia and the Pacific) for their valuable financial support. Partial support from the Centennial Fund of Chulalongkorn University for researcher exchange under Dr. Tawatchai is also acknowledged. The author is grateful to Bayer Material Science Ltd., for all the MWCNT samples.

The author would like to thank Prof. Dr. Suttichai Assabumrungrat, Asst. Prof. Dr. Nattaporn Tonanon, and Lecturer Dr. Apinan Soottitantawat for their helpful comments and participation in the dissertation defence committee.

Furthermore, the author is grateful to her colleagues in the Center of Excellence in Particle Technology (CEPT), Chulalongkorn University, for their co-operation and assistances during this doctoral study.

Finally, the author wishes to offer her sincere thanks to her family for their unfailing support and understanding even at the most difficult moments.

CONTENTS

CHAPTER Page

CHAPTER Page

CHAPTER Page

LIST OF TABLES

Page

LIST OF FIGURES

Page

Page

Page

Page

CHAPTER I

INTRODUCTION

1.1 Background

Macroporous materials are interesting to employ in wide-ranging applications since their porous structures extremely could affect mass transfer rates and pressure drop occurs during their usage (Nishihara et al., 2005). Being simple and environmental-friendly, freezing or ice templating is an effective technique to produce macroporous materials whose the pore morphology was dependent on the freezing method (Mukai et al., 2004; Mukai et al., 2005; Nishihara et al., 2005; Abdelwahed et al., 2006; Nakagawa et al., 2006; Hottot et al., 2007). It was reported by several researches that the freezing protocol and initial formulation of starting solution are key parameters for designing porous systems because they directly affected ice-crystal sizes (Jennings, 1999; Fukasawa et al., 2002; Mukai et al., 2003; Yunoki et al., 2006; Deville et al., 2007; Landi et al., 2008; Lau et al., 2008). Freeze-drying of frozen samples is considered a more useful technique than sintering and leaching because it could prevent the collapse of the remaining porous structure of prepared samples after drying and also does not destabilize thermally sensitive products (Geankoplis, 1993; Tamon et al., 2000; Fukasawa et al. 2002; Yunoki et al., 2006; Hottot et al., 2007).

Recently, macroporous bulk materials composed of carbon nanotubes (CNTs) have attracted a great deal of attention because of the superior properties of CNTs such as electronic, adsorptive, mechanical and thermal properties (Serp et al., 2003; Romanenko et al., 2007). A well-interconnected macroporous structure in the bulk

matrix offers a desirable combination of the high internal reactive surface along the CNT nanostructure with the facile molecular transport through broad highways provided by the macropores (Gutierrez et al., 2007). Moreover, the bulk materials made from CNTs are also expected to overcome the difficulties in handling and controlling as-received CNTs whose nano-scale sizes are not suitable and unsafe to employ in daily-life applications. Nabeta et al. (2005) prepared sponge-like bulk materials from CNTs. By dispersing acidified CNTs in gelatin solution and subsequent freeze-drying, CNTs sponges were obtained. In their samples, porous structures derived from self-networking nature of the gelatin were obtained after the freeze-drying process. Leroy et al. (2007) also employed the freeze-drying technique to produce foam-like materials from CNTs, though their porous structures were created by bubbling during the freezing step. Some studies attempted to develop porous materials by freeze-drying chitosan containing dispersed CNTs, and utilizing them as scaffolds for tissue engineering (Abarrategi et al., 2008; Lau et al., 2008) or electrode for a fuel cell (Gutierrez et al., 2007). One may surmise from these reports that porous bulk material can be produced from CNTs, which were supported by a surface active agent that helped to disperse the CNTs in a starting solution and kept its bulk structure after freeze-drying. In our point view, it will be a great challenge to develop macroporous CNT foams with a controlled pore size by using ice-crystal templates whilst the matrix of the obtained CNT foams should have dual characteristics derived from both the “nanomaterial” and the “bulk structure”. However, few studies dealing with the preparation of bulk matrix made of CNT to yield bi-functional property have been reported from the viewpoint of nanomaterial development.

In this work, we focused on the preparation of macroporous CNT foams by freezing multi-walled carbon nanotubes (MWCNTs) dispersed in a carboxymethyl cellulose (CMC) sodium salt solution and subsequent freeze-drying. The characteristics of the prepared macroporous CNT foams (i.e. bulk density, porosity, morphology, pore size distribution, electric resistance) as well as the influence of the preparation conditions (i.e. initial formulation, freezing condition, freezing method) on their macroporous structures were investigated. Finally, the potential application of the prepared macroporous CNT foams to gas identification was studied.

1.2 Objectives of study

The objective in this work is to prepare and characterize the obtained macroporous carbon nanotube (CNT) foams using the freeze-casting method with subsequent freeze-drying in order to control the macropore sizes and structures of the foams. In addition, the bi-functional property of the prepared CNT foams, that is, dual characteristics derived from both the CNTs and bulk structures was also determined.

1.3 Scope of research

1.3.1 Preparation of macroporous CNT foams induced by ice crystals (Fig. 1.1) using two different freezing methods;

(1) Contact freezing with plate heat exchanger

(2) Immersion freezing in a cooling bath

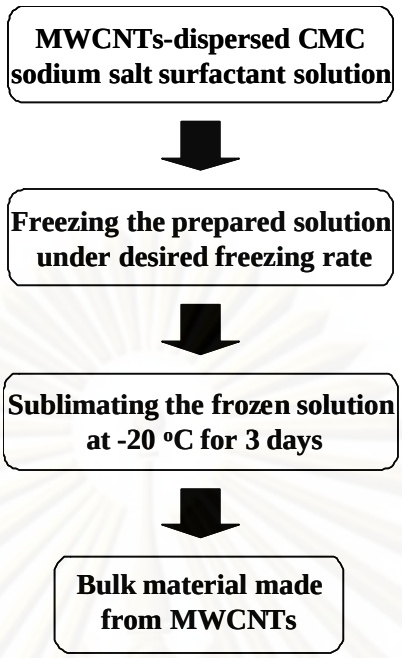

Figure 1.1 Schematic diagram for preparation of macroporous CNT foams

1.3.2 Determination of the characteristics of the obtained macroporous CNT foams, such as *bulk density*, *porosity*, *pore size distribution (by image analysis)*, *morphology (SEM and optical microscope), and electric resistance (by multimeter).*

1.3.3 Investigation of the influence of the preparation conditions on the macropore sizes of CNT foams;

(1) Initial formulation

MWCNT content: 0.5, 1.0, or 1.5 wt.%

CMC sodium salt surfactant concentration: 0.5, 1.0, or 2.0 wt.%

(2) Freezing condition

Cooling rate: -0.1, -0.5, or -3.0 K min^{-1}

Immersion rate: 20, 67, or 180 μm s^{-1}

1.3.4 Study on potential application of the prepared CNT foams to gas identification.

1.4 Expected benefits

1.4.1 The knowledge of the mechanism of the preparation of macroporous CNT foams was obtained.

1.4.2 An understanding of how to develop the CNT foams with the desirable macropore sizes and structures was obtained.

1.4.3 Some potential application of the prepared macroporous CNT foams as gas identifier was indicated.

CHAPTER II

FUNDAMENTAL KNOWLEDGE AND LITERATURE REVIEW

2.1 Carbon nanotubes

Carbon nanotube (CNT) is a hexagonal network of carbon atoms that can be thought of as a layer of graphite sheet rolled-up into a cylinder, and having a diameter of few nanometers but length of many micrometers (Paradise et al., 2007; Sayago et al., 2008). Depending on the arrangement of its graphene cylinder, CNT is categorized into two types, i.e. single-walled carbon nanotube (SWCNT) and multi-walled carbon nanotube (MWCNT) as shown in Fig. 2.1. The structure of SWCNT is only one single layer of graphite sheet wrapped into a cylinder, while MWCNT consists of multiple layers of graphite sheets rolled up into a cylindrical tube. Although graphite is a semiconductor, CNT can be either metallic or semiconducting, depending upon the tube diameter and the helicity of the arrangement of graphite rings.

(a) (b)

Figure 2.1 Carbon nanotubes: (a) SWCNT and (b) MWCNT

(Zarbin, 2007)

Since their unique properties such as mechanical, electrical, magnetic, optical and thermal properties, CNTs have been employed in many applications (Serp et al., 2003; Romanenko et al., 2007; Sun et al., 2007; Chang et al., 2008).. In this research, only electrical properties of CNTs will be considered due to the produced CNT foam will be tested for gas sensing application. CNTs can be used as a superior material to adsorb gas molecules due to their unique electrical property (Sun et al., 2007). Electron transfer can be promoted when gas molecules were adsorbed on CNTs wall. Romanenko et al. (2007) also reported that the change in electric conductivity of CNTs is connected with processes of gas adsorption–desorption on the nanotubes surface. Electrical conductivity is dependent on the interaction of adsorbed molecules and CNTs wall. CNTs were also provided the fast response, high sensitivity as well as wide employing in various gases (Suehiro et al., 2006; Quang et al., 2006; Paradise et al., 2007).

2.2 Porous materials

Porous material is defined as the solid with cavities or channels which are deeper than they are wide (Rouquerol et al., 2001). Some of the principal terms and properties associated with the porous materials are defined in Table 2.1.

Table 2.1 Definitions: porous materials (Rouquerol et al., 2001)

Term	Definitions
Open pore	Cavity or channel with access to the surface
Interconnected pore	Pore which communicates with other pores
Blind pore	Pore with a single connection to the surface
Closed pore	Cavity not connected to the surface
Void	Space between particles
Pore size	Pore width (diamter of cylindrical pore or distance between opposite walls of slit)
Pore volume	Volume of pores determined by stated method
Porosity	Ratio of total pore volume to apperent volume of particles
Surface area	Extent of total surface area as determined by given method under stated conditions.
Apparent density	Density of material including closed and inaccessible pores, as determined by stated method

Pores can be classified by the International Union of Pure and Applied Chemistry (IUPAC) based on their inner pores width (D_p) into three groups: micropores, mesopores and macropores.

1. Micropores: $0.3 \text{ nm} < D_p < 2 \text{ nm}$

In micropores, the adsorption proceeds via the mechanism of volume filling in which the adsorption behavior is dominated almost entirely by the interactions of the adsorbate and the pore walls, and as not a layer-by layer surface coverage.

2. Mesopores: $2 \text{ nm} \leq D_p \leq 50 \text{ nm}$

The process of filling mesopore volume with adsorbate takes place via the mechanism of capillary condensation. Capillary condensation in mesopores is generally associated with a shift in the vapor-liquid coexistence in pore compared to

the bulk fluid. This means a fluid confined in a pore condenses at a pressure lower than the saturation pressure at a given temperature, since the condensation pressure depends on the pore size and shape, and also on the strength of the interaction between the fluid and pore walls. Besides the significant contribution to the adsorption of mesopores, they also perform as main transport arteries for the adsorbate.

3. Macropores: 50 nm < D_p

The macropore volumes are not entirely filled with adsorbate via the mechanism of capillary condensation. The values of their specific surface area are negligibly small compared to the surface of the remaining types of pore, and consequently, the macropores are not important in the adsorption process. Macropores merely act as accessible transport arteries for the adsorbate molecules.

2.3 Freeze-drying process

Freeze drying, also termed “lyophilization”, is a drying process whereby water or another solvent is removed from the frozen product by sublimation (Swarbrick et al., 2002; Velardi et al., 2008). Sublimation occurs when a frozen solvent goes directly to the gaseous phase without passing through the liquid phase. The removal of solvent by sublimation creates an open network of “pores”, which allows pathways for escape of solvent vapor from the product. Here, only the solution system of water and solutes is focused in this study.

The lyophilization technique is performed through several successive steps as follows.

2.3.1 Freezing stage

In general, the first step of freeze-drying process is the formation of the ice from the water contained in product solution, which this process is also termed as a freezing stage (Jennings, 1999; Swarbrick et al., 2002). Nakagawa (2007) elucidated the temperature profile during freezing process which is represented in Fig. 2.2. Firstly, the starting solution is cooled down at constant freezing rate until some supercooled level at which the starting point of ice nucleation. Next, the temperature rapidly increases due to the heat evolution caused by the sudden ice crystallization, and then the temperature slightly decreases due to the latent heat generates by ice-crystal growth up to the end of ice-crystal growth period corresponding to the total ice freezing. Finally, the temperature continues to decrease until complete solidification of cryoconcentrated phase.

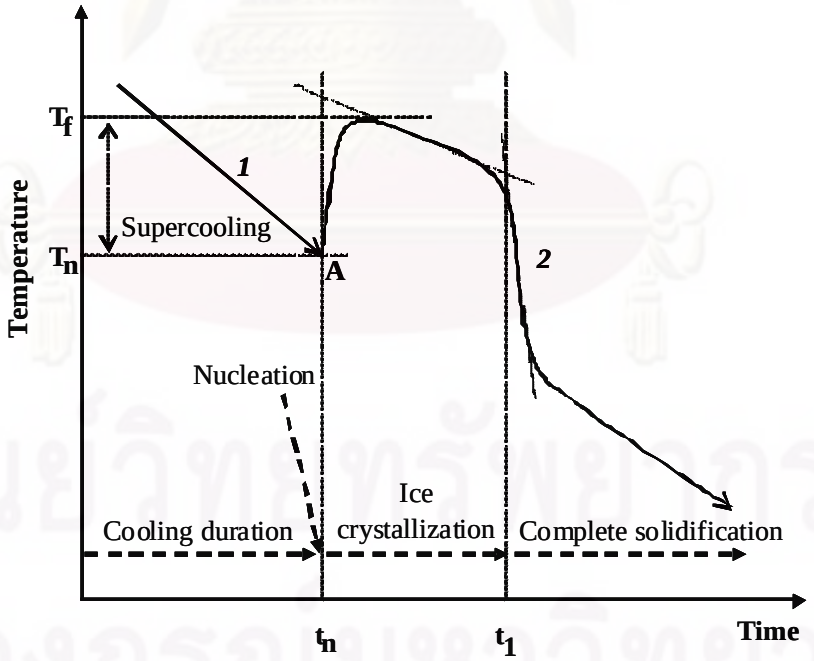

Figure 2.2 Schematic of temperature profile during freezing process

(Nakagawa, 2007)

In general, there are two common freezing parameters in the definition of the freezing process, i.e. the degree of supercooling and the rate of ice crystallization (Jennings, 1999; Swarbrick et al., 2002).

1. Degree of supercooling

It is the difference between the equilibrium freezing point and the nucleation temperature (primarily the formation of ice crystals. The degree of supercooling determines the number of ice nuclei (in turn the number of ice crystal formation in the sample). A high degree of supercooling produces a large number of ice crystals with the total amount of frozen water is fixed, resulting in the small in size of ice crystals occurs after complete solidification by freezing. Since, a thermal property of the formulation directly effects to the equilibrium freezing temperature (Jenning, 1999), the degree of supercooling (in case of formulation is fixed) is mostly varied by controlling the nucleation temperature (Nakagawa et al., 2006). It is well-known that the supercooled solution for the same freezing rate and experimental conditions starts its nucleation quite randomly, and leading to the corresponding nucleation temperature is largely distributed. However, the nucleation can be initiated by introduction of foreign particulate and this gives rise to heterogeneous nucleation. The particulate may either be a solid particle or droplet. In fact, most of the nucleation in nature is heterogeneous in character. These foreign particulates, which help nucleate ice, are more commonly known as ice-forming nuclei (Hazra et al., 2003).

2. Rate of ice crystallization

It is often called freezing rate (of the solution), where is the temperature change of the heat sink (in solution) for ice crystal formation. The rate of ice crystal growth

determines the residence time of the product in a freeze-concentrated fluid state. A rapid growth rate minimizes the residence time, normally allowing less degradation during freezing process (in case of thermally sensitive products). The heat transfer limits the rate of ice growth. In general, a rapid ice growth is promoted by a low shelf temperature. A rapid freezing produces a large number of ice crystals when the total amount of frozen water is fixed, and results in the small ice crystals appearance after complete freezing process.

In short, it has been reported that the adopted freezing condition is the key parameter to control the ice crystal size, while the ice crystal shape was mainly controlled by the freezing method (Jennings, 1999; Kang et al., 1999; Fukasawa et al., 2002; Mukai et al., 2003; Nishihara et al., 2005; Yunoki et al., 2006; Deville et al., 2007; Landi et al., 2008; Lau et al., 2008). The obtained ice crystal is commonly in turn the pore morphology (i.e. size and shape) in bulk matrix of product.

In this research, the two freezing methods are proposed for the study, i.e. a contact freezing (with a plate heat exchanger) and an immersion freezing (in a cooling bath).

1. Contact freezing

Contact freezing is a freezing technique in which the heat-transfer media (liquid or gas coolants) is in contact with only the bottom of the container, as shown in Fig. 2.3a.

2. Immersion freezing

Immersion freezing is a freezing technique in which the heat-transfer media (liquid or gas coolants) is in contact with both the bottom and the walls of the container (Jennings, 2008), as shown in Fig. 2.3b.

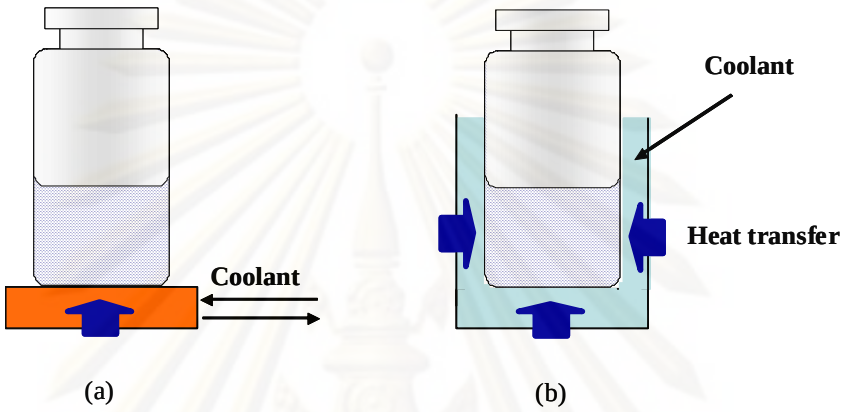

Figure 2.3 Scheme of freezing system: (a) contact freezing and (b) immersion freezing

2.3.2 Freeze-drying stage

Drying characteristic is one important database for every process materials that has a purpose to remove water or organic solvent from a solute matrix since it is usually useful to estimate the size of dryer needed, the various operating conditions (either temperature or pressure used), and predict the time needed to perform the amount of drying required (Geankoplis, 1993). A freeze-drying is one drying process in which the water is removed from the frozen material by mainly sublimation. Freeze-drying of frozen material is very useful technique for several materials since it could prevent the collapse of the remaining porous structure of produced samples after drying and also does not destabilize thermally sensitive products (Geankoplis, 1993; Tamon et al., 2000; Hottot et al., 2007). In general, there are two steps

occurring during freeze-drying process, i.e. primary and secondary freeze-drying stages (Swarbrick et al., 2002; Velardi et al., 2008).

1. Primary freeze-drying stage

In this stage, the ice is generally sublimated under vacuum system. The sublimation occurs when a frozen solvent goes directly to the gaseous phase without passing through the liquid phase. The driving force for the sublimation process is provided by the partial pressure difference of water at the sublimating ice surface and at the drying chamber. The boundary between frozen and dried regions generally moves from the top of the product toward the bottom of the vial as primary freeze-drying proceeds. It should be noted that an increase in shelf temperature before all products have completed primary freeze-drying should be careful due to it can carry a high risk of product collapse.

2. Secondary freeze-drying stage

The last stage of the freeze-drying process is a desorption of the residual moisture, which is strongly bounded by adsorption phenomena to the partially dried cake. The secondary freeze-drying generally starts from the end of the primary drying (i.e. when all frozen solvent is removed). As earlier mentioned, it is noted the shelf temperature setting during primary freeze-drying should be taking care because it may lead a product collapse. Similarity, the structural collapse may also occur during secondary freeze-drying, particularly if the freeze-dried product contains high levels of residual moisture. However, such an event is a less common problem during the secondary freeze-drying than that is collapse during the primary freeze-drying. In

general, the secondary freeze-drying is usually carried out at high vacuum and moderate temperature (20–60 ^{o}C).

In short, the removal of solvent by sublimation creates an open network of “pores”, which allows solvent vapor to escape from the product. A produced small pore size in the sample results in a high resistance to water vapor transport during primary freeze-drying, and consequently, a long primary freeze-drying time. Besides, the small pore size also means a high specific surface area in the freeze-dried product, which decreases the secondary freeze-drying time.

2.4 Literature review of macroporous bulk material preparation by freeze-drying process

Recently, the ordered macroporous bulk materials has been of interest in a wide range of applications due to their porous structures could affect mass transfer rates and pressure drop during their usage (Nishihara et al., 2005). As previous section, the freezing is a practical process to design a pore structure of product, while that pore size can be manipulated by either the freezing condition or the formulation of solution (Jennings, 1999; Fukasawa et al., 2002; Mukai et al., 2003; Yunoki et al., 2006; Deville et al., 2007; Landi et al., 2008; Lau et al., 2008). Freeze-drying of the frozen product is a very useful technique to prevent a risk of the pore collapse during drying process. In short, ice crystals produced via freezing process directly relates to the final pore morphology of product after complete freeze-drying (Tamon et al., 2000; Hottot et al., 2007).

Some of the published literatures relates to the porous bulk materials produced by freeze-drying process were briefly summarized as below.

Kang et al., (1999) developed the macroporous gelatin scaffolds for tissue engineering by combination of the porogen method using only water as a solvent and the freeze-drying technique. Macroporous networks in gelatin gel were produced by crosslinking this gel with glutaraldehyde in an aqueous solution. After complete solidification of the gelatin gel by freezing process, the ice formed in the network of gelatin gel was removed by freeze-drying. As this report, ice acts as templates to create the pore structures during freezing step, and the porous structures in a bulk are controlled by the freezing condition. The frozen gelatin gel in liquid nitrogen had the two-dimensional structure of pores while the three-dimensional structure with interconnected macropores was made by freezing the gelatin gel at -20 ^{o}C. They also suggested that the macropore structure gradually became more two-dimensionally ordered when the freezing temperature was lowered.

Fukasawa et al., (2002) fabricated the macroporous silicon nitride by using freeze-drying process. Firstly, the silicon nitride powders were mixed with the additive and surfactant solution, and then put this solution into a container at where only its bottom was immersed in a freezing bath (-50, -80 ^{o}C). After complete solidification, the frozen sample was sublimated under vacuum in order to remove ices in the bulk matrix of sample, and finally the macroporous material was obtained. They found that the macropore size of samples could be controlled by the freezing temperature and slurry concentration, that is, a lower freezing temperature and high slurry concentration led to smaller macropore in size.

Nazarov et al., (2004) produced the macroporous silk scaffolds by three preparation techniques, i.e. freeze-drying, salt leaching and gas foaming. High macroporosity (up to 99%) was promoted by freeze-drying process. On the contrary, the scaffolds produced by the freeze-drying had a lowest compressive strength. The gas foaming was the best preparation technique in their study in terms of compressive strength (up to 280 ± 2 kPa) and macropore size (> 100 μm), as well as the general requirements related to bone tissue engineering.

Nishihara et al., (2005) employed the immersion freezing (into a cold bath) and subsequent freeze-drying to produce the ordered macroporous bulk silica. The obtained macropore structure had a homogeneous honeycomb monolith. Besides the ordered macropore, micro/mesopore also developed on the honeycomb walls by their preparation technique. The results show that the macropore size of bulk silica was precisely controlled by changing the immersion rate (freezing rate) and the freezing temperature without any changing in the micro/mesopore on the honeycomb walls. The micro/mesoporosity could be controlled by hydrothermal treatment of as-prepared bulk silica in the basic aqueous solution. Moreover, the size of micro/mesopore on the honeycomb walls affected the heat stability of product, that is, the heat stability of porous bulk silica could be enhanced with an increase micro/mesopore size on the honeycomb walls.

Deville at al., (2006) fabricated the macroporous hydroxyapatite scaffolds with total porosity ranging from at least 40% to 65% by freezing the hydroxyapatite aqueous suspensions and subsequent freeze-drying and sintering. The problem of a lack in strength of porous materials could be overcome by their preparation technique. The resultant porosity was open and unidirectional, and exhibited a lamellar morphology. The macropore size of scaffolds was mainly controlled by modifying the

freezing rate of the slurry and the slurry concentration. Moreover, it was found that the compressive strength of produced scaffolds was affected by macropore size. Macropore size (i.e. defect size) decreased as the freezing rate increased, so that the compressive strength also increases as the defects (macropore) become smaller. It was also suggested that the produced hydroxyapatite scaffold with high compressive strength (i.e. up to 145 MPa for 47% porosity and 65 MPa for 56%) allowed considering the potential of such materials for some load-bearing biological applications.

Yunoki et al., (2006) produced the macroporous hydroxyapatite/collagen composite with the controlled pore structure by using the unidirectional ice growth with the liquid N_2 and followed by freeze-drying process, and also investigated its mechanical properties with the uncontrolled one (by solidification in a freezer at -20 ^{o}C). They found that the composite with the unique pore structure offered the high mechanical strength and modulus against the compression parallel to the pore axis.

Deville et al., (2007) prepared the macroporous bulk materials made from alumina powder by freeze-drying technique in order to investigate relationships between freezing conditions and final macropore structures. In their study, the initial formulation of starting solution was also varied to observe microstructures of the obtained material as well. This report suggested that the morphology of macropore structure was controlled by initial formulation of starting solution and the freezing conditions. At high alumina content, the lamellar structure was lost and the macropores were not interconnected. At low almina content, the obtained material became weaker and difficult to handle. As freezing condition, a faster cooling rate led to a decrease of ice dendrite tip radius, consequently, the homogeneous and thinner lamellae structures were obtained.

Landi et al., (2008) developed the macroporous hydroxyapatite/gelatine scaffolds by using the freeze-drying technique. In their preparation process, the ice was in a unidirectional growth, and consequently, the lamellar morphology with a channel-like pore was obtained after freeze-drying process. They found that the slurry concentration and freezing temperature strongly influenced on the characteristics of prepared samples. The thinner lamellar and high porosity were produced at a low solid loading of slurry and a high temperature gradient between the bottom and top of the sample holder. Moreover, they also suggested that the mechanical properties of obtained sample could be improved by increasing the freezing rate.

Ren et al., (2008) developed the macroporous materials made from titanium dioxide (TiO_2) by freeze casting technique. The starting solution composed of TiO_2 powder, ammonium polyacrylate (NH_4PAA, dispersant) and polyvinyl alcohol (PVA). They also studied the influence of PVA concentration (3, 6 wt.%) on the final macropore structure of obtained material. The results show that the PVA concentration affected macropore structure of the obtained samples because PVA gelation phenomena during freezing step influenced a growth manner of ice crystal. The growth manner of ice crystal changed from dendritic into parallel columnar when the PVA concentration changed from 3 wt.% to 6 wt.%. As the change of the growth manner, the macropore structure of obtained material was also varied according to the ice shape that determined the macropore structure of freeze-dried samples. The produced samples had about 56.99 to 60.39 % of porosity.

To date, there have been a few published reports dealing to the porous bulk materials made of CNTs produced by freeze-drying process. Here, some of the published literatures were briefly summarized as follows.

Nabeta et al., (2005) developed the sponge-like bulk materials made from CNTs by freeze-drying the acidified CNTs dispersed in gelatin solution. In their obtained samples, porous structures derived from self-networking nature of gelatin were appeared after freeze-drying process. As freeze-dried sample, CNTs were covered with gelatin on the pore wall, and also those samples act as insulator after electrical resistivity measurement. The gelatin was removed by heat treatment, consequently, CNTs appeared on the surface of pore wall. The electric resistivity of pyrolysed samples was quite high, about 10^3 Ω cm. Owing to the tar was still covered on the pyrolysed samples after the heat treatment, it affected the resistivity of bulk material. Moreover, the pyrolysed samples were shrunk by the heat treatment as well.

Gutierrez et al., (2007) produced the macroporous bulk materials composed of MWCNT surface decorated with Pt and chitosan by using unidirectional ice growth with the liquid N_2 and followed by freeze-drying process. The prepared samples had a monolith structure with specific gravity of (4.0-9.4) x 10^{-2} and exhibited excellent electron conductivity (0.17-2.5 S cm^{-1}). It was found that the morphology of the resulting structure was strongly dependent on the MWCNT content. The high MWCNT content favors the formation of pillars crossing between layers.

Leroy et al., (2007) developed the foam-like materials from CNTs by freeze-drying technique, while the porosity of obtained materials were made by bubbling the surfactant solution containing with CNTs during freezing process. In this study, SDS (sodium dodecyl sulphate), carboxymethyl cellulose (CMC) sodium salt and Tergitol were used as surfactant. Porosity of obtained material was 90 %. The pore size in bulk material was limited by viscosity of solution during the bubble formation.

Abarrategi et al., (2008) developed the porous CNT scaffolds for tissue engineering by freeze-drying technique. Briefly, acidified MWCNTs were dispersed

into chitosan solution. Then this solution was frozen by unidirectional dipping at constant speed into the liquid N_2. The frozen samples were placed in the freeze-dryer in order to sublimate the ice crystals, and freeze-dried samples were obtained after complete ice removal. The obtained material had a monolithic structure.

Lau et al., (2008) produced the conductive macroporous chitosan-based CNT scaffolds by freeze-drying process. In their experiment, the chitosan solution containing CNT was filled in a container, subsequently frozen on the plate heat exchanger at -20 ^{o}C, and finally sublimated the frozen samples under reduced pressure. The prepared samples showed a high macroporous material with a porosity of 97%, and their porous structure had a spherical-like shape. It was found that the CNT content in the starting solution influenced on the pore size and electric resistivity of obtained samples. A high concentration of CNT gave a smaller macropore and a lowered electric resistivity as well.

2.5 Process of gas adsorption on CNTs

Adsorption is defined as the enrichment of material or increase in the density of the fluid in the vicinity of an interface (Rouquerol et al., 2001). It is brought about by the interaction between the solid and the molecules in the fluid phase (liquid or gas states). Two kinds of forces are involved, i.e. physisorption and chemisorption.

In general, the gas adsorption process is considered as a physisorption process because the molecular forces involved are normally of the van der Waals type (Roque-Malherbe, 2007). The physical adsorption of gases and vapors in solids could also be classified as mobile adsorption, which occurs when the adsorbed molecules behaves as a gas molecule in the adsorption space, and immobile adsorption, which

occurs whenever the adsorbed molecule is forced to vibrate around adsorption site. Physical adsorption of gases in solid surfaces occurs in the case where no reaction involving exchange of electrons between the solid surface and the gas molecules with the formation of chemical bonds is required during the adsorption process. In case where a reaction by means of electron exchange between the solid surface and the gas molecules occurs during adsorption, the phenomenon is called chemical adsorption.

The interaction of CNTs with their environment, and in particular with gases adsorbed either on their internal or external surface has attracted increasing attention due to the possible influence of the adsorption on some of the tubes properties and to the possibility of using these materials for efficient gas storage (Serp et al., 2003). Adsorption properties on SWCNT samples, usually found in bundles or ropes, should not be considered in terms of individual nanotubes but in term of adsorption on the exterior or interior surfaces of such bundles. A similar situation exists for MWCNT where adsorption could occur either on or inside the tube or between aggregated MWCNT. Additionally, it has been shown that the curvature of the graphite sheets can results in a lower heat of adsorption with respect to this on a planar graphitic surface. Indeed, the rolling up of the graphite sheet to form the tube causes a rehybridization of carbon orbital (non-planar sp^2 configuration), thus leading to modifications of the π-density of the graphite sheet.

Several studies dealing with the adsorption of N_2 on MWCNT and SWCNT have highlighted the porous nature of these materials. Pores in MWCNT can be mainly divided into inner hollow cavities of small diameter (narrowly distributed, mainly 3-6 nm) and aggregated pores (widely distributed, 20-40 nm) formed by interaction of isolated MWCNT, the latter being much more important for the adsorption. On as-prepared SWCNT, N_2 adsorption has clearly evidenced the

microporous nature of SWCNT samples, contrarily to the MWCNT mesoporous nature. Experimentally, the specific surface area of SWCNT is often larger than that of MWCNT. Typically, total surface area of as-produced SWCNT ranged between 400 and 900 m^2 g^{-1} (micropore volume, 0.15-0.3 mL g^{-1}), whereas for as-produced MWCNT values ranging between 200 and 400 m^2 g^{-1}. In case of SWCNT, the diameter of the tubes and the number of tubes in the bundle will affect mainly the BET value. In addition, it is worthy to note that opening/closure of the central canal noticeably affects the adsorptive properties of nanotubes.

Adsorption sites in the SWCNT bundle can be either the inside of the tubes (pore), the interstitial triangular channels between the tubes, the outer surface of the bundle or the grooves formed at the contact between adjacent tubes on the outside of the bundle (Fig. 2.4). For MWCNTs, adsorption can occur in the aggregated pores, inside the tube or on the external walls, in the latter case the presence of the defects, as incomplete graphene layers, has to be taken into consideration. Higher condensation pressure and lower heat of adsorption were found on the nanotubes with respect to graphite. These differences mainly result from a decrease in the lateral interactions between the adsorbed molecules, in direct relationship with the curvature of the graphene sheets.

In short, it appears that CNTs present specific adsorption properties when compared to graphite or activated carbon, mainly due to their peculiar morphology, the role of defects, opening/closing of the tubes.

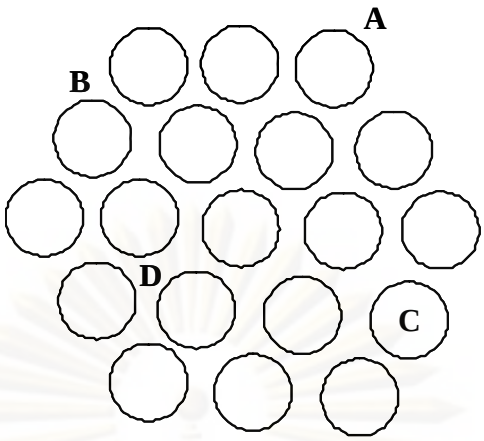

Figure 2.4 Different adsorption sites in SWCNT bundles: (A) surface; (B) groove; (C) pores; (D) interstitial (Serp et al., 2003)

2.6 Literature review of applications of carbon nanotubes in gas detection and gas identification

Several studies revealed that CNTs are good candidate to be utilized as gas detector since their excellent electronic and adsorption properties over the traditional carbon, resulting in a faster response and a higher sensitivity (Suehiro et al., 2003; Serp et al., 2003; Romanenko et al., 2007; Sun et al., 2007; Chang et al., 2008; Sayago et al., 2008; Ueda et al., 2008). The basic concept of chemical gas detection using CNT based sensor is that a CNT network has a characteristic electronic conductance when the analyte molecules come into contact with it. As an analyte comes into contact with the CNT, the network conductance is modified to produce a detection signal.

Some of the published literatures relates to CNT as a gas sensor were briefly summarized as below.

Romanenko et al., (2007) investigated the conductivity of MWCNT in five gas environments (i.e. He, H_2, O_2, air and methane) at the temperature interval 4.2-300 K. Their sensor devices were made by pressing the MWCNT powder in a glass ampoule. It was found that a change of the gas in volume at where their MWCNT as sensor led to the change in the temperature dependence of the conductivity of MWCNT. Mostly, the largest decrease of conductivity took place in the vicinity of the melting and condensation temperatures of the tested gases (i.e. H_2, O_2, air and methane). The melting and vaporization of those gases resulted in the formation of non-conductive layers between MWCNTs, thus leading to the decrease of the number of current paths. So, the observed conductivity at the melting and condensation temperatures finally decreased.

Wang et al., (2007) fabricated the four MWCNT composites based sensor for detection of three organic vapors (i.e. methanol, chloroform and tetrahydrofuran) at room temperature. Four composites based gas sensor composed of the MWCNTs grafted with polystyrene, poly(4-vinylpyridine), poly(styrene-*b*-4-vinylpyridine) and poly(styrene-*co*-4-vinylpyridine). The gas sensitivities of their sensors for all tested vapors depended on both the composite compositions of the polymers and the nature of the detected organic vapors. It evidenced a possibility to construct sensor array based on composites of CNTs bonded with polymers having different composition for the selective detection of three tested organic vapors.

Chang et al., (2008) developed the MWCNTs/polyaniline/Au composites based sensor for NH_3 detection. As the processing preparation of composites, Au nanoparticles decorated on the MWCNT/polyaniline that produced via by in situ polymerization. The electric resistance of the developed sensor dramatically increased upon exposed to NH_3 gas, and then decreased upon return to pure dry air. The sensing

mechanism was governed by the protonation/deprotonation phenomena between semiconducting polyaniline and NH_3 gas.

Ma et al., (2008) investigated the gas-sensing behaviors of both the polypyrrole and the CNT-polypyrrole composite films to trimethylamine vapors. Their experimental results showed that the gas sensitivity of that composite film to the trimethylamine exposure was decreased, but the resistance of that composite film to moisture was improved greatly whilst the rapid response was still remained. Besides, they also found that the developed sensor could be reversibility at room temperature even the desorption rate is much slower than that of adsorption. However, this problem could be eliminated by increasing the flux of N_2 gas to accelerate the desorption rate. In addition, the gas responses of the composite film to a series of vapors (trimethylamine, ammonia, triethylamine) were examined. The gas sensitivity and response rate to similar vapor differed. The order of gas sensitivity of the composite film to chemical vapors was trimethylamine > ammonia > triethylamine. Similarity, the observed trend was similar to that of response rate of the composite film to chemical vapors, that is, trimethylamine > ammonia > triethylamine.

Zhang et al., (2008) studied the effect of water vapor containing in gaseous THF on the resistance change of MWCNT/polystyrene composites. Their sensor devices were made by in situ polymerization of polystyrene filling MWCNTs and coating as thin film. It was found that the resistance increased until reaching its maximum value after the mixed vapors of THF and water vapor came to contact the sensing device because the swelling of polymer enlarged the distance among MWCNTs and destroyed the conductive networks. Then, this sensing device was moved to the dry air, and leading to an appearance of the strange phenomenon of the resistance change, that is, their resistance sharply increased until its maximum and finally slightly

decreased. This phenomenon deviated from the case of only pure THF, namely, the resistance immediately decreased when the composites was transferred into the dried air. As mentioned to the strange behavior, they suggested that the desorption rate of water is faster than the drop rate of resistance because of the stronger interaction force between THF molecules and polystyrene (similar polarity).

Sayago et al., (2008) investigated the sensitivity of CNT network with the different employed CNT materials (i.e. MWCNTs, DWCNTs, acidified DWCNTs) for detection of NO_2, H_2, NH_3, toluene and octane. Their sensor devices made by airbrushing dispersion of CNTs as thin film on alumina substrates. The electric resistance change (either rise or drop), when the CNT network was exposed to the tested gases, was explained by the characteristics of interaction between semiconducting CNT and reducing/oxidizing gases adsorbed on CNT surface. Sensor resistance decreased in the presence of NO_2 (oxidizing gas), increased when exposed to H_2 and NH_3 (reducing gases), and remained unchanged when exposed to toluene and octane (non reducing/oxidizing gases). The higher sensitivity value was obtained when using the acidified DWCNT networks at high temperature (100-200 ^{o}C) because of the nature of carboxylic groups, leading to additional enriched hole carriers in the DWCNTs.

Ueda et al., (2008) fabricated the CNT (both SWCNT and MWCNT materials) based gas sensor, which could operate at room temperature, for the detection of NO and NO_2 gases (2-10 ppm of gas concentration). Both SWCNT and MWCNT thin films were grown on Al_2O_3 substrate with interdigitated Pt-electroded to make a gas sensor. The electrical sensitivity of the SWCNT gas sensor to the exposure of NO_x was higher than that of the MWCNT gas sensor. The low sensitivity of MWCNT gas sensor resulted from the current leakage by the Fe/Al catalytic layer (it was a material

in the MWCNT production) on the Pt electrodes. The electric resistance decreased when exposing the CNT thin films to the tested gases due to the interaction between semiconducting CNT and oxidizing gases adsorbed on CNT surface.

For the subject of CNT sensor array, each sensing element must be made from a unique CNT material that can provide a specific interaction with target analytes in varying degrees (Lu et al., 2006; Star et al., 2006). A number of different CNT sensors can provide a pattern for a specific gas. Each gas will have its own pattern from the same set of sensors. Hence, when an unknown subject is introduced into the system where CNT sensor array is placed on, the sensor response of an unknown subject are compared with the smellprints of several known substances. Finally, the unknown subject can be identified by matching its pattern to one of the known substances in the library.

Some of the published literatures relates to the CNT gas sensor array were briefly summarized as below.

Lu et al., (2006) developed the CNT based gas sensor array with 32 sensing elements on a silicon based chip for discriminating NO_2, HCN, HCl, Cl_2, acetone and benzene (in ppm levels). The 32 sensing elements were composed of the different nanomaterials: (1) pristine SWCNTs, (2) CNTs coated with different polymers (chlorosulfonated polyethylene and hydroxypropyl cellulose), (3) CNTs loaded with Pd nanoparticles and monolayer protected clusters of gold nanoparticles. The array data was normalized and autoscaled for eliminating concentration and background noise. The post process array data was then undergone a principal component analysis (one of pattern recognition techniques). Each sensor responded to different

gases/vapors in the different ways (i.e. large or small, positive or negative). The histogram of sensor responses from 32 sensors to different gases/vapors gave the patterns for each gas/vapor. The developed CNT sensor array led to be used as gas/vapor identifiers.

Star et al., (2006) fabricated the electronic sensor array based on metal-decorated SWCNTs. The sensor array with the difference in catalytic activity of 18 catalytic metals (Mg, Al, Ti, V, Cr, Mn, Fe, Co, Ni, Zn, Mo, Rh, Pd, Sn, W, Pt, Au, Pb) was tested electronically for the detection of H_2, CH_4, CO, NH_3 and H_2S gases. The output of the sensor array was analyzed by using the PLS (partial least squares) regression method to yield recognition of the gases. The signal output for the four analyte gases (H_2, CH_4, NH_3, H_2S) demonstrated the selective responses of developed sensor array. On the other hand, there was a lack of sensor array sensitivity toward CO gas. They claimed that their fabricated sensor array has been suitable to real life applications due to its small-size, low power consumption, and especially it could detect and identify the toxic/combustible gases for personal safety and air pollution monitoring.

CHAPTER III

EXPERIMENTAL

3.1 Materials

3.1.1 Chemicals used in CNT foam preparation

Commercial multi-walled carbon nanotubes (MWCNTs) (Bayer Materials Science Ltd.) synthesized by chemical vapor decomposition were used in this work. MWCNT specifications provided by the supplier are listed in Table 3.1. Carboxymethyl cellulose (CMC) sodium salt surfactant (Fluka, Sweden) was used as a dispersing agent. Maximum solubility of CMC sodium salt in water is ca. 2.0 %. Distilled water was used throughout this work.

Table 3.1 MWCNT specifications (Bayer Materials Science Ltd.)

Specification	Value	Unit	Method
Purity	> 95	%	Elementary analysis
Free amorphous carbon	Not detecttible	%	TEM
Number of walls	3-15	-	TEM
Outer mean diameter	13-16	nm	TEM
Outer diameter distribution	5-20	nm	TEM
Inner mean diameter	4	nm	TEM
Inner diameter distribution	2-6	nm	TEM
Length	1 - >10	μm	SEM
Loose agglomerate size	0.3-1	mm	PSD
Electric conductivity	$> 10^4$	S cm^{-1}	N/A

3.1.2 Chemicals used in testing of gas identification of CNT foams

Graphite adhesive (Graphi-bond 551-A, Aremco Products, Inc., New York) was used for bonding wires to CNT foams in the preparation of CNT foams as sensing devices. Helium (99.99% in purity), ethane (99.0% in purity) and iso-butane (99.0% in purity) were used as test gases for experiments of gas identification for CNT foams. All gases used were supplied from Sumitomo Seika Chemicals Co., Ltd., Japan.

3.2 Preparation of macroporous CNT foams by freeze-drying technique

MWCNTs (0.5, 1.0, 1.5 wt.%) were dispersed in 10 mL of 0.5, 1.0 or 2.0 wt.% of surfactant solution by an ultrasonic homogenizer (UH-300, SMT company, Japan) for 30 minutes at 15 watts output. Then the prepared solution was frozen by either of two different freezing methods, i.e. contact freezing and immersion freezing. The preparation conditions in this work are listed in Table 3.2.

Table 3.2 The preparation conditions of CNT foam in this research

Freezing method	Sample code	MWCNT content (wt.%)	Surfactant concentration (wt.%)	Pre-cooled temperature (^{o}C)	Cooling rate (K min^{-1})
Contact freezing	C1	0.5	1.0	5	-3.0
	C2	1.0	0.5	5	-3.0
	C3	1.0	1.0	5	-0.1
	C4	1.0	1.0	5	-0.5
	C5	1.0	1.0	5	-3.0
	C6	1.0	1.0	30	-3.0
	C7	1.0	2.0	5	-0.5
	C8	1.0	2.0	5	-3.0
	C9	1.5	1.0	5	-0.5
	C10	1.5	1.0	5	-3.0
Freezing method	Sample code	MWCNT content (wt.%)	Surfactant concentration (wt.%)	Bath temperature (^{o}C)	Immersion rate (μm s^{-1})
Immersion freezing	I1	1.0	1.0	-40	20
	I2	1.0	1.0	-40	67
	I3	1.0	1.0	-40	180
	I4	1.0	1.0	-196	180

3.2.1 Contact freezing with plate heat exchanger

The prepared solution was put into a cylindrical sample holder (8.0 mm inner diameter, 5.0 mm height), which made from the acrylic resin, equipped with a cooling device (Fig. 3.1). Cooling fluid (methanol) was continuously circulated through the heat exchanger to control the temperature of the sample. The temperature of interest was monitored by a type K thermocouple and indicated with a digital multimeter (Keithley 2700, U.S.) at every second. The thermocouple was buried in the wall of the sample holder in order to avoid the thermocouple becoming a nucleation site during the freezing step (Fig. 3.1). Initially, the temperature of the sample solution was stabilized at a selected pre-cooled temperature (either 5 or 30 °C) for 15 minutes, and subsequently reduced at a constant cooling rate (-0.1, -0.5, or -3.0 K min^{-1}) down to -40 °C and held constant thereafter. It should be noted that the obtained frozen samples via this contact freezing method were consecutively freeze-dried on the same cooling shelf (Fig. 3.4).

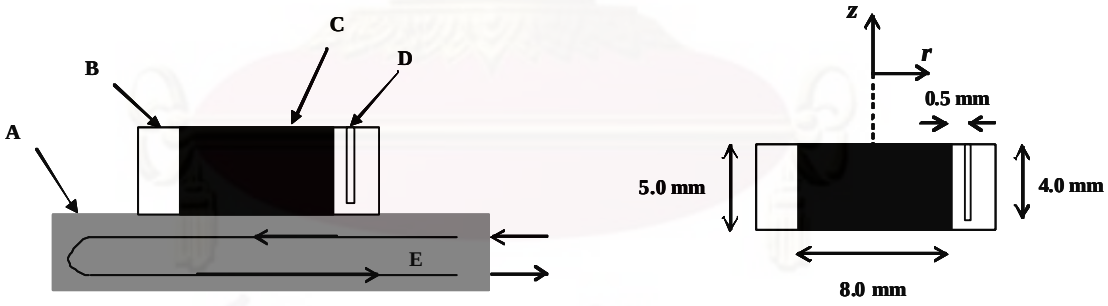

Figure 3.1 Main components of the contact freezing system: (A) heat exchanger, (B) sample holder, (C) sample solution, (D) hole for thermocouples and (E) cooling fluid

3.2.2 Immersion freezing in a cooling bath

The prepared solution was put into a quartz tube section (8.0 mm inner diameter, 5.0 mm height) with a thin square copper plate attached at its bottom end, and then the sample solution was placed in a much bigger dipping cage (Fig. 3.2). The cage was connected to an immersion device which is capable of lowering the cage into a cooling bath at a fixed speed controlled via an electric gear system (Fig. 3.3). The temperature of the isothermal cooling bath was set at a certain selected temperature (-40 °C with methanol, or -196 °C with liquid nitrogen). Before being dipped into the bath, the temperature of the sample solution was left to stabilize for at least 15 minutes, and then the sample was connected to the immersion system and set up so as to locate the sample bottom just above the surface of the pre-cooled coolant. In order to ensure uniform good contact between the copper plate and the surrounding coolant, short plastic tubes were placed between the bottom of the sample holder and the dipping cage. The solution was quickly frozen by lowering the sample cage into the bath at a desired immersion speeds (slow: 20 μm s^{-1}, medium: 67 μm s^{-1}, fast: 180 μm s^{-1}) until the liquid coolant level arrived near the top of the sample holder and the sample was held stationary until complete solidification was achieved. In order to prevent the frozen sample from melting, it was promptly transferred from the cage to the cooling shelf of a freeze-dryer (Fig. 3.4) to commence freeze-drying.

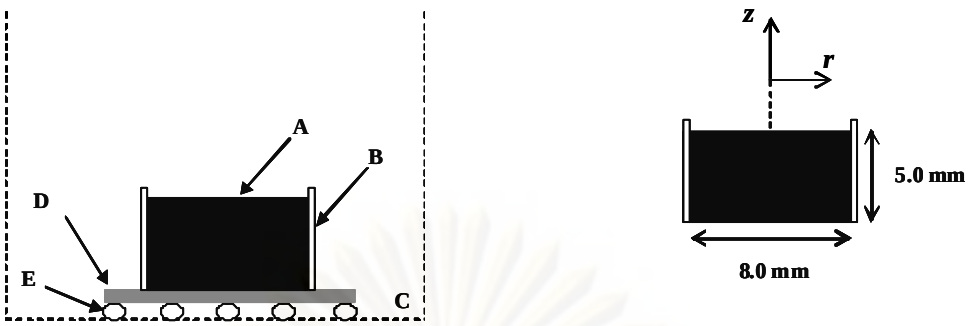

Figure 3.2 Main components of the immersion freezing system: (A) sample solution, (B) quartz tube, (C) dipping cage, (D) copper plate and (E) plastic tubes

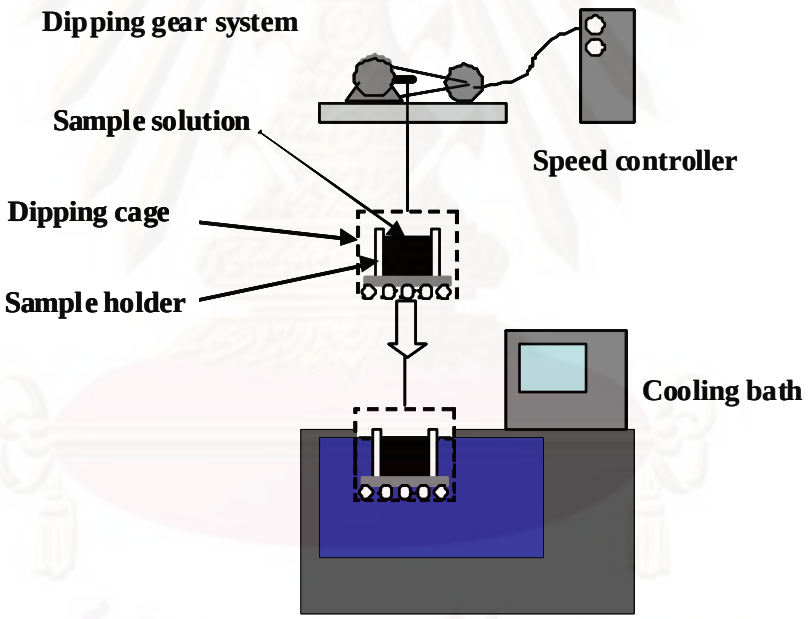

Figure 3.3 Schematic diagram of the immersion freezing system

3.2.3 Freeze-drying procedure

The frozen samples were kept on the cooling shelf of the freeze-dryer at -40 ^{o}C for 1 h in order to stabilize their structures in this frozen state before subsequent lyophilization at a chamber pressure of 25 Pa and -20 °C for 2 days in order to completely remove the ice. Any residual adsorbed moisture was removed from the CNTs and surfactant by drying at a temperature of 20 ^{o}C for 1 day. A schematic diagram of the freeze-dryer was illustrated in Fig. 3.4.

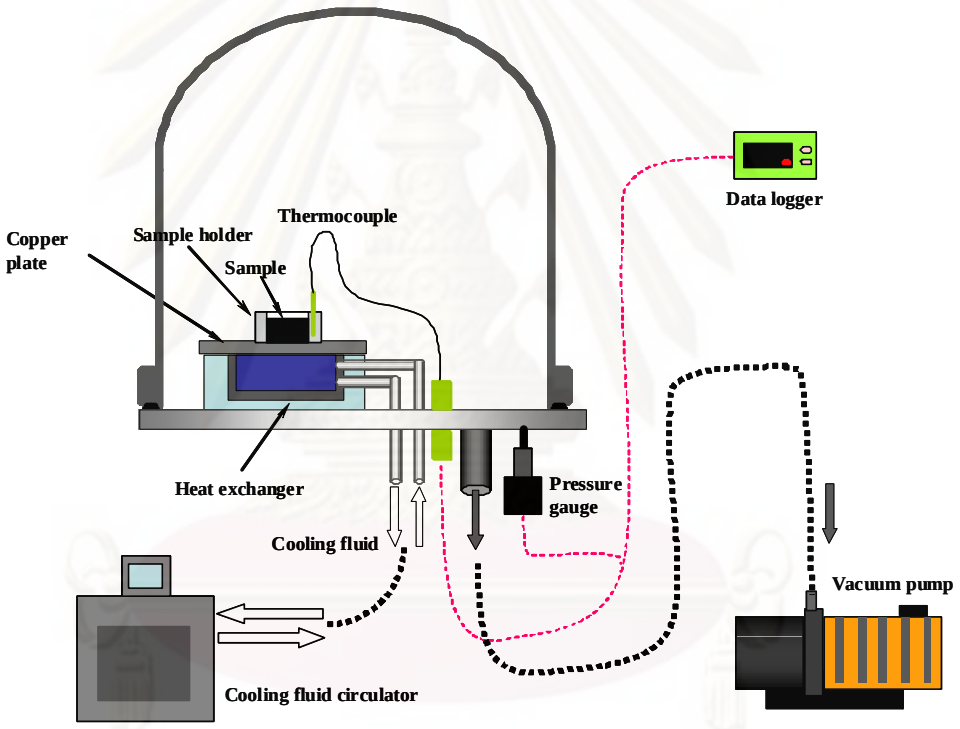

Figure 3.4 Schematic diagram of the freeze-dryer (Nakagawa, 2007)

3.3 Procedure for obtaining preliminary drying characteristics of macroporous CNT foams

The contact freezing system was used to prepare bulk CNT foams in these cases. The formulation of the starting solution contained 1.0 wt.% of MWCNTs and 1.0 wt.% of surfactant. 0.25 mL of the sample solution, which corresponds to the volume of samples prepared by the contact freezing method mentioned in section 3.2.1, was poured into each of the 10 sample vials (7.0 mm inner diameter, 25.0 mm height). The 10 sample vials were simultaneously placed on the plate heat exchanger (cooling shelf) of the freeze-dryer system (see Fig. 3.4). Here the same freezing procedure as described in section 3.2.1 was adopted with a fixed pre-cooled solution at 5 ^{o}C. Each batch of 10 sample solutions were cooled down to -40 ^{o}C at a constant cooling rate of either -0.5 or -3.0 K min^{-1}, and ice sublimated out of the frozen samples under absolute pressure of 25 Pa, -20 ^{o}C. It should be noted that the vacuum system of the freeze-drying chamber had to be shut down at each sampling time in order to allow the taking out of a sample vial. The particularly vial would immediately be covered with an air tight cap in order to avoid atmospheric moisture leaking into the vial, thereby resulting in an error of its dry. Of course, the vacuum condition was restored as soon as possible to prevent the melting of the remaining frozen samples. The residual water content of a sample versus the drying time was obtained by subtracting the observed total weight of the vial, cap and sample from the weight of only the vial and cap. The temperature of each sample versus the drying time was monitored with a type K thermocouple, which was attached to the exterior wall of the sample vial in order to avoid the thermocouple becoming a nucleation point during the freezing step. The temperature was indicated with a digital multimeter (Keithley 2700, U.S.).

3.4 Characterization of the obtained macroporous CNT foams

After obtaining the macroporous CNT foams via freeze-drying, the characteristics of the freeze-dried samples (i.e. bulk density, porosity, pore size distribution, porous structures, morphology and electric resistance) were determined as follows.

3.4.1 Bulk density and porosity

The bulk density of the obtained macroporous CNT foam was calculated from its final weight and bulk volume. The porosity of the bulk sample is defined as the ratio of the volume of pore spaces to the total volume of the bulk sample. The volume of pore spaces was calculated by subtracting the total volume of all residual constituent materials from the total volume of the bulk sample. The residual volume of the constituent materials was measured with a pycnometer.

3.4.2 Pore size distribution

The micro/mesoporous structure of the obtained CNT foams was obtained via N_2 adsorption at 77 K using a standard adsorption apparatus (BELSORP18, BEL Japan Inc.). The specific surface area and mesopore size distribution were determined using the BJH method whilst the t-plot method was employed to analyze for the micropore volume.

The macropore size distribution of the same sample was determined by image analysis (ImageJ 1.38v software). Images taken with the SEM (scanning electron microscope) as well as a digital optical microscope were used for this analysis. About 200 pore areas in each image were counted in the analysis. It should be noted that the

macropore size distribution obtained by SEM observations differed slightly from that obtained from images of the digital optical microscope.

3.4.3 Macroporous structure and morphology

Macroporous structures of the freeze-dried samples were observed on SEM micrographs (S-2400, Hitachi, Japan) and/or digital optical microscope (Moticam1000/L-814, Hozan, Japan). Two different microscopes were used because of differences in the morphology and porous structures of the obtained CNT foams produced by the two freezing methods (i.e. contact freezing and immersion freezing). The latter freezing method ran into difficulty in the cutting of the samples for observation with only a SEM. For your information, we initially prepared the CNT foams via the contact freezing method and it turned out that the obtained CNT foams were easy to cut for SEM analysis without any breakages.

In the SEM image analysis, the obtained CNT foams were first dipped into the liquid N_2 in order to harden their structures before cutting for SEM observation. The samples thus pretreated were vertically cut in halves in order to reveal its central cross section, which corresponds to the axial direction of the samples. To obtain the porous networks in the bulk samples, SEM images were taken at several different positions as described in Fig. 3.5. It should be noted that SEM analyses were carried out mainly to investigate the effects of the initial formulation and the freezing condition (i.e. controlling by cooling rate) on the porous walls of bulk samples.

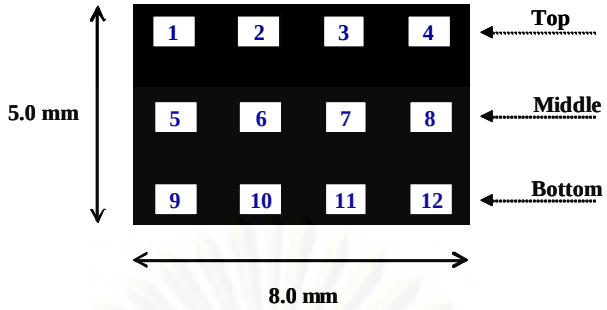

Figure 3.5 Locations for SEM observation of macroporous CNT foam specimen

As for the observation with the digital optical microscope, the obtained CNT foams were first embedded in epoxy resin (EpoFixResin, Struers, Denmark) in order to avoid the breakage of their macropores while the samples were being cut along various selected cross sections. The embedded samples were cut either vertically or horizontally with respect to the direction of freezing in order to analyze their macropore sizes and morphology. The microscopic images were taken to elucidate the porous networks in the bulk samples.

3.4.4 Electric resistance

In order to find out the potential application for a usage of prepared CNT foams in gas identification, the electronic property of obtained samples was screened via measuring the electric resistance of bulk CNT foams by using two-probe method with digital multimeter (Keithley 2700, U.S.). It was done by directly touching two electrodes on the surface of bulk foams (8.0 mm in apart).

3.5 Electric resistance test of the macroporous CNT foams for gas identification

Electric resistances of the prepared macroporous CNT foams could be measured via two methods, i.e. the four-probe and two-probe methods. The selected technique depends on which one is more simple and convenient to use in specific experimental set-up as explained in more details later.

3.5.1 Four-probe method

In our preliminary tests, dry air was used as base case. The electric resistance of a prepared macroporous CNT foam was measured with the four-probe method under controlled pressure of dry air. Four probes (each 0.5 mm in diameter, 4.0 mm in length, 1.5 mm apart) were vertically inserted into the sample. The device set up with this CNT foam was put in a vacuum chamber (same as the freeze-dryer in Fig. 3.4). The change of the electric resistance was investigated as the chamber pressure was varied. In all, three CNT foams produced with different initial formulations via the contact freezing method, namely, samples C1, C5 and C10, were tested in the presence of dry air.

3.5.2 Two-probe method

The obtained CNT foams were found to display different dynamic electric resistance as the pressure and type of the gas were varied. Therefore, the dynamic responses of CNT foams with different porous structures against three different gases (i.e. helium, ethane, iso-butane) were investigated. Six freeze-dried CNT foams produced under different freezing conditions and different freezing methods but with

the same initial formulation, namely, samples C3, C4, C5, C6, I1 and I3, were tested here. An experimental system was designed and set up to manipulate and feed a test gas into the testing chamber conveniently (Fig. 3.6). The two-probe method was selected because it is more flexible and practical to set up within the small space of the testing chamber at where several samples were placed in a testing chamber. The electrical contacts made of 0.5 mm Cu-Sn wire were horizontally inserted into each foam samples at the same positions (1.0 mm in length, 6 mm apart). A photograph of the typical two-probe set-up is shown in Fig. 3.7. Before actual measurement, the sample was kept in vacuum (0.1 MPa) at room temperature for 2 h in order to remove residual moisture and stabilize the initial absolute resistance of the sample. Next the test gas of interest was introduced into the testing chamber at a constant flow rate while the electric resistance was recorded. The dynamic responses of the electric resistance and gas pressure as a function of time were observed in each test gas environment. Before starting a new experiment, the sample was evacuated in vacuum to expel the residual gas and moisture inside.

It should be noted that the dynamic responses in the testing chamber were measured by using a digital multimeter (Keithley 2700, U.S.) and recorded on a data logger. All tests were carried out at ambient temperature, about 20 ^{o}C in Himeji, Japan.

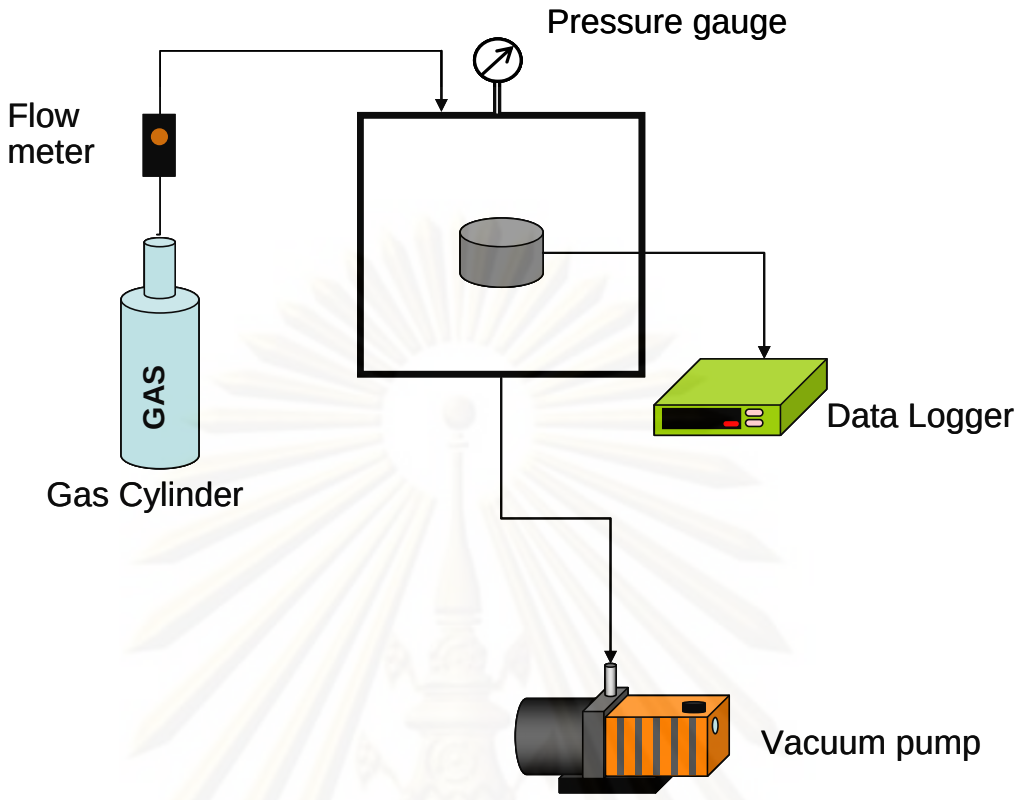

Figure 3.6 Schematic diagram of the set-up used for measuring the dynamic response of the CNT foam

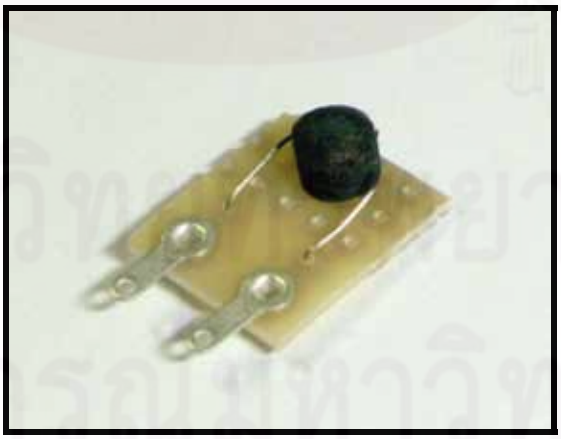

Figure 3.7 A setup of CNT foam with two probes

CHAPTER IV

RESULTS AND DISCUSSION

4.1 General characteristics of prepared macroporous CNT foams

A typical sample of the bulk CNT foam produced in this work was displayed in Fig. 4.1. All prepared samples exhibited a sponge-like nature due to their elasticity and, as a result, their original shapes can repeatedly be recovered after being gently squeezed to a significant extent. Table 4.1 lists the physical properties of the prepared freeze-dried CNT foams. The obtained bulk samples were highly macroporous with porosity of ca. 97% and bulk density of 0.05 to 0.06 g cm^{-3}. N_2 adsorption-desorption isotherms revealed that the as-received multi-walled carbon nanotube (MWCNT) used in this work was a mesoporous material (isotherm type IV) (Fig. 4.2a), while the prepared CNT foams exhibited a different mesoporous structure (isotherm type V) (Fig. 4.2b). It was considered that the mesoporous structure observed around the reoriented macroporous CNT foams came from the inter-space between MWCNT-embedded surfactant networks in macroporous bulk matrix due to the lower specific surface area is around 47.4 m^2 g^{-1} as compared to that as-received MWCNTs (275.5 m^2 g^{-1}). It is noteworthy that our preparation technique successfully produced an ordered macroporous material with mesopores developed inside the foam walls through directional freezing of a solution of MWCNTs-dispersed carboxymethyl cellulose (CMC) sodium salt surfactant, and subsequent freeze-drying.

In addition, the electrical property of the freeze-dried bulk samples was screened by measuring their electric resistivity between contacting electrodes on the surface of

each sample. These measurements indicate that the freeze-dried CNT foams are conductive with electric resistivity in the range of 1-10 kΩ m^{-1} (depending on the preparation conditions). This conductivity can be attributed to the effective interconnection between the CNTs in the porous network of the bulk samples. This fact is one of the evidences that our bulk samples retain part of the MWCNT characteristics.

Table 4.1 Physical characteristics of typical freeze-dried samples made of different formulations prepared via the contact freezing method

Sample code	MWCNT content (wt.%)	Surfactant concentration (wt.%)	Cooling rate (K min^{-1})	Bulk density (g cm^{-3})	Porosity (%)	Avg. pore diameter (μm)
C4	1.0	1.0	-0.5	0.06	97.0	72.7 (68.1)
C5	1.0	1.0	-3.0	0.05	97.6	71.0 (57.7)
C7	1.0	2.0	-0.5	0.05	97.1	61.1 (57.8)
C8	1.0	2.0	-3.0	0.05	97.4	51.7 (50.4)
C9	1.5	1.0	-0.5	0.05	97.7	73.6 (64.3)
C10	1.5	1.0	-3.0	0.05	97.4	48.9 (45.6)

Remark: 1. Apparent density of MWCNTs in this study is 2.5 g cm^{-3}.
2. For average pore sizes, values outside and inside the parentheses are estimated via analysis of SEM images and optical microscopic images, respectively.

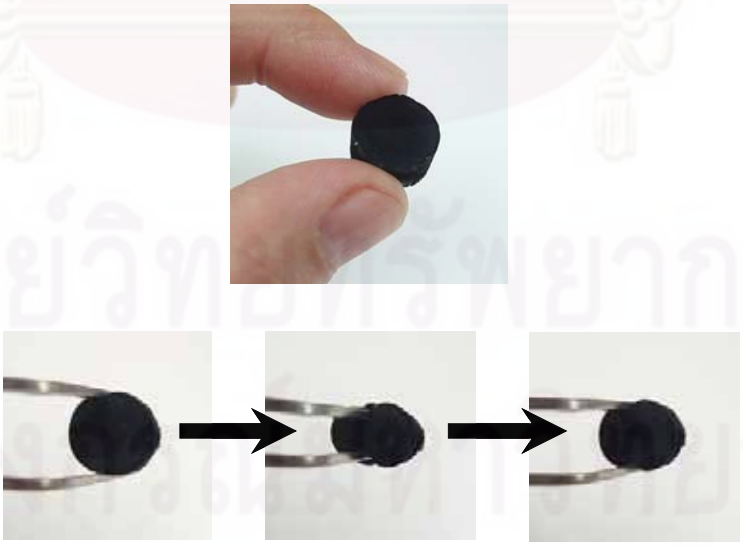

Figure 4.1 Elastic nature of the prepared CNT foam

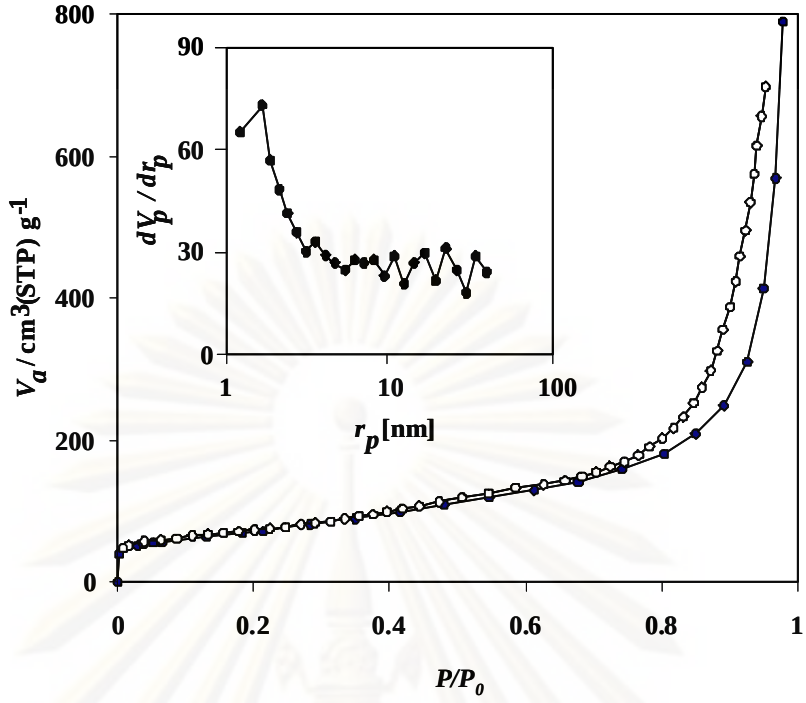

(a)

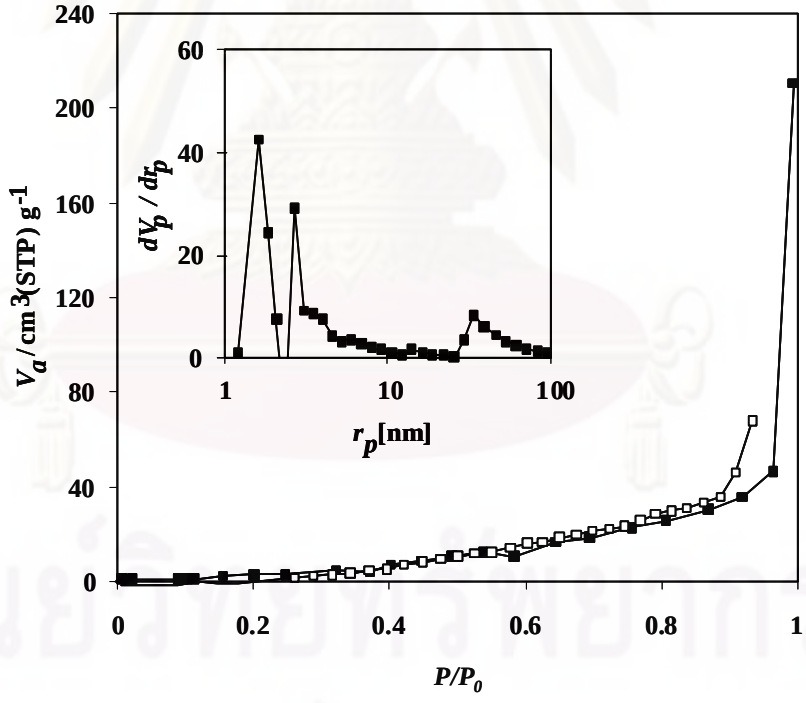

(b)

Figure 4.2 Isotherms of N_2 adsorption (open symbols) and desorption (solid symbols) and mesopore size distribution data of typical samples: (a) as-received MWCNTs and (b) freeze-dried CNT foam (sample C5)

Fig. 4.3 shows SEM images of the inner wall surface of a pore in a prepared CNT foam specimen. One can see that the MWCNTs were mainly embedded inside the CMC sodium salt (Fig. 4.3a). The freeze-dried sample was next calcined in N_2 flow at 500 ^{o}C for 3 h to remove residual surfactant on the pore walls, thereby revealing the inside of these walls. In this manner, it was confirmed that the calcined sample still kept its foam-like structure after the CMC sodium salt surfactant was partly removed. One can recognize the MWCNTs on the pore walls of the calcined CNT foam as shown in Fig. 4.3b. It was suggested that the CMC sodium salt surfactant played a key role in constructing the porous network and incorporating the MWCNTs into the foam walls. The calcined sample could maintain its porous structure though it lost the elastic nature of the original freeze-dried products.

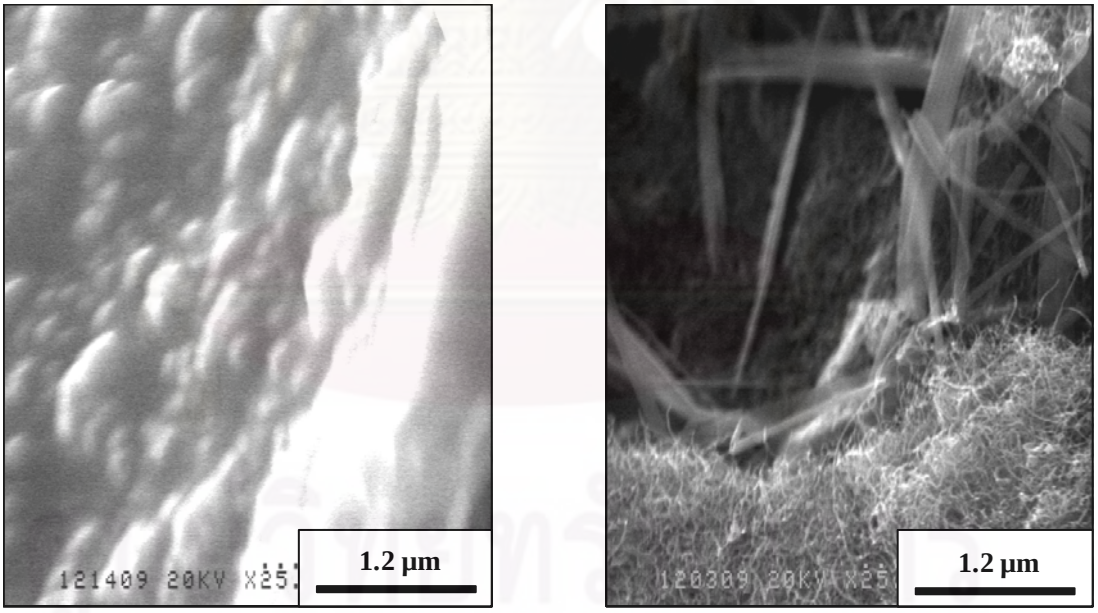

(a) (b)

Figure 4.3 SEM images of inner surfaces of CNT foam prepared via the contact freezing method: (a) freeze-dried sample and (b) calcined sample

4.2 Influence of the preparation condition on the macropore size of CNT foams

As noted in the previous section, spatially ordered macroporous CNT foams with mesochannels in the foam walls can successfully be produced with our processing technique, i.e. the directional freezing of a solution of MWCNTs-dispersed CMC sodium salt surfactant, and subsequent freeze-drying. In this section, we will focus on the macropore structural control (i.e. size and shape). It has been reported that the constituent materials in the starting solution and the adopted freezing condition were the key parameters to control the macropore size, while the macroporous shape was mainly controlled by the freezing method (Jennings, 1999; Kang et al., 1999; Fukasawa et al., 2002; Swarbrick et al., 2002; Mukai et al., 2003; Nishihara et al., 2005; Yunoki et al., 2006; Deville et al., 2007; Landi et al., 2008; Lau et al., 2008). Here the effect of the initial formulation (concentrations of CNTs and CMC sodium salt surfactant) of the starting solution and then that of the freezing condition on the macropore size of CNT foams produced via two different freezing methods, i.e. contact freezing with a plate heat exchanger, and immersion freezing in a cooling bath, will be investigated, as follows.

4.2.1 CNT foams prepared via the contact freezing method

(1) Effect of the initial formulation

The contact freezing of the starting solution with plate heat exchanger was used to prepare bulk CNT foams for investigating the effect of the initial formulation. In the starting solution, MWCNT content was varied as 0.5, 1.0, or 1.5 wt.%, whereas the concentration of CMC sodium salt surfactant was varied as 0.5, 1.0, or 2.0 wt.%. It was found that the samples prepared with either the lowest MWCNT content (0.5

wt.%) or the lowest surfactant concentration (0.5 wt.%) were rather fragile and, as a consequence, they could not be characterized. As expected, the strength of a foam sample depends on the concentration of the surfactant as well as the MWCNT content. Both of them constitute the foam wall (Mukai et al., 2004). Table 4.1 summarizes the average macropore sizes of freeze-dried bulk samples made of different MWCNT contents and surfactant concentrations. Fig. 4.4 shows SEM images of the freeze-dried bulk samples made of two different concentrations of MWCNTs and surfactant, and Fig. 4.5 shows the cumulative pore size distributions of the corresponding samples. Evidently a higher MWCNT content led to a smaller macroporous structure in the bulk matrix. Similarly, when the samples were prepared at a higher surfactant concentration, smaller pores appeared in the matrix of the bulk samples. This straight-forward relationship was subsequently confirmed to be governed by the ice crystal growth rate during freezing (Table 4.2). In other words, a higher ice crystal growth rate produces smaller ice crystal sizes (in turn resulting in smaller pore diameter) in which the details will be described in the next section. In fact, the effect of both parameters became clearer when the samples were prepared at a faster cooling rate ($-3.0\ K\ min^{-1}$).

There are reports that the concentration of the starting slurry influences the ice crystal size because the volume of liquid water directly affects ice crystal growth in the freezing process (Fukasawa et al., 2002; Deville et al., 2007; Landi et al., 2008; Lau et al., 2008). Logically, the ice crystal growth was limited by the available volume of water. At a small volume of water, there is lower probability of the ice dendrites to combine. This is why a smaller ice crystal size was obtained with either a higher surfactant concentration or MWCNT content. Since the ultimate pore sizes of a foam are associated with the ice crystals in the frozen samples, it is reasonable to

expect that, when the initial formulation is fixed, the macropore diameters can be designed and manipulated via the control of the ice crystal growth, that is, the freezing condition. The influence of the freezing condition on the pore size of the prepared CNT foams will be discussed in the next section.

Table 4.2 Ice crystal growth rates during freezing process

Sample code	MW CNT content (wt.%)	Surfactant concentration (wt.%)	Cooling rate (K min^{-1})	Ice-crystal growth rate (cm min^{-1})
C3	1.0	1.0	-0.1	4.6×10^{-2}
C4	1.0	1.0	-0.5	8.3×10^{-2}
C5	1.0	1.0	-3.0	14.2×10^{-2}
C7	1.0	2.0	-0.5	10.3×10^{-2}
C8	1.0	2.0	-3.0	12.3×10^{-2}
C9	1.5	1.0	-0.5	8.5×10^{-2}
C10	1.5	1.0	-3.0	12.8×10^{-2}

Remark: These bulk samples were prepared via the contact freezing method.

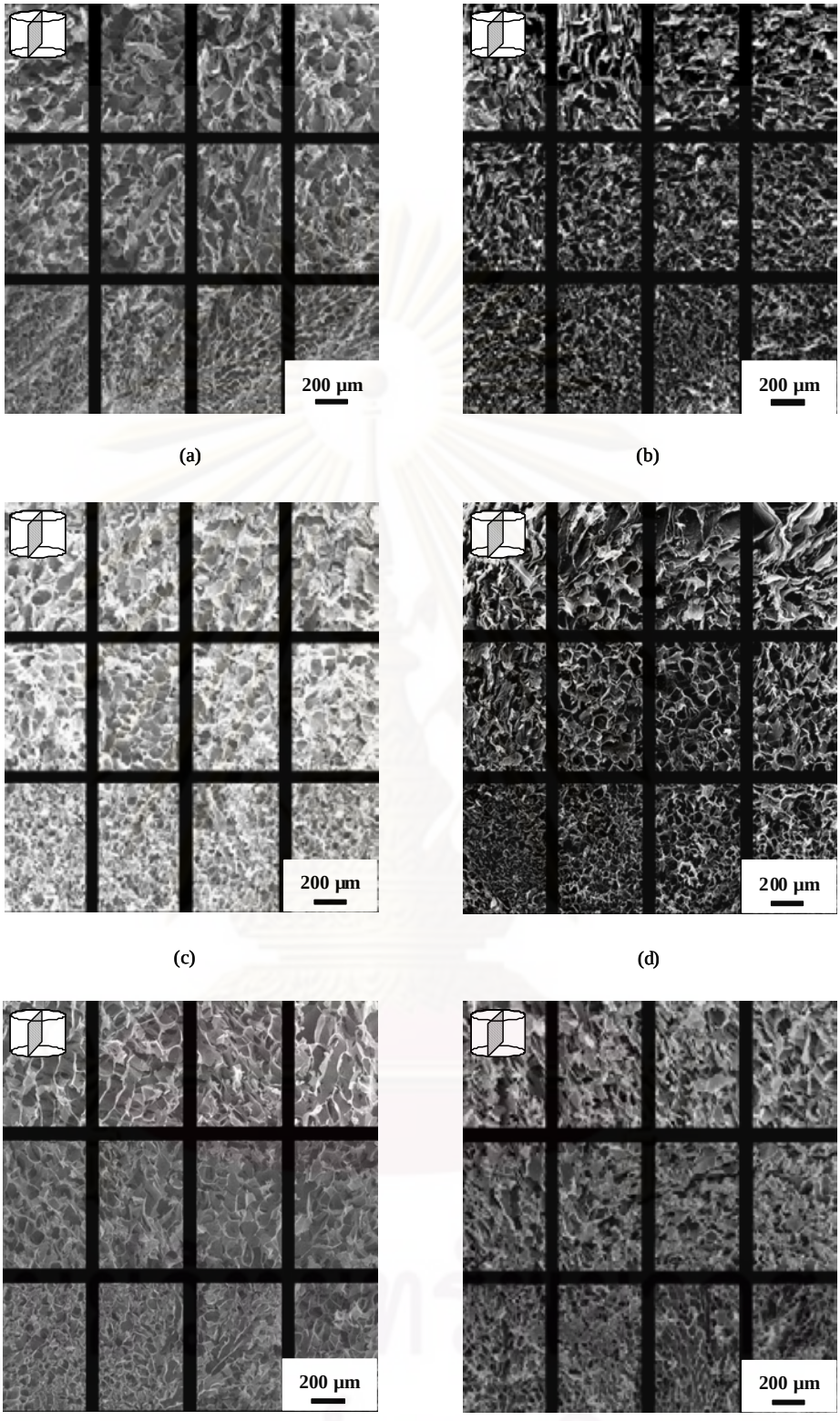

Figure 4.4 SEM images of freeze-dried samples prepared via the contact freezing method under different experimental conditions: (a) sample C4, (b) sample C7, (c) sample C5, (d) sample C8, (e) sample C9 and (f) sample C10

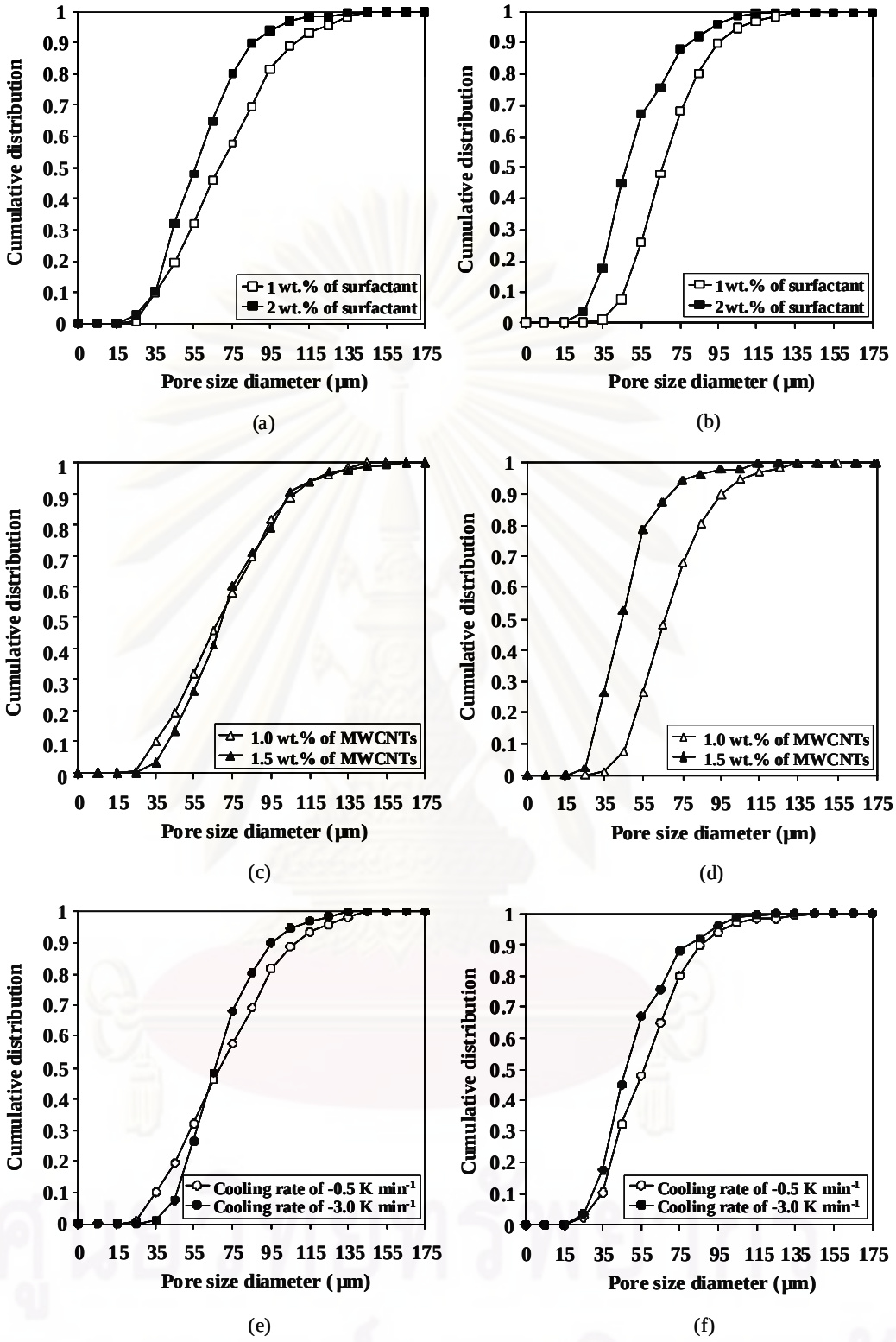

Figure 4.5 Cumulative distribution of pore size as estimated by SEM images for freeze-dried samples prepared via the contact freezing method under different preparation conditions: (a) sample C4, (b) sample C7, (c) sample C5, (d) sample C8, (e) sample C9 and (f) sample C10

(2) Effect of the cooling rate

It was reported that nucleation temperature during the freezing process and freezing condition influence the ice crystal morphology which in turned is controlled by the ice crystal growth rate and temperature distribution in the freezing system (Nakagawa et al., 2006; Hottot et al., 2007). As a result, the nucleation temperature and freezing condition are expected to be the major control factors (Hazra et al., 2003; Nakagawa, 2007). However, in reality the nucleation process in a supercooled solution occurs as a random phenomenon due to the spontaneous nature of nucleation. Therefore, a mechanism to artificially break down the supercooling should be employed if the nucleation phenomenon is to be controlled. As a matter of fact, the observed nucleation temperature of the present system was approximately close to each other and it lay between -5 to -8 ^{o}C. It is reasonable to consider that the uniformly dispersed MWCNTs play a key role as nucleation sites for initiating ice crystal nucleation during the freezing process (Hazra et al., 2003). As a result, the whole system nucleated at essentially the same subcooled temperatures, and the morphology of the samples prepared in this work should mainly be controlled by the freezing condition, i.e. cooling rate (in case of the contact freezing with plate heat exchanger).

Fig. 4.6 shows typical examples of the temperature profiles inside the sample solutions during freezing. The average ice crystal growth rate was calculated from the temperature profile of each experimental condition and summarized in Table 4.2. As expected, a faster cooling rate gave a higher ice crystal growth rate. Average macropore sizes of the freeze-dried bulk samples prepared under different cooling rates are listed in Tables 4.1 and 4.3. It can be seen that the cooling rate (ice crystal growth rate) clearly affects the ice crystal size and in turn the pore sizes. The

cumulative pore size distributions (Figs. 4.5e vs. 4.5f) indicate that a faster cooling rate led to better homogeneity of the macropore network in the bulk matrix of MWCNTs. Morphological differences of the bulk samples due to the different cooling rates can clearly be seen in the images taken with an optical microscope upon comparing Figs. 4.7a vs. 4.7b. These images reveal that, though the macropore shapes are similar to one another, the aspect ratio of the ice crystal growth in the z- and r-directions (Figs. 4.7a vs. 4.7b) as well as their macropore sizes in the bulk samples were significantly different from one another (Tables 4.1 and 4.3). Similar evidences were observed in the SEM images of the corresponding samples (Figs. 4.4a to 4.4c and Figs. 4.4b to 4.4d).

Table 4.3 Average macropore sizes of freeze-dried bulk foams made of 1.0 wt.% of MWCNTs and 1.0 wt.% of surfactant

Freezing method	Sample code	Pre-cooled temperature (^oC)	Cooling rate (K min^{-1})	Position	Average pore diameter* (μm)
Contact freezing	C3	5	-0.1	Top	94.7
				Middle	99.1
				Bottom	85.5
	C4	5	-0.5	Top	62.3
				Middle	78.6
				Bottom	63.5
	C5	5	-3.0	Top	59.6
				Middle	60.9
				Bottom	52.5
	C6	30	-3.0	Top	72.5
				Middle	78.8
				Bottom	65.2
Freezing method	Sample code	Bath temperature (^oC)	Immersion rate (μm s^{-1})		Average pore diameter* (μm)
Immersion freezing	I1	-40	20		40.2
	I2	-40	67		32.5
	I3	-40	180		30.4
	I4	-196	180		15.6

* refers the values of average pore sizes are estimated via analysis of optical microscopic images.

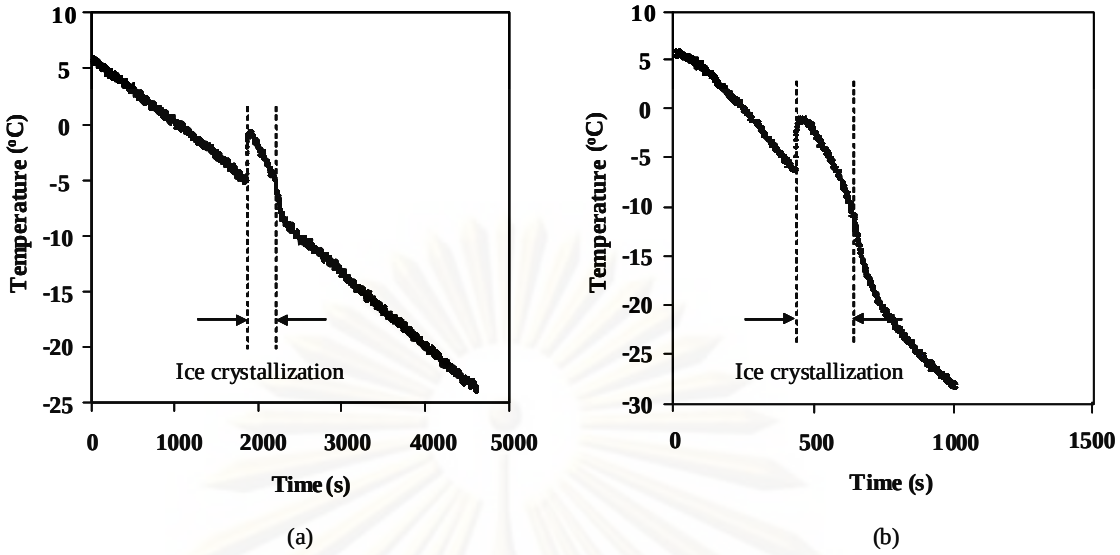

Figure 4.6 Freezing curves of freeze-dried samples made of 1.0 wt.% of MWCNTs and 1.0 wt.% surfactant, and produced via contact freezing under different freezing conditions: (a) cooling rate of -0.5 K min^{-1} and (b) cooling rate of -3.0 K min^{-1}

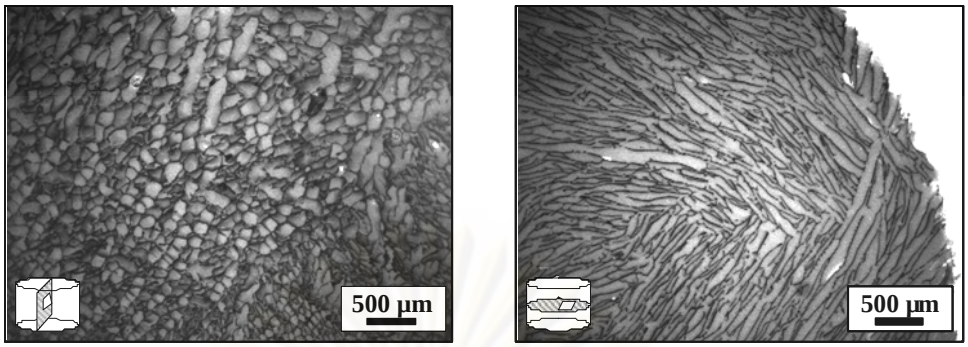

(a)

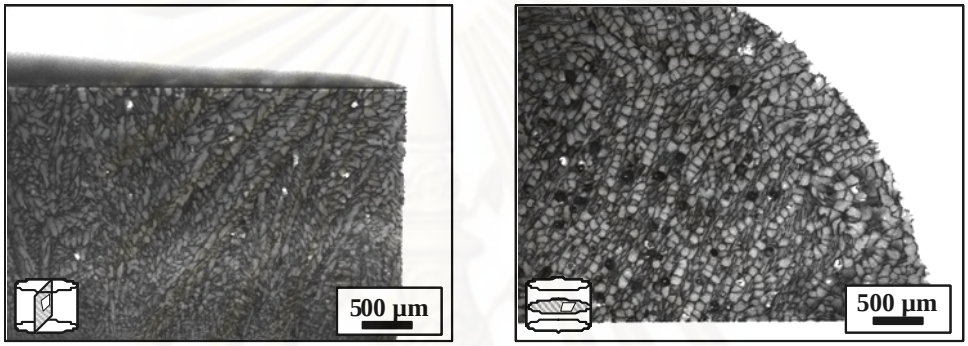

(b)

Figure 4.7 Microscopic images in vertical and horizontal cross section of freeze-dried CNT foams prepared via contact freezing: (a) cooling rate of -0.1 K min^{-1} and cooling rate of-3.0 K min^{-1}

Moreover, it was also confirmed in the present work that the spatial temperature distribution inside the pre-cooled solution was another factor that affected the ice morphology. The effect of this factor was studied by varying the pre-cooled temperature of solution (i.e. 5 and 30 ^{o}C) before freezing under a constant cooling rate at -3.0 K min^{-1}. The results show that the sample solution pre-cooled at a lower temperature (5 ^{o}C) gave a smaller macropore size, as listed in Table 4.3. The reason might be a short induction time for ice nucleation in the case of a lower pre-cooled temperature, leading to a higher ice crystal growth rate. However, an exact

comparison of this factor was not made because we did not monitor the temperature profile during the freezing process of the pre-cooled solution at 30 ^{o}C.

In short, all the results shown in this section reveal that CNT foams produced via the contact freezing method had macroporous structures that grew somewhat randomly in the z- and r- directions, and their macropore sizes could be adjusted by controlling the concentrations of MWCNTs and CMC sodium salt surfactant as well as the cooling rate.

4.2.2 CNT foams prepared via the immersion freezing method

It was shown in the previous section that samples frozen via contact freezing with a plate heat exchanger exhibited a random macroporous structure in the bulk matrix of CNT foams. However, the porous shape of the CNT foams is one important feature that should be designed to suit specific desirable application. Recently, monolithic honeycomb structure has gained attention for several applications because of its uniform straight parallel pore structure, leading to a narrow pore size distribution and lowered pressure drop compared to other porous shapes. The monolith-type materials could be prepared via the immersion freezing method, in which the target solution filled container was quickly frozen by unidirectionally immersing it into a cryo-bath at the desired immersion rate (Nishihara et al., 2005). Yunoki et al. (2006) found that the mechanical strength against compressive forces acting parallel to the pore axis could be improved by porous materials with the monolithic pore structure.

In this work, the macroporous structure of CNT foams produced via the immersion freezing method, especially the effect of the preparation condition on the

resultant macropore sizes was investigated. The effect of the immersion rate (20, 67, or 180 μm s^{-1}) on the pore structures was focused, and the formulation of all samples was fixed at 1.0 wt.% of MWCNTs and 1.0 wt.% of CMC sodium salt surfactant. The effect of freezing temperature was preliminarily investigated.

(1) Effect of the immersion rate

Fig. 4.8 shows typical microscopic cross-sectional images of CNT foams produced via the immersion freezing at different immersion rates. The overall tendency of the present effect is similar to that of the cooling rate on the macropore size, that is, a higher immersion rate led to a smaller average macropore. A faster immersion rate leads a faster ice crystal growth, resulting in the final creation of smaller-sized pores.

It is interesting here to compare the results between the two freezing methods when the immersion rate of 20 μm s^{-1} was close to the experimentally detected of about 24 μm s^{-1} ice crystal growth rate observed with a cooling rate of -3.0 K min^{-1} of the contact freezing method. The results show that a smaller macropore size was produced via the immersion freezing method (Table 4.3). The observed difference may be attributed to the fact that in the immersion system, the heat withdrawal flux was transported through the solution in two directions, i.e. z- and r- directions whilst it occurred in just one direction (i.e. z- direction) in the contact freezing system. This resulted in a faster and more oriented ice crystal growth in the former system, and consequently, monolithic macropores with smaller pore sizes were appeared in the bulk matrix.

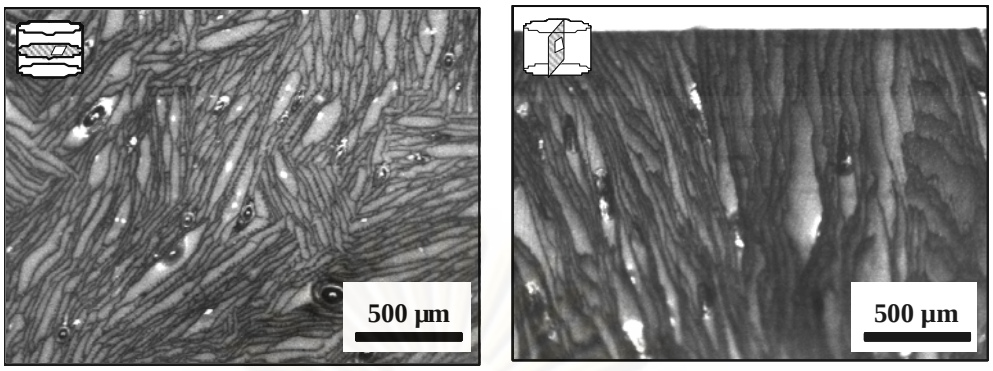

(a)

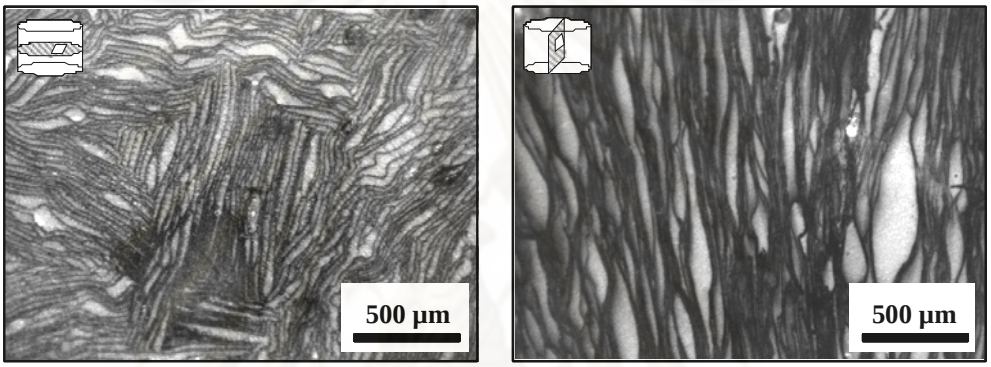

(b)

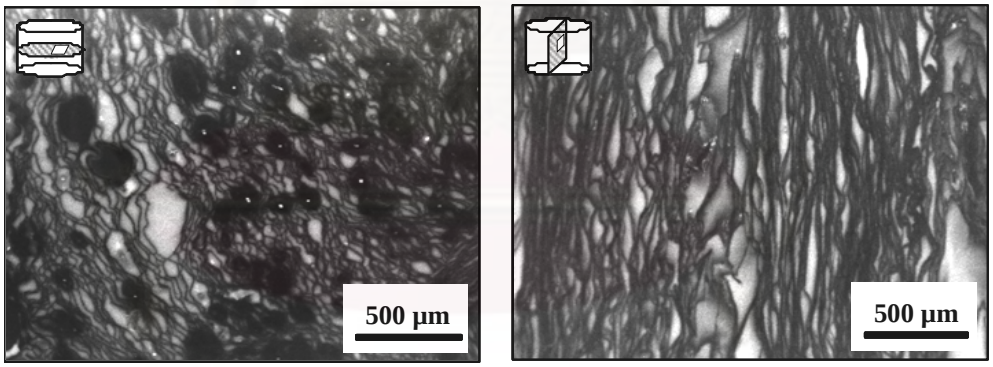

(c)

Figure 4.8 Microscopic cross-sectional images of the vertical and horizontal plane of the freeze-dried CNT foams prepared via the immersion freezing with a cryo-bath temperature of -40 ^{o}C: immersion rate of (a) 20 µm s^{-1}, (b) 67 µm s^{-1} and (c) 180 µm s^{-1}

As seen from Table 4.3, we also found that the freezing temperature significantly affected the average macropore size of the bulk samples, that is, a lower freezing temperature decreased the macropore size. This finding suggests that the decrease of macropore size in bulk sample could be attributed to the increase of heat flow along the vertical direction during freezing process (Kang et al., 1999; Yunoki et al., 2006). It is possible that a large number of ice nuclei was initially formed at a lower freezing temperature.

4.2.3 Comparison between the contact freezing and immersion freezing methods

Sections 4.2.1 and 4.2.2 reveal that the freezing method strongly influenced the macropore shape of the bulk CNT foams. The microscopic cross-sectional images reveal that a somewhat random macroporous structure was produced by the contact freezing method, whereas a rather uniform monolithic honeycomb structure was produced by the immersion freezing method. In addition, the average macropore size of the bulk samples could be adjusted by varying the preparation condition, namely, the initial formulation of the starting solution and the freezing condition. Fig. 4.7b shows the vertical and horizontal cross-sections of the bulk samples prepared via contact freezing under a rapid cooling rate. One can see that both of them were assembles of mostly columnar pores. Little differences and no tendency in the morphology were clearly observed. It means that the growth directions of ice crystals were quite random in z- and r- directions. In contrast, Fig. 4.7a reveals the lamellar structures on the horizontal cross-section of the bulk sample prepared at a slow cooling rate, while only columnar structures are seen on the vertical cross-section. This interesting fact suggests that the ice crystal growth toward the z direction is restricted due to the slow cooling condition. A sketch for the pore morphology of

macroporous CNT foams prepared via the contact freezing method under different cooling rates is illustrated in Fig. 4.9a.

The immersion freezing system shows an obvious morphological difference from that of the contact freezing system (Fig. 4.8). Continuous lamellar structures commonly appeared on the vertical cross-sections (Figs. 4.8a to 4.8c), while columnar structures appeared on the horizontal cross-sections. Moreover, one can see that the immersion rate influenced the aspect ratio of the columnar cross sections (Figs. 4.8a vs. 4.8c). More specifically, the aspect ratio became larger when the sample solution was immersed more slowly. The aspect ratio is controlled by a kinetic balance between the ice crystal growth rates in the z- and r- directions. In short, it suggests that, in the immersion freezing system, ice crystals predominantly grew up in the z-direction, and the resulting bundle of uniformly arranged ice crystals made the monolithic honeycomb structure. A sketch of the pore morphology of macroporous CNT foams prepared via immersion freezing method at different immersion rates is illustrated in Fig. 4.9b.

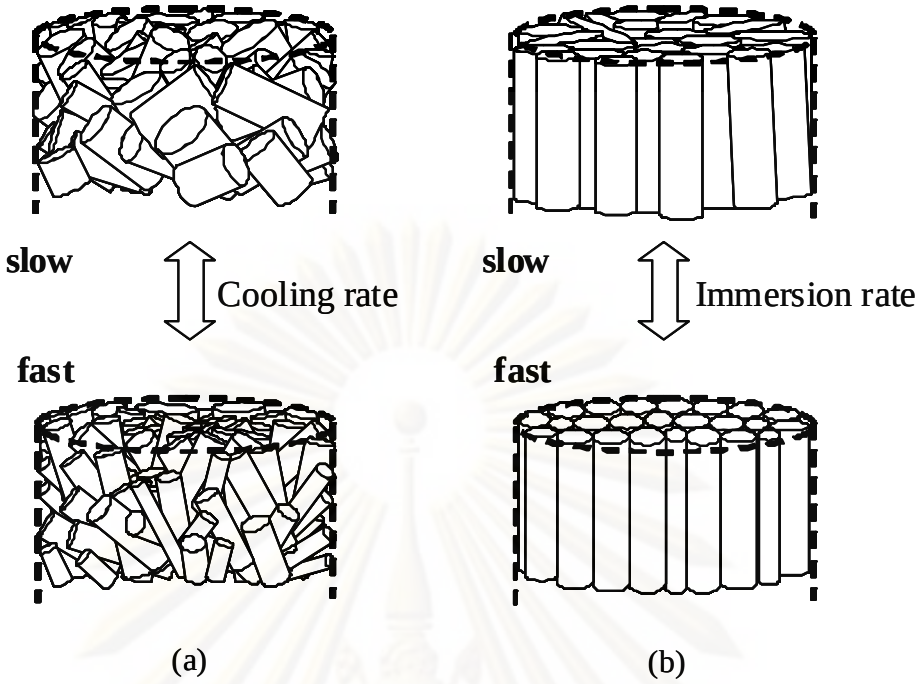

Figure 4.9 Schematic sketch of pore morphology of CNT foams produced via different freezing processes: (a) contact freezing and (b) immersion freezing

One can conclude that the macroporous morphology of CNT foams prepared from the two freezing methods (i.e. contact freezing and immersion freezing) were clearly different owing to the difference in the ice crystal growth behavior during freezing. The heat withdrawal flux is transported through the solution in two directions, i.e. z- and r- directions in the immersion freezing system, whereas the contact freezing system, only one direction (i.e. z- direction) is effectively employed for heat flow. Kang et al. (1999) suggest that, if ice is formed in the absence of any external forces, the ice crystals will tend to form in a random fashion without any preferred direction. By contrast, if ice crystals are subjected to an external stress, for example, rapid cooling, their growth will be oriented due to the temperature gradient induced in the sample solution.

Regarding the set-up of experimental apparatus, the contact freezing with a plate heat exchanger is more simple than the immersion freezing with a cryo-bath system. However, the former system suffers from a broader pore size distribution, especially, samples frozen at slow cooling condition. To obtain uniform parallel pore structure (i.e. honeycomb monolith), it is recommended that the sample solution should be frozen via immersion freezing with a cryo-bath system, or via contact freezing with a plate heat exchanger at a very rapid cooling rate (especially, for a good thermally conductive sample holder). Moreover, it has been reported that the mechanical strength of the porous materials against compressive forces acting parallel to the pore axis could be improved with the monolithic pore structure (Yunoki et al., 2006), though the mechanical property of the obtained CNT foams in this work could not be determined.

4.3 Drying characteristics of macroporous CNT foams during freeze-drying

Generally, two drying stages are observed during freeze-drying, i.e. the constant-rate and falling-rate (Swarbrick et al., 2002; Velardi et al., 2008). In the primary constant-rate freeze-drying stage, unbound ice crystals are sublimated to water vapor under vacuum, while the falling-rate freeze-drying stage is for the desorption of residual water, which is strongly bounded by adsorption to the partially dried cake. In practice the shelf temperature used in the constant-rate stage is much lower than required for efficient removal of residual water in the falling-rate stage, which is normally carried out under high vacuum and moderate temperature (20–60 ^{o}C) and the shelf and the product temperatures are nearly identical. The critical period during freeze-drying mostly occurs in the primary drying step because a premature

increase in the shelf temperature before the constant-rate period has been completed carried a high risk of collapse in the product structure (Swarbrick et al., 2002; Abdelwahed et al., 2006). In this study, the drying characteristics of some CNT foam product were in obtained. The obtained data should be useful for predicting the drying time needed (Geankoplis, 1993). The product temperature response is the most common indicator of the end of freeze-drying. When the product temperature becomes identical to the shelf surface temperature, it indicates the completion of whole freeze-drying process.

As CNT itself is porous nanomaterial, the drying behavior of the bulk foam composed of CNTs might not be straight-forward. A typical freeze-drying characteristic curve for a sample frozen via the contact freezing method is illustrated in Fig. 4.10. The shelf temperature of the freeze-dryer was set constant by setting the methanol coolant temperature at -20 ^{o}C. Apparently, two major steps were observed, i.e. steps A and B. It was confirmed from N_2 adsorption-desorption analysis that the obtained macroporous freeze-dried CNT foams show a mesopore structure on the foam wall, thereby leading to a difference in the sublimation rates between macro-ice crystals and meso-ice crystals in steps A and B, respectively. As shown in Fig. 4.10 that the drying rate is constant during step A. This is attributed to the sublimation of unbounded ice crystals in the macroporous structure of the frozen core sample, in which these ice crystals are entirely unbounded water in the solid state and they act as if there is no presence of solutes, i.e. CNTs and surfactant (Geankoplis, 1993). Therefore, the rate of sublimation under the selected vacuum conditions is independent of the solutes and its constant rate continues as long as the macro-ice crystals are sublimated. The process to sublimate macro-ice crystals took about 6 hr (Fig. 4.11a). Fig. 4.11b shows the temperature indicated by the thermocouple (TC)

buried in the side wall of the frozen sample holder. The TC temperature was determined by the rate of heat transfer by radiation and convection from the surrounding air vacuum space in the freeze-dryer to the TC and the rate of heat transfer by conduction from the TC through the frozen sample to the shelf surface. When these two rates were equal, the TC temperature will remain constant. By the way, since heat conductions within the wall of the sample holder were relatively faster and remained unchanged during the drying process, their roles would not be discussed here. When the former rate was faster than the latter, the TC temperature would rise. The latter rate would drop when the effective thermal conductivity of the sample decreased because solid ice crystals were gradually sublimated as drying proceeded, thereby being replaced by voids.

When the macro-ice crystals were completely sublimated, the effective thermal conductivity of the sample stopped its monotonic decrease, and the TC temperature stopped at a temporary maximum at around 6 hr in Fig. 4.11b. After that the drying rate fall down in step B due to the removal by sublimation of meso-ice crystals existing in the interconnecting spaces between the CNTs and the subsequent removal of meso-ice crystals existing inside the CNTs, thereby leading to a non-liner falling rate step.

Fig. 4.11 clearly reveals that the freeze-drying process took around 30 to 45 hr to end. In short, the freeze-drying characteristic curve explain why the drying time required was quite long mainly because of water strongly bounded to the large external and internal surface areas (step B). In any case, it should be remarked that only the drying behavior of CNT foams prepared via the contact freezing method was experimentally investigated in this study because of the difficulty in recording the changes during the freeze-drying of samples made by the immersion freezing system.

Nevertheless, our fundamental knowledge of the expected heat and mass transfer during the freeze-drying process tells us that a similar drying characteristic and required drying time can be expected.

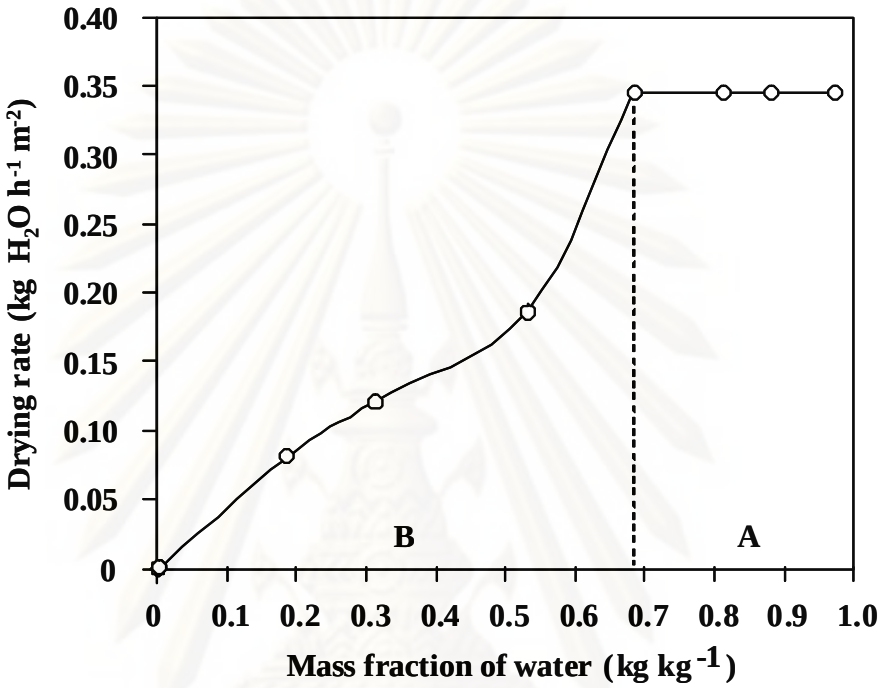

Figure 4.10 Freeze-drying characteristics of sample C4

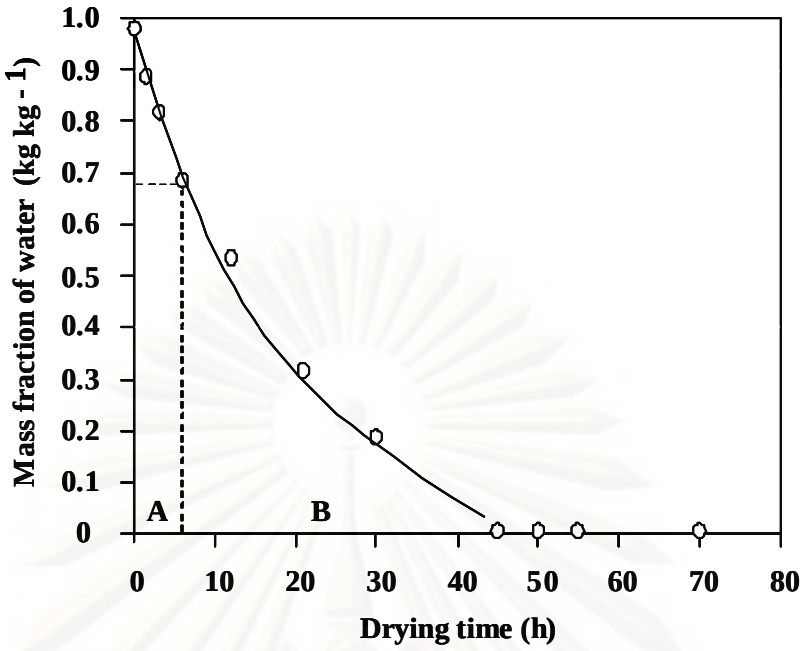

(a)

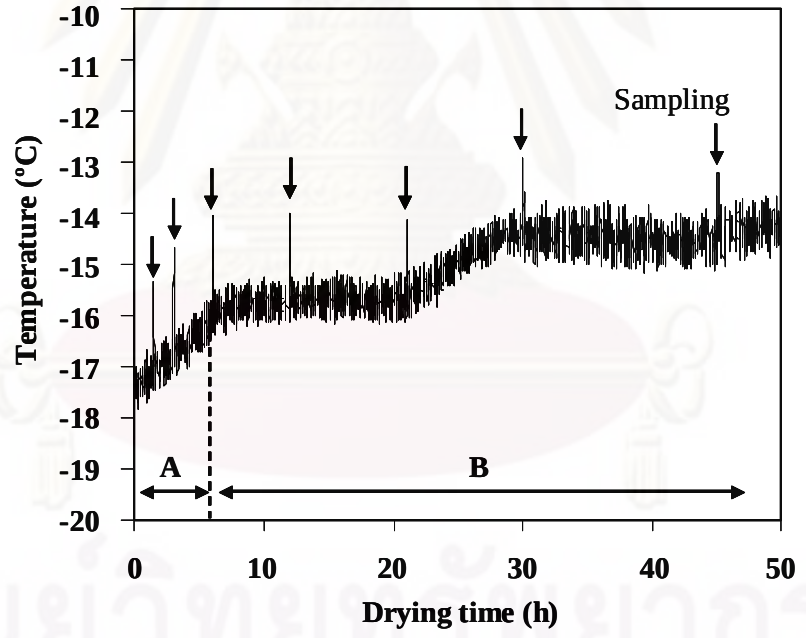

(b)

Figure 4.11 Typical freeze-drying curves of sample C4: (a) mass fraction of water vs. drying time and (b) TC temperature vs. drying time

By the way, some studies stated that ice crystal morphology should affect the sublimation rate during the constant-rate freeze-drying stage, that is, the larger ice crystal led to a higher sublimation rate (Swarbrick et al., 2002; Nakagawa et al., 2006). As for the falling-rate stage, the water vapor mass transfer resistance can be expressed as a function of the average pore diameter (macro-ice crystal) based on the hypothesis of molecular diffusion by Knudsen regime (Hottot et al., 2007). This hypothesis indicates a shorter time for the falling-rate period with larger ice crystals. In this work, the effect of the average macropore size was investigated on CNT foams prepared under cooling rate of -0.5 K min^{-1} and -3.0 K min^{-1}.

The obtained drying curves for both bulk samples are depicted in Fig. 4.12. No significant difference can be observed from these results, though the drying rate for the sample prepared at a slower cooling rate appeared to be slightly faster than that prepared at a more rapid cooling rate. The result may be ascribed to the foot that a slightly larger macropore diameter of the sample prepared at the slower cooling rate (68.1 μm in average pore diameter) compared to that prepared at the faster one (57.7 μm in average pore diameter) while both samples have similar macropore shapes, as reported in “the section 4.2.1”.

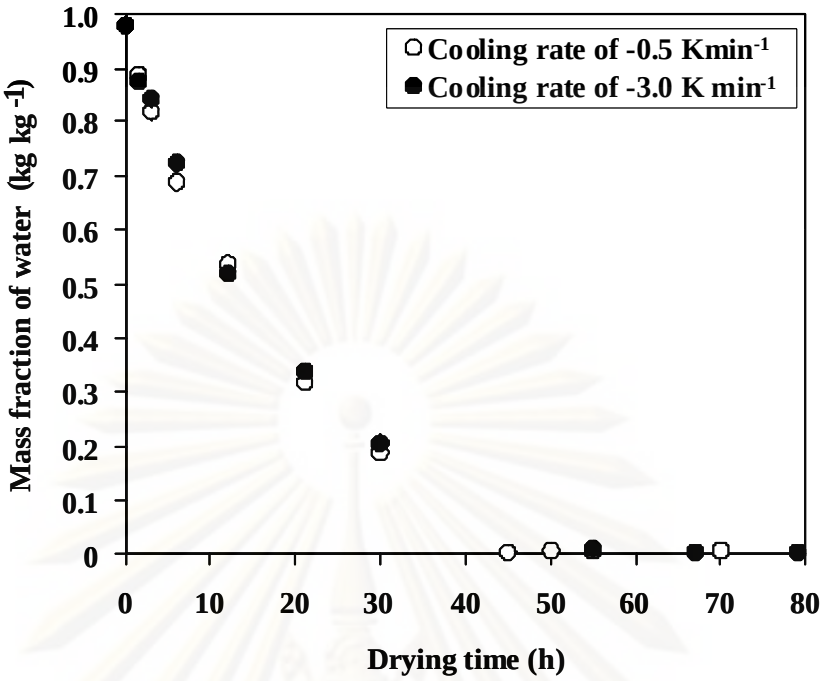

Figure 4.12 Freeze-drying curves for samples C4 (opened circles) and C5 (closed circles)

4.4 Simplified mechanism of macroporous CNT foam formation

It was clearly revealed that the two freezing methods (i.e. contact freezing and immersion freezing) significantly influenced the ice crystal shapes (in turn, the macroporous shapes) in the bulk matrix of CNT foams, whereas the preparation condition of each freezing method also affected the obtained ice crystal sizes (in turn, the macropore sizes). To gain more understanding, a simplified mechanism of macroporous CNT foam formation via each freezing method and subsequent freeze-drying process is proposed here. In our solution or suspension, there are three components consisting of the CNTs, CMC sodium salt surfactant and water. Water is the main component to be solidified during freezing process. Fig. 4.13 shows schematic sketches of how a pore system can be prepared in a typical bulk foam made from CNTs via freeze-casting with subsequent freeze-drying process.

First, ice nuclei initiate localized freezing in the supercooled solution, resulting in ice crystals gradually growing up from the bottom to the top of the sample. Of course, the ice crystal growth direction will depend on the dynamic balance between the growth rates in the z- and r- directions, as mentioned in “the section 4.2.3”. During the freezing process, the CMC sodium salt surfactant (attached to the CNTs) is pushed into the interdendritic spaces by the growing ice dendrites, and consequently, the CMC sodium salt with its embedded CNTs is assembled onto the ice crystal surface. After complete solidification in the bulk matrix is achieved, the frozen sample is lyophilized to remove the ice crystals from the bulk sample. According to the drying characteristics data (Fig. 4.10), it should be noted that ice crystals that correspond to future macropores (macro-scale ice crystals) are preferentially sublimated at the first step of freeze-drying (period A). Subsequently, ice crystals embedded together with CNTs (meso-scale ice crystals) continue to sublimate, followed by desorption of the adsorbed water inside the CNTs (period B). Finally a typical dried bulk of CNT foam is obtained.

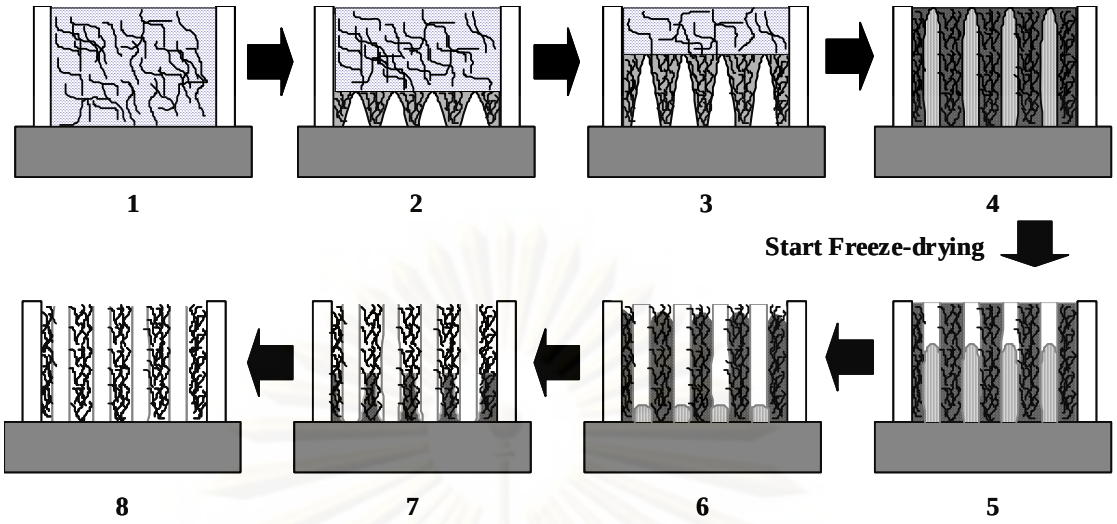

1: CNTs dispersing solution
2, 3: Ice crystal nucleation and growth
4: Complete solidification
5: Sublimation of macro-ice crystals
6: Sublimation of macro- and meso-ice crystals
7: Sublimation of meso-ice crystals and adsorbed water inside CNTs-embedded surfactant
8: Complete sublimation

Figure 4.13 Sketches of a simplified mechanism for macroporous CNT foam formation

4.5 CNT foams as potential gas identifier

The previous sections have revealed the successful production of macroporous CNT foams by freezing solutions of MWCNTs dispersed in CMC sodium salt surfactant, and subsequent freeze-drying. It was shown that their macroporous characteristics could reasonably be controlled with the preparation condition (i.e. freezing condition, and concentrations of MWCNTs and surfactant). In this section, a key characteristic of the obtained CNT foams, i.e. electric conductivity, will be discussed. It is well recognized that the CNT is a potentially superb material to adsorb gas molecules due to its huge surface-to-volume ratio, hollow geometry, and unique electrical properties (Sun et al., 2007; Chang et al., 2008). In addition, a detectable change in electric conductivity of the CNT is connected to the process of gas

adsorption–desorption on the nanotube surface (Romanenko et al., 2007). Electron transfer through the CNTs was promoted when certain gas molecules were adsorbed on the CNT walls (Chang et al., 2008). In other words, the electrical conductivity of the CNT is dependent on the interactions between the adsorbed gas molecules and CNT wall. Similarly, it was reported that the electric resistance of the CNTs responded sensitively to the adsorption of various gases (Suehiro et al., 2003; Quang et al., 2006). In this sense, the CNT has recently become a good candidate as a sensitive material for the detection of gases such as H_2, O_2, NO_x, NH_3, VOCs, etc., with an improved real-time monitoring (Sayago et al., 2008). It can be deduced from these reports that our CNT foam preparation would present a very fascinating technique if it could retain these characteristics of the CNT in the bulk samples.

As mentioned in “the section 4.1”, it was preliminarily tested and tentatively proved that the obtained CNT foams retain part of the MWCNT characteristics in terms of electric conductivity. In fact, the ideal bulk foams are expected to display significant characteristics of the original MWCNTs in combination with the characteristics of the macroporous structure in the matrix of their bulk foams.

4.5.1 Dynamic response of electric resistance of CNT foams in dry air

For the sake of simplicity, we will measure the electric resistance of our samples instead of the electrical conductivity. Here, we just aim to investigate the dynamic response of the obtained CNT foams in dry air in order to predict their potential application in gas detection. The electric resistance measurements were carried out in a freeze-dryer (Fig. 3.4), which is amenable to the injection-rejection of dry air into the closed system. In short, it was an experimental study for determining the dynamic response of the electric resistance of CNT foams in the presence/absence of dry air

(humidity ~0%). Typical bulk CNT foams produced via the contact freezing method were subjected to transient dry air exposure. By manipulating the internal absolute pressure of the system, the absolute number of dry air molecules (mainly N_2 and O_2) in the system was manipulated as a function of time.

Fig. 4.14 shows typical examples of the relationship between the electric resistivity of the CNT foam and the gas pressure (the chamber total pressure). It is obvious that the resistivity responded quite rapidly to the rise and drop in the pressure. It is reasonably attributed to the change in electric resistivity to the adsorption and desorption of dry air on the foam walls composed of strands of CNTs. In fact the absolute resistivity value decreased as the bulk MWCNT content or density increased (Figs. 4.14a to 4.14c). Furthermore, the absolute resistivity value of the macroporous CNT foam should also be a function of the weight ratio of MWCNT to CMC sodium salt surfactant. As the MWCNT content ranged from a maximum of 1.5 wt.% to a minimum of 0.5 wt.%, the electric resistivity of our CNT foams increased from 0.03 to 0.35 Ω m (Fig. 4.14), which is about ten orders of magnitude smaller than typical insulating polymers (10^{12} Ω m) (Lau et al., 2008). However, it is still 3 to 4 orders of magnitude higher than the electric resistivity of as-received MWCNTs, which is lower than 10^{-6} Ω m. This means that a reasonably effective network of tube-tube and tube-surfactant contacts can be created to render highly conductive CNT foams via the proposed preparation technique.

It should be noted that a proper comparison with the reported values in the literature is quite difficult because most of the reported values are for two-dimensional films of CNTs-polymer composites. On the order hand, a discussion on the resistivity of three-dimensional matrices is generally based on the mass % of CNTs in the original media solution (Lau et al., 2008). As reported by Lau and his co-

workers, the electric resistivity of their macroporous CNT scaffolds in a chitosan system dropped approximately two orders of magnitude from 3.6 to 0.04 Ω m when the concentration of CNTs in the original solution was increased from 0.8 to 2.5 wt.%. Gutierrez et al. (2007) reported that the electric resistivity of their macroporous CNT foams in a chitosan system decreased from 0.06 to 0.004 Ω m as the CNT content in the original solution increased from 2.0 to 8.0 wt.%. These studies are two typical examples of the electric resistivity values of three-dimensional bulk structure of CNT specimens produced via the freeze-drying process.

Here, a CNT foam specimen is called as sample xi-bj-uk;

where x = C (contact freezing method) or I (immersion freezing method),

b = production batch, u = usage, i = formulation of CNT foam (Table 3.2),

j = number of production batch, k = number of use

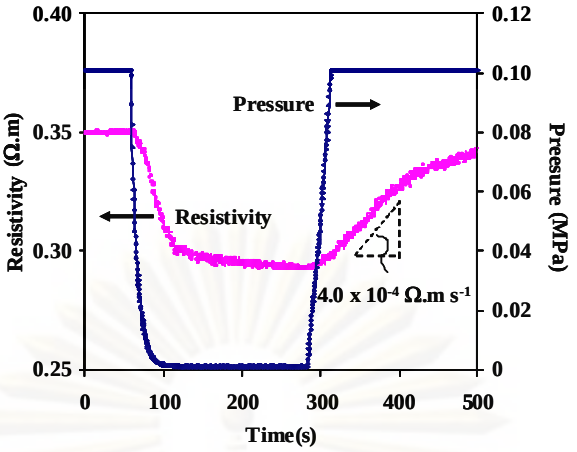

(a)

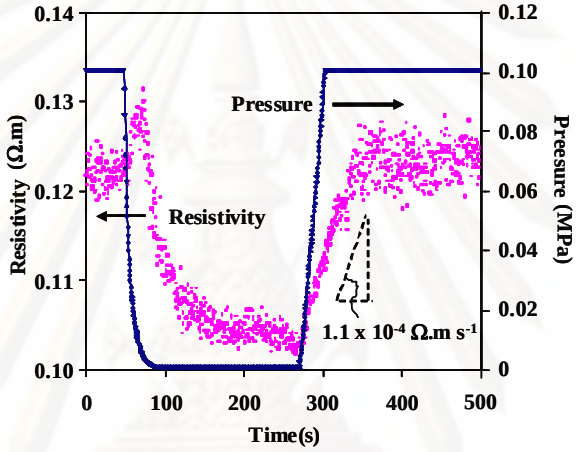

(b)

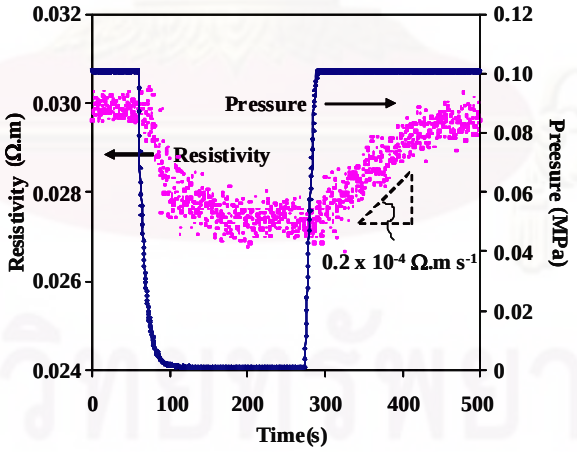

(c)

Figure 4.14 Relationship between electric resistivity and gas pressure for freeze-dried CNT foams with 1.0 wt.% surfactant produced via the contact freezing method: (a) sample C1-b1-u1 (0.5 wt.% MWCNT), (b) sample C5-b1-u1 (1.0 wt.% MWCNT) and (c) sample C10-b1-u1 (1.5 wt.% MWCNT)

Table 4.4 The absolute uptake rates of resistivity and their normalized values for CNT foams made of different MWCNT contents

CNT foam specimens	dR/dt (Ω.m s^{-1})	1/ΔR(dR/dt) (s^{-1})
C1-b1-u1 (0.5 wt.% MWCNT)	4.0 x 10^{-4}	N/D
C5-b1-u1 (1.0 wt.% MWCNT)	1.1 x 10^{-4}	5.4 x 10^{-3}
C10-b1-u1 (1.5 wt.% MWCNT)	0.2 x 10^{-4}	8.1 x 10^{-3}

Interestingly, the specific value of resistivity difference, ΔR (corresponding to 0.1 MPa pressure difference) also showed a similar trend (Figs. 4.14a to 4.14c). It is reasonable to deduce from these results that the level of contacts between the CNTs embedded in the bulk foam walls was influenced by the CNT concentration, and the difference in the contacts appeared as a difference in the measured electric resistances of the bulk samples. It should be noted that this characteristic of the electric conductivity was affected by the preparation condition of the CNT foam. Therefore, to utilize the CNT foam as a pressure sensing material, we can control its sensitivity by selecting a proper preparation condition, which will in turn influence the degree of homogeneity and macropore size of the bulk network.

As discussed in section 4.2.1, bulk CNT foams containing a higher MWCNT content had smaller macropore sizes. The average macropore size of the bulk CNT foam decreased as the MWCNT content increased (Table 4.1). When the absolute uptake rate of resistivity (dR/dt) during pressure change with respect to time was examined, it was found that the foam containing a higher amount of MWCNT gave a lower absolute uptake rate (Fig. 4.14 and Table 4.4). It is considered that gas molecules were more rapidly transported, adsorbed and desorbed within larger macropores. However, as mentioned above, the observed specific value of the resistivity difference (ΔR) decreased with the increased amount of MWCNT. As a

result, we scrutinize the normalized uptake rate of resistivity ($1/\Delta R(dR/dt)$ [s^{-1}]) during the gas pressure drop and rise with time (Table 4.4) in order to make a fair comparison among each foam in spite of a ΔR value difference. Here it was found that the foam containing a lower amount of MWCNTs shows a higher normalized uptake rate.

It is clearly seen from Fig. 4.14a that a bulk foam made with 0.5 wt.% of MWCNTs tends to show a lowest normalized response of the uptake rate of resistivity. This might be due to a natural collapse of its fragile macropore structure in the case of the bulk foam composed of low amount of MWCNTs, especially after a sudden pressure increase, leading to a not-well interconnection between CNTs in the porous network. In short, one can mention that the properly designed macroporous CNT foam containing MWCNTs and even surfactant shows potential characteristics for such usage as pressure sensor, gas detector and so on.

4.5.2 Dynamic response of electric resistance of CNT foams against helium, ethane and iso-butane

It was indicated in the previous section that the macroporous bulk foams consisting of CNTs and CMC sodium salt surfactant might function as gas sensing materials because their electric resistivity changed drastically upon exposure to gas molecules and returned to the original value after their desorption. With carbon and CNTs acting as conductive fillers in the polymer matrix, both carbon-polymer and CNT-polymer composites have been extensively studied for the detection of several gases in the literature. It was demonstrated that gas sensors based on these composites have the advantages of ease of manufacture, cost effectiveness, diversity of potential polymer candidates and a wide spectrum of detectable gases. Generally, it is

considered that the swelling of the polymer matrix, which leads to increased inter-filler distance and might eventually damage the conduction networks in the composite, accounts for the variation of the electric resistance.

Recently, sensor arrays made of different composite materials, the so-called “electronic nose”, have been fabricated by several researchers (Hu et al., 2004; Lu et al., 2006; Star et al., 2006). Since each conductive composite has its own response characteristics as determined by specific interactions between the polymer matrix and the gas of interest, the response pattern given by the detector array contains hidden information about odor species and concentration, which can be extracted through signal processing. We can deduce from these studies that our macroporous CNT foam would be an alternative candidate as electronic nose, if its macroporous structure possesses the function of gas identification.

The focus of study here is the transient response pattern of the electric resistance of each CNT foam against one of the three kinds of gas molecules, i.e. helium, ethane and iso-butane. The selection of the test gases is based on the difference in their sizes and shapes. In this section, the effect of the macropore morphology on the transient response pattern of electric resistance was investigated. To focus on the morphological effect, the formulation of all composite samples was fixed at 1.0 wt.% of MWCNTs and 1.0 wt.% of CMC sodium salt surfactant, and the bulk foam specimens were produced via one of the two different freezing methods.

Figs. 4.15a, 4.16a and 4.17a show typical examples of the transient electrical response behavior of CNT foam to a step change in the gas environment, whereas Figs. 4.15b, 4.16b and 4.17b show the corresponding chamber temperature profile observed. Obviously, as the gas molecules were adsorbed, the CNT foam showed a corresponding significant increase in its electric resistance. However, after reaching a

maximum, the resistance had a tendency to gradually decline as time passed (Fig. 4.15a). This declining behavior was observed in all bulk specimens and test gases.

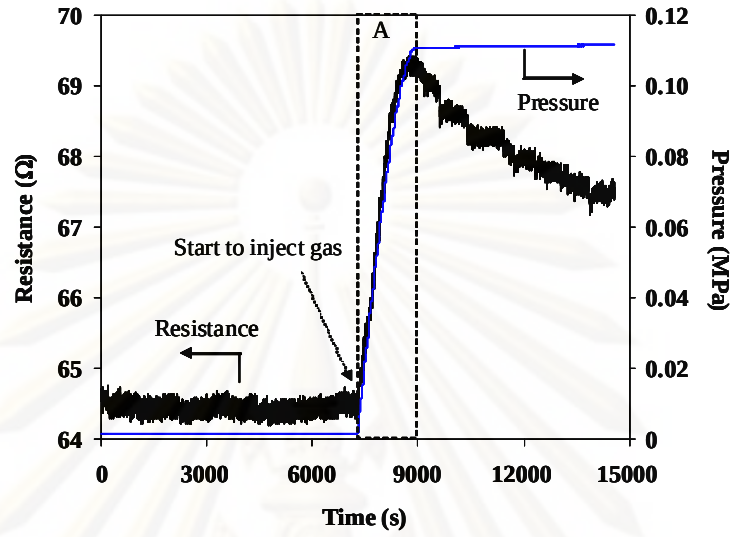

(a)

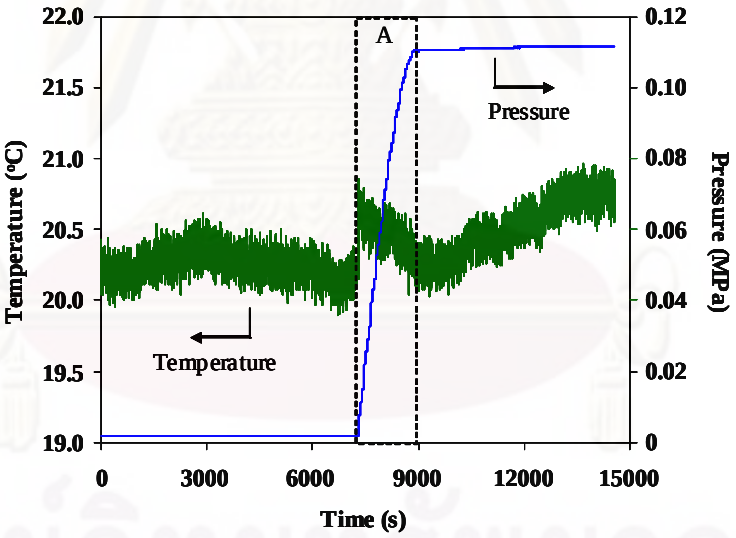

(b)

Figure 4.15 Dynamic response behaviors of bulk sample C4-b2-u1 in helium (He) atmosphere: (a) electric resistance vs. chamber pressure and (b) chamber temperature vs. chamber pressure

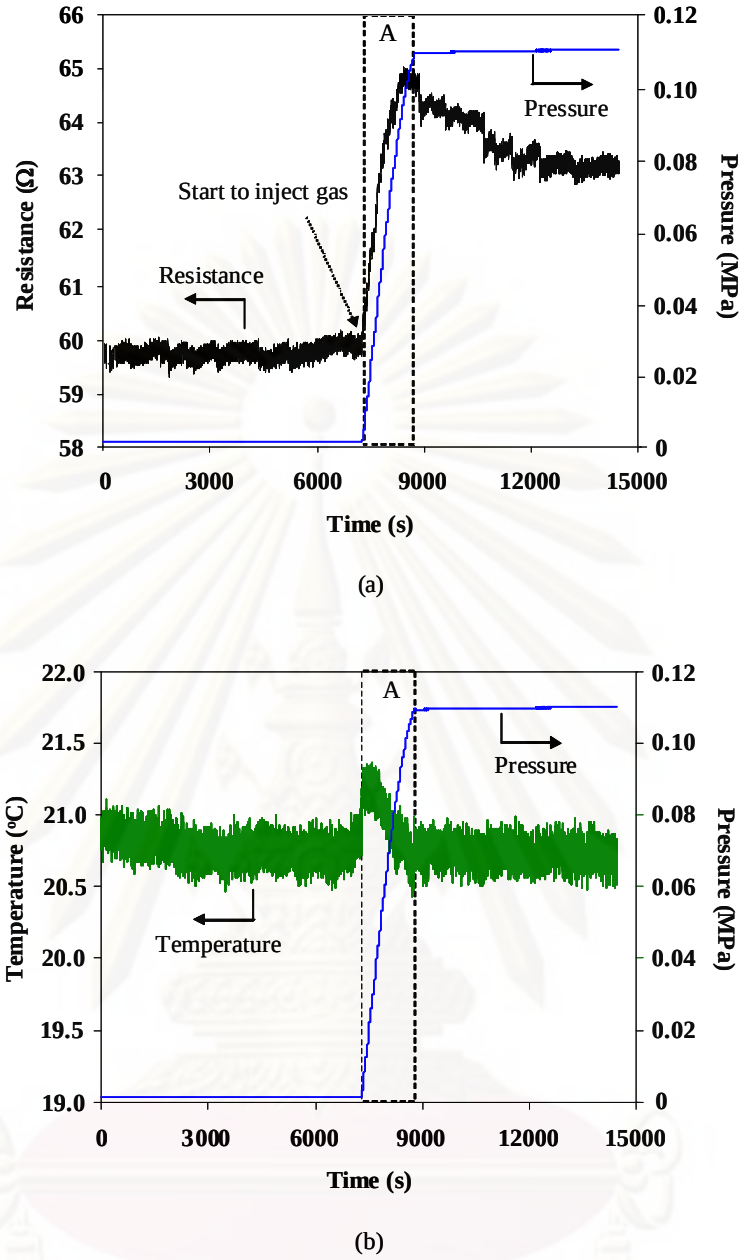

Figure 4.16 Dynamic response behaviors of bulk sample C4-b2-u2 in ethane atmosphere: (a) electric resistance vs. chamber pressure and (b) chamber temperature vs. chamber pressure

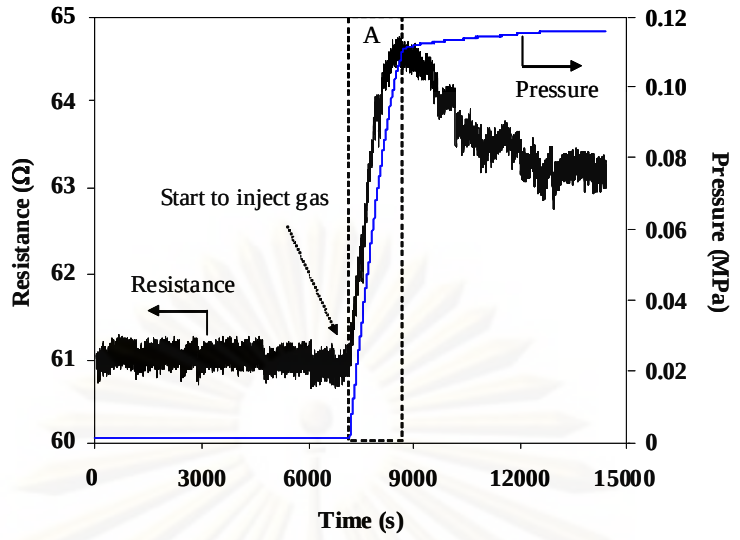

(a)

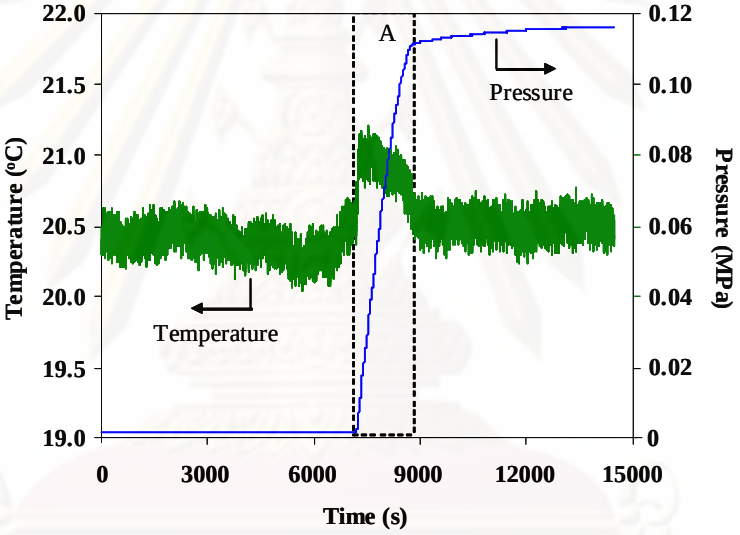

(b)

Figure 4.17 Dynamic response behaviors of bulk sample C4-b2-u3 in iso-butane atmosphere: (a) electric resistance vs. chamber pressure and (b) chamber temperature vs. chamber pressure

In order to explain the observed phenomena, we should understand the electronic property of our CNT foams. The electronic property of the CNT foams was evaluated by measuring its sensitivity before and after exposing a foam sample to UV light. A UV lamp was installed in the measurement system. As shown in Fig. 3.6, the

UV lamp (wavelength λ=365 nm) was put in front of the CNT foam sample at a distance of around 2 cm to activate the foam at room temperature. Then the transient resistance change upon UV irradiation was observed. The sensitivity (S) is defined here as the ratio of the resistance change due to UV light exposure to its baseline resistance in air without UV light:

$$S(\%) = \begin{cases} \dfrac{(R_{t,UV} - R_o)}{R_o} \times 100 & \text{(with UV)} \quad (4.1) \\ \dfrac{(R_t - R_o)}{R_o} \times 100 & \text{(without UV)} \quad (4.2) \end{cases}$$

where $R_{t,UV}$ and R_t are the sensor resistances in the presence and absence of UV light, respectively, and R_o is the fresh sensor resistance in air in the absence of UV light.

Fig. 4.18 shows the calculated sensitivity of CNT foam to UV irradiation. The result reveals that the CNT foam behaved as a semiconductor because it was sensitive to UV light exposure. In short, when the MWCNT was exposed to a reducing gas, electrons were transferred from the MWCNT surface to the gas molecules, thereby leading to the formation of positive holes on the MWCNT and a corresponding increase in the electric resistance (Sayago et al., 2008; Ueda et al., 2008; Van Hieu et al., 2008). Meantime, Figure 4.15a still shows an increase in the electric resistance of the CNT foam sample after exposing it to He, even though He is not a reducing gas. This strongly implies that there should be another dominant mechanism contributing to the increase in its electric resistance upon exposure to the test gases.

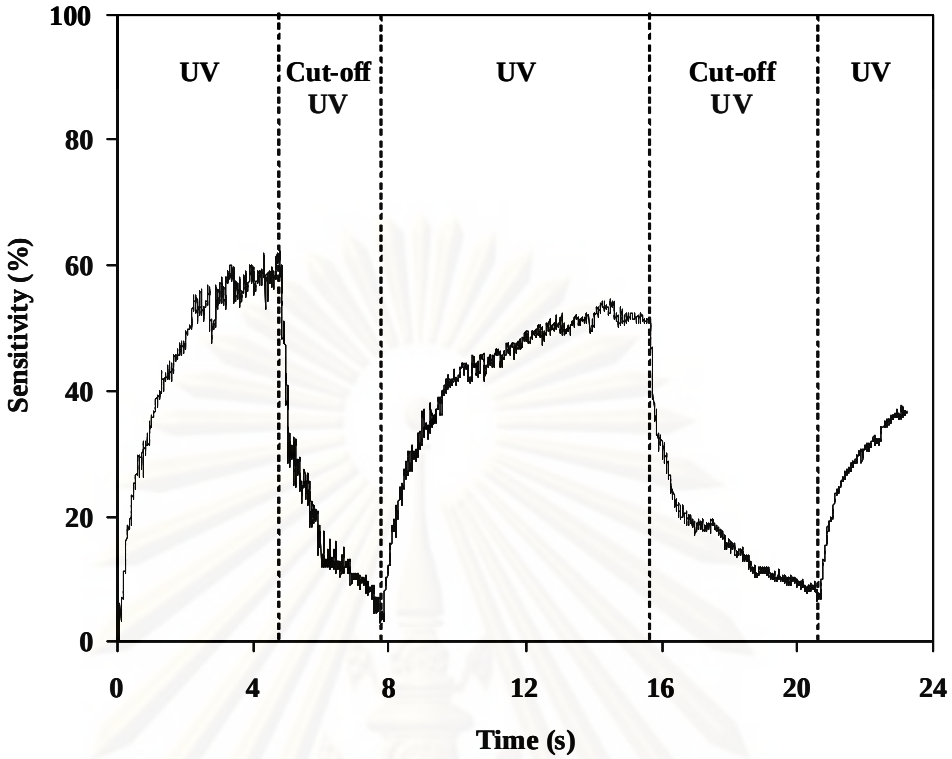

Figure 4.18 Sensitivity of CNT foam (bulk sample C5-b3) to UV irradiation at ambient condition

In fact, it has been reported that the change in the resistance of CNT-polymer composite could be attributed to the swelling of the polymer matrix (Carrillo et al., 2005; Chen et al., 2005; Zhang et al., 2008). The swelling behavior is associated with two parameters: gas permeation and polymer-solvent interaction between the gas and polymer matrix (Srisurichan, 2008). Regarding our CNT foam-gas system, permeation of gas into the polymer matrix might be dominant. Here permeation is defined as the rate at which the gas molecules pass through the polymer, and the mechanism involves three kinds of steps: (1) adsorption, (2) diffusion, and (3) desorption of gas molecules. Diffusion is frequently the rate-controlling step and the diffusion process is closely connected to a property of the polymer named the free volume, i.e. a small amount of tiny unfilled volumes between the polymer chains.

When gas molecules manage to diffuse into the polymer free volume, they can sometimes force a rearrangement of the surrounding polymer chains, thereby resulting in an increased spacing between the chains, as illustrated in Fig. 4.19. We may deduce from our experimental results that, when the gas-free CNT foam sample was exposed to the introduced gas, the gas molecules rushing into the free volume could locally rearrange the surrounding polymer (or surfactant) chain as well as the MWCNTs (Fig. 4.20). Obviously, two possibilities can be envisioned: formation of a new entangling lump of MWCNTs, or a loosening of the MWCNT network. Our experimental results would correspond to the latter case as more dominant. In other words, matrix swelling induced by the gas molecules partially disconnects the agglomerated CNTs and leads to the increase in the electric resistance of the CNT foam (Figs. 4.15a, 14.16a, 14.17a). Interestingly, after reaching a maximum, the resistance tended to gradually decline to some extent. This may be attributed to the relaxation of the forced rapid swelling with time to gain a more stable equilibrium status.

The above phenomenon was further complicated by the joint effects of chamber temperature and vapor pressure (Chen et al., 2005). Accordingly to the ideal gas law, surplus thermal energy is released and the temperature rises when free-roaming gas molecules enter a restrictive free volume and get adsorbed. As the temperature rises, the saturated vapor pressure of the adsorbate is bound to increase, thereby accelerating the adsorption on the CNT foam and increasing the resistance (see Figs. 4.15a and 4.15b). On the other hand, the elevated temperature also increases the rate of physical desorption, thereby expelling the absorbed gas molecules from the CNT foam (Li et al., 2003; Chen et al., 2005). This latter phenomenon should to some extent contribute to a subsequent reduction in the electric resistance of the CNT foam.

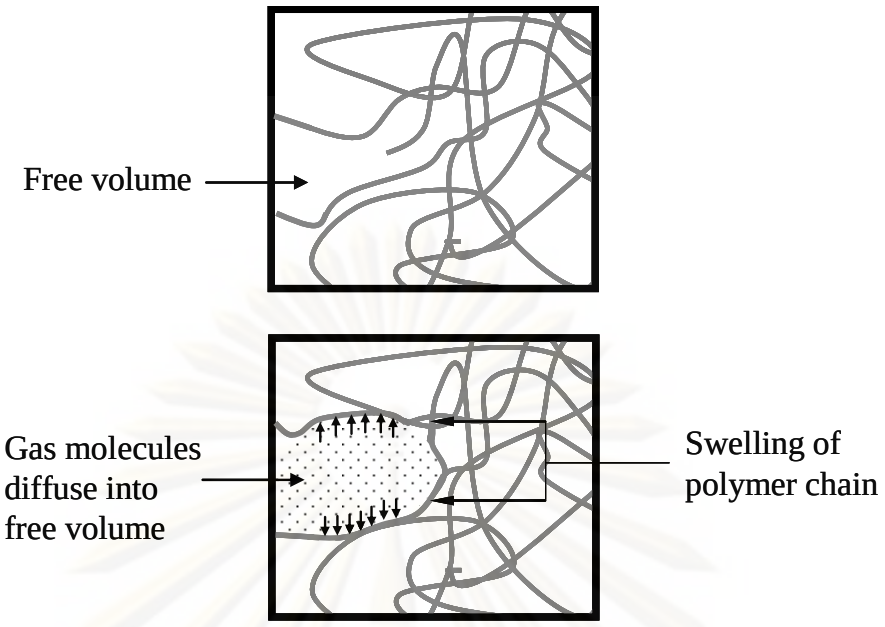

Figure 4.19 Swelling of polymer chain after gas molecules diffused into a free volume (Srisurichan, 2008)

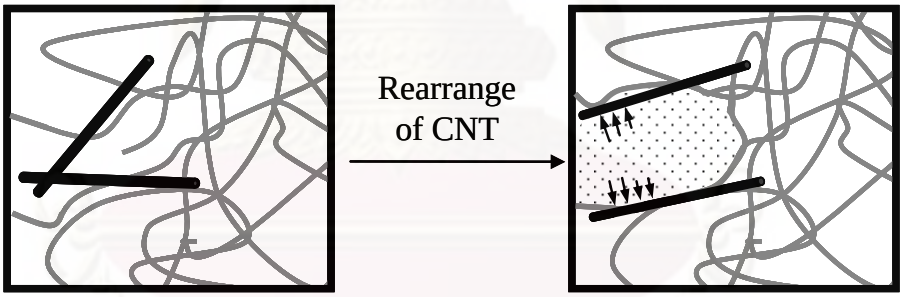

Figure 4.20 Rearrangement of polymer chains and disentanglement of MWCNTs (Srisurichan, 2008)

By the way, our experimental observations of the significant differences in the absolute values of the electrical resistance and the gas-uptake resistance response of the CNT foams against the three test gases in zone A of Figs. 4.15a, 4.16a and 4.17a, respectively, have revealed the potential of using the CNT foams as sensor array for

identifying what gas is coming into contact. In reality, the sample resistance measured with the two-probe technique generally includes the probe characteristic resistance as well as the contact resistance and spreading resistance of the probe (Schroder, 1998). Since we were unable to distinguish between these effects, it was decided to normalize the transient electric resistance change in order to fairly compare the resistance response patterns of each foam specimen with respect to a different test gas.

As revealed in “the sections 4.2.1 and 4.2.2”, the bulk CNT foams produced via contact freezing possessed a rather random macroporous structure, whereas the immersion freezing method gave a rather uniform monolithic honeycomb structure. Nevertheless, the freezing condition (i.e. either the cooling rate or immersion rate) still significantly affected the macropore size. In short, a bulk CNT foam produced with a faster freezing rate usually possessed a smaller macropore size. Figs. 4.21a and 4.21b show the dynamic gas-uptake electrical responses of two CNT foams produced via the contact freezing but with a different cooling rate and consequently a different average macropore size. The CNT foams in Figs. 4.21a and 4.21b exhibited average macropore sizes of 93.1 μm and 68.1 μm, respectively. We can see that, for the same formulation (MWCNT content and surfactant concentration), the gas-uptake electrical response was significantly different and depended on the pore structures. As expected, the larger macropores gave a faster response in electric resistance change after the foam came into contact with one of the tested gases (Figs. 4.21a vs. 4.21b). In fact, the two inset figures reveal that the higher absolute resistance belonged to the larger macroporous foam. The observed results can be attributed to the gas diffusion process, that is, a larger macropore naturally led to a faster diffusion process (Feller et al., 2004). It should be noted that the freezing condition did not influence the micro/meso-porosity of the walls of the bulk material (Nishihara et al., 2005). Hence, it is

reasonable to consider that the macropore size of the CNT foam is a key parameter that controls its mass transfer capability during its usage.

Among of the three tested gases, it was found that He attained an equilibrium state most slowly, around 25 min (Figs. 4.21a and 4.21b). In fact the required gas adsorption equilibrium time increased in the following order: iso-butane = ethane < He. The result may be attributed to the fact that He is an inert gas, whereas the CNT is electro-negative. As it turned out, the adsorption equilibrium times for iso-butane and ethane were essentially the same. The required time might be attributed to two competitive mechanisms: van der Waals interactions, which dominate the sorption between the adsorbate and CNT foam, and the shape of the adsorbate molecule, which affects the packing efficiency (Shih et al., 2008). Ethane is a saturated hydrocarbon with short linear chain, whereas iso-butane has a longer with triangular shape. Hence, ethane can diffuse into CNTs faster than iso-butane. On the other hand, CNTs and iso-butane show stronger van der Waals interactions and faster adsorption velocity.

Moreover, since the iso-butane molecule is the biggest among the three, it could not enter the restricted free volume between the polymer chains as easily as He and ethane. More specifically, the uptake rate of the absolute resistance increased in the following order: iso-butane (2.6×10^{-3} Ω s^{-1}) < ethane (3.6×10^{-3} Ω s^{-1}) = He (3.6×10^{-3} Ω s^{-1}) as seen from Figs. 4.15a, 4.16a and 4.17a. It is also noticed that the absolute uptake rates of resistance for ethane and that for He was identical. This might be due to besides, ethane molecules transport into a restricted free volume of polymer chains, and they can be also adsorbed on CNTs governed by van der Waals interaction.

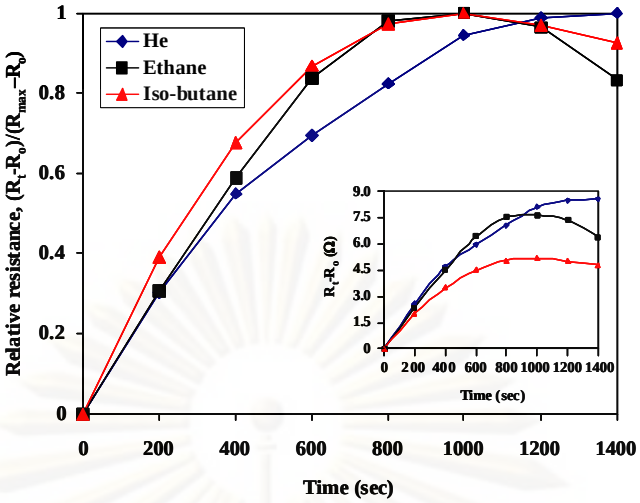

(a)

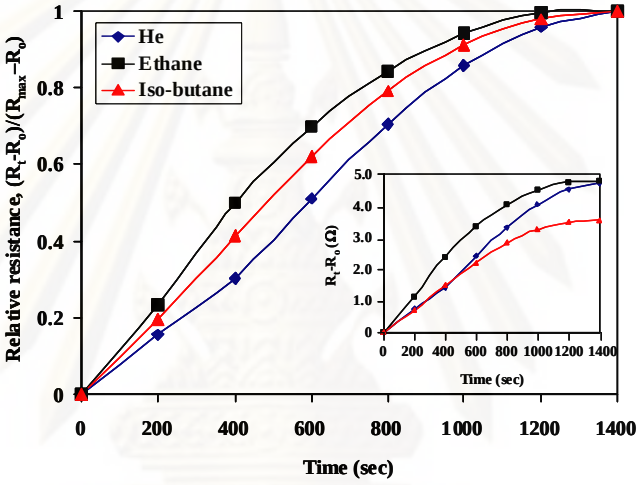

(b)

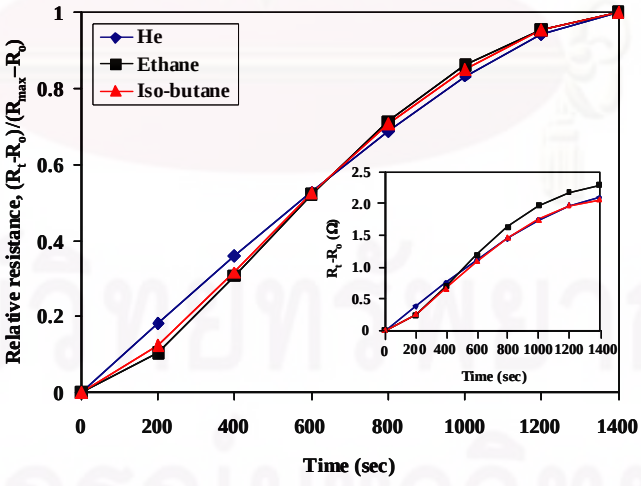

(c)

Figure 4.21 Dynamic electrical response of CNT foams against uptake time for He, ethane, and iso-butane: (a) sample C3-b2-u1, (b) sample C4-b2-u2 and (c) sample I3-b2-u3

Interestingly, we can observe apparently inconsistent patterns of the normalized gas-uptake electric response of each CNT foam specimen after coming into contact with each of the three test gases (Figs. 4.21a vs. 4.21b). Indeed, the seemingly strange patterns are related to several intertwining parameters. However, we can not yet fully explain the observed phenomenon. Nevertheless, the pattern difference corresponding to a different freezing condition can clearly be recognized and attributed to the diffusion process. In other words, one can say that the pattern of the normalized gas-uptake electric response for each gas species depends on the macropore size of the CNT foam.

Next we briefly look at the effect of the pore morphology on the normalized gas-uptake electric response. As mentioned earlier, a somewhat random macroporous structure was produced by the contact freezing method, whereas a rather uniform monolithic honeycomb structure was produced by the immersion freezing method. It is logical to expect that the resulting difference in the macropore morphology of CNT foams should to a certain extent exhibit a different pattern in the normalized gas-uptake electric response for each gas species. Figs. 4.21a (or 4.21b) and 4.21c compare the dependence of the normalized gas-uptake electrical response of CNT foams on the different freezing methods. Surprisingly, no significant differences in the normalized responses were observed for the three different gases in the case of honeycomb-monolith CNT foams obtained via immersion freezing (Fig. 4.21c). This behavior is the reverse of the case of CNT foams with somewhat random macroporous structure obtained via contact freezing (Figs. 4.21a and 4.21b). Though further studies are needed, the honeycomb-like structure may be assumed to be a key parameter or factor. In any case, more in-depth study and relevant experiments are needed to utilize the full potential of the CNT foam as a gas identifier.

4.5.3 Cyclic dynamic response of CNT foams

Stability of the CNT foam as gas sensor will definitely determine its reliability during long-term use. In the previous section, the change in electrical resistance of the CNT foam could be attributed to the matrix swelling and the gas diffusion as well as adsorption-desorption process. In order to evaluate the stability of the response behavior of the CNT foam, repeated measurements of the electric resistance were carried out under cyclical gas pressures. The electric resistance measurements were carried out in a testing system, as shown in Fig. 3.6. In short, it was an experimental study for determining the cyclic dynamic response of the electric resistance of CNT foams in the presence/absence of dry air (humidity ~0%). Typical bulk CNT foams produced via the contact freezing method were subjected to transient dry air exposure.

As revealed in Fig. 4.22, we can see that the initial electrical resistance of CNT foam was not identical from cycle to cycle. The initial electrical resistance at atmospheric pressure slightly increased after every cycle (< 5% increase after 3 cycles). It might be come from imperfect rearrangement of CNTs to their original positions after the desorption process. Interestingly, it can be observed that the maximum difference in electrical resistance within each cycle appeared to remain essentially constant. In addition, the increase in the maximum resistance tended to become smaller as the number of cycles increased. It remains to be seen whether the increase in maximum and minimum resistances will monotonically approach zero after, say, 10 cycles.

By the way, it should be noted that all experiments involving gas identification in this study were repeated three times with a fresh CNT foam specimen, and the obtained results generally gave a similar trend. In other words, our experimental results have good reproducibility. In short, the present CNT foams show reasonable

potential for application as a gas identifier, though additional investigations are necessary before a final conclusion may be made.

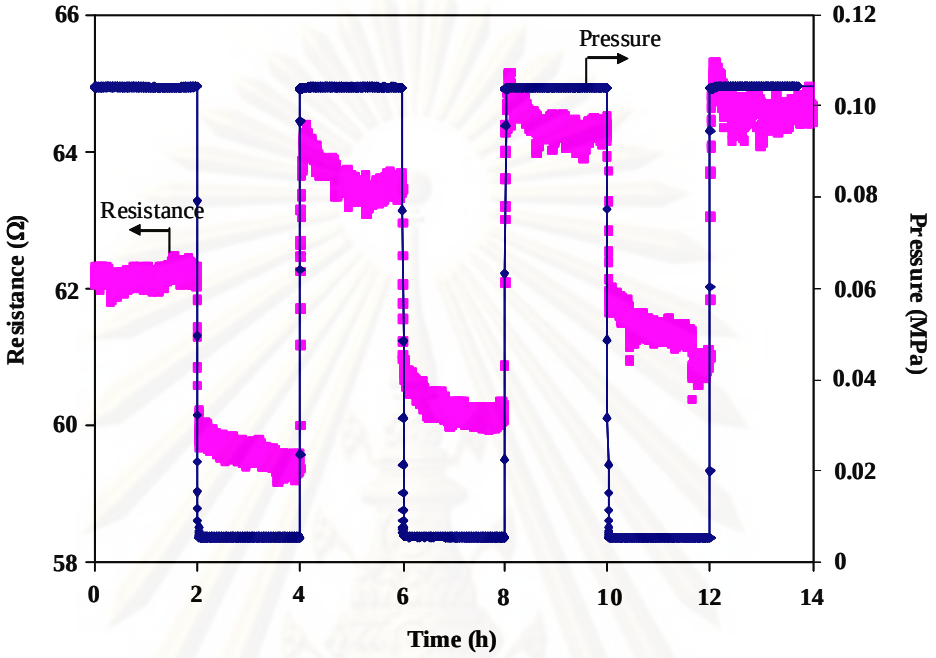

Figure 4.22 Cycle of electric response of typical CNT foam (sample C4-b4) in the presence of air

CHAPTER V

CONCLUSION AND RECOMMENDATION

5.1 Conclusion

5.1.1 Characteristics of macroporous CNT foams prepared via freeze-drying technique

Macroporous carbon nanotube (CNT) foams with mesoporous structures in the foam walls were obtained via freezing suitable aqueous solutions of carboxymethyl cellulose (CMC) sodium salt surfactant and multi-walled carbon nanotubes (MWCNTs), followed by the conventional freeze-drying process. The freeze-dried CNT foams were lightweight conductive sponge-like materials with high macroporosity (< 97%) and bulk density of 0.05 to 0.06 g cm^{-3}. The macropore sizes of the bulk specimens could be designed indirectly by manipulating the ice crystal sizes, which were controlled by adjusting the initial formulation of the starting solution (i.e. MWCNT content and concentration of surfactant) and the freezing condition.

Higher concentrations of MWCNTs and/or the surfactant as well as a more rapid freezing rate gave a similar decreasing trend in the average macropore size in the bulk matrix of the specimens. Furthermore, the pore morphology was strongly dependent on the freezing method (i.e. contact freezing vs. immersion freezing). The immersion freezing system gave a rather well-ordered macropore structure resembling honeycomb monolith, especially at a more rapid immersion rate. On the other hand, a more random macropore structure was produced via contact freezing, although well-

oriented pore structure resembling honeycomb monolith might also be produced at a rapid cooling rate.

Since the macropore size and structure of CNT foams could be controlled to a significant extent through our freeze-drying technique, it is expected that bulk CNT foams with desirable macropore size characteristics suitable for specific applications could be produced, which combine the functionality of CNT nanomaterials with the mass transfer characteristics of the macropore structure.

5.1.2 Potential applications of prepared macroporous CNT foams to gas identification

It has been shown that the electric resistance of bulk CNT foam samples responded rapidly and sensitively to a step change in the gas pressure, as the produced CNT foams behaved as semiconductor. Interestingly, it was observed that the electric resistance of CNT foam increased after exposed to even inert gas molecules (helium). The experimental results indicated that the rearrangement of polymer chains and MWCNTs entanglement would take place due to swelling and the gas diffusion as well as adsorption-desorption processes.

The dynamics of the electric resistance responses were found to strongly depend on the preparation conditions of the sensitive CNT foams. A larger macropore in the bulk specimen generally gave a faster response in the electric resistance after the specimen was exposed to any test gases. In addition, for gas identification, difference in the normalized gas-uptake electric resistance response pattern for each gas species was observed in CNT foams with different macropore sizes. Nevertheless, the preliminary tests of CNT foams as potential gas identifier are just qualitative

evaluation, and additional experiments should be carried out to investigate the effect of gas concentration on quantitative analysis.

5.2 Recommendations for future work

5.2.1 Suggestions for bulk solid foams made of nanomaterials prepared via freeze-drying technique

The CNT foams obtained in the present work with well-controlled macropore sizes show essentially hydrophilic surface property, thereby leading to limited usage. A further study should be focused on how to prepare hydrophobic CNT foams. Here the surfactant in the starting solution must display the following features**:**

(1) The bulk structure of the prepared CNT foam can be maintained during and after the freeze-drying process, and no significant shrinkage is observed.

(2) No handling difficulty appears after the heat treatment process (i.e. calcination) of the freeze-dried bulk samples.

The author and collaborators have successfully prepared CNT foams using other different surfactants or dispersing agents. However, more study and experiments must be carried out. For instance, chitosan has been used as a dispersing agent in the preparation of bulk CNT foams through freeze-casting, followed by freeze-drying (Abarrategi et al., 2008; Lau et al., 2008; Thongprachan et al., 2008). It is known that chitosan is a hydrophobic material, which can provide more hydrophilic property after soaking in an acid media (pH approximately 5.0). In fact, we got an idea to employ chitosan in the making of hydrophobic CNT foams via freeze-drying. Here frozen acid water was sublimated, thereby leaving some acid in the freeze-dried samples. As

anticipated, the freeze-dried CNT-chitosan foams displayed hydrophobic surface property. SEM observations revealed that the CNT foams prepared with the aid of chitosan had well-organized macropore structure, and the pore morphology of the bulk samples made with chitosan was quite similar to that made with CMC sodium salt (Thongprachan et al., 2008). It was found that the CNT content in the starting solution mainly influenced the electronic property (i.e. electric conductivity) of the foams. At a low concentration of CNT (1.0 wt %), the CNT foams mimicked an insulator, whereas they shifted to a conductive material as the concentration of CNT gradually increased. However, an excessive amount of CNT in the formulation (5.0 wt %) led to handling difficulty of the obtained bulk samples. In fact, the mechanical strength of the CNT foams can be improved by increasing the concentration of chitosan. However, the problem of poor CNT dispersion in chitosan solution before the start of the freezing process occurred. Some further research is needed.

By the way, the preparation of bulk solid foams made of different nanomaterials is a practical approach to widen the range of applications. For instance, titanium dioxide (TiO_2)-CNT composite could be an effective photocatalyst in wastewater or gas treatment (Lee et al, 2005; Wang et al., 2005). Nakagawa et al. (2008) reported the development of bulk solid foams made of several nanomaterials, such as CNT, TiO_2, etc. via freeze-casting and subsequent freeze-drying. In any case, a breakthrough in controlling the hydrophobicity of the bulk solid foams should be achieved first.

5.2.2 Suggestion for further study on the potential application of prepared macroporous CNT foams as gas identifier

From our study, the produced CNT foams show reasonable potential to be utilized as gas identifier though more study is needed. As of now, our experiments are just qualitative evaluation, so an investigation into the effect of gas concentration is needed in order to achieve quantitative evaluation. Besides, the tests in this work were carried out only with pure gas exposure, leading to severe limitation of the CNT foam application in real situation. Therefore it is necessary to investigate the dynamic responses of CNT foams in a binary or multi-component gas system in order to simulate the natural environment as well as to create a database for various gases.

Finally, the long-term stability of the response behavior of the CNT foams should be evaluated by carrying out repeated sensing experiments in different gases and at different concentrations.

REFERENCES

Abarrategi, A., Gutierrez, M.C., Moreno-Vicente, C., Hortiguela, M.J., Ramos, V., Lopez-Lacomba, J.L., et al. Multiwall carbon nanotube scaffolds for tissue engineering purposes. Biomaterials 29 (2008): 94-102.

Abdelwahed, W., Degobert, G., and Fessi, H. Freeze-drying of nanocapsules: Impact of annealing on the drying process. International Journal of Pharmaceutics 324 (2006): 74–82.

Carrillo, A., Martin-Dominguez, I.R., Glossman, D., and Marquez, A. Study of the effect of solvent induced swelling on the resistivity of butadiene based elastomers filled with carbon particles: Part I. Elucidating second order effects. Sensors and Actuators A 119 (2005): 157-168.

Chang, Q., Zhao, K., Chen, X., Li, M., and Liu, J. Preparation of gold/polyaniline/multiwall carbon nanotube nanocomposites an application in ammonia gas detection. Journal of Materials Science 43 (2008): 5861-5866.

Chen, S.G., Hu, J.W., Zhang, M.Q., and Rong, M.Z. Effects of temperature and vapor pressure on the gas sensing behavior of carbon black filled polyurethane composites. Sensors and Actuators B 105 (2005): 187-193.

Deville, S., Saiz, E., Tomsia, A.P. Freeze casting of hydroxyapatite scaffolds for bone tissue engineering. Biomaterial 27 (2006): 5480-5489.

Deville, S., Saiz, E., Tomsia, A.P. Ice-templated porous alumina structures. Acta Materialia 55 (2007): 1965-1974.

Feller, J.F., Langevin, D., and Marais, S. Influence of processing conditions on sensitivity of conductive polymer composites to organic solvent vapours. Synthetic Metals 144 (2004): 81-88.

Fukasawa, T., Ando, M., Ohji, T., and Kanzaki, S. Synthesis of porous ceramics with complex pore structure by freeze-dry processing. Journal of the American Ceramic Society 84 (2001): 230-232.

Fukasawa, T., Deng, Z.-Y., Ando, M., Ohji, T., and Kanzaki, S. Synthesis of porous silicon nitride with unidirectionally aligned channels using freeze-drying process. Journal of the American Ceramic Society 85 (2002): 2151-2155.

Geankoplis, C.J. Transport processes and unit operations. New Jersey: Prentice-Hall, Inc., 1993.

Gutierrez, M.C., Hortigiiela, M.J., Amarilla, J.M., Jimenez, R., Ferrer, M.L., and Monte, F. Macroporous 3D architectures of self-assembled MWCNT surface decorated with Pt nanoparticles as anodes for a direct methanol fuel cell. The Journal of Physical Chemistry C 111 (2007): 5557-5560.

Hazra, A., Paul, S., De, U.K., Bhar, S., and Goswami, K. Investigation on ice nucleation/hydrate crystallization by aqueous solution of ammonium sulfate. Progress in Crystal Growth and Characterization of Materials 47 (2003): 45-61.

Heyden, A., Duren, T., and Keil, F.J. Study of molecular shape and non-ideality effects on mixture adsorption isotherms of small molecules in carbon nanotubes: A grand canonical Monte Carlo simulation study. Chemical Engineering Science 57 (2002): 2439-2448.

Hottot, A., Vessot, S., and Andrieu, J. Freeze drying of pharmaceuticals in vials: Influence of freezing protocol and sample configuration on ice morphology and freeze-dried cake texture. Chemical Engineering and Processing 46 (2007): 666-674.

Hu, J.W., Chen, S.G., Zhang, M.Q., Li, M.W., and Rong, M.Z. Low carbon black filled polyurethane composite as candidate for wide spectrum gas-sensing element. Materials Letters 58 (2004): 3606-3609.

Jennings, T.A. Lyophilization: Introduction and Basic Principles. US: Interpharm Press Inc, 1999.

Kang, H.-W., Tabata, Y., and Ikada, Y. Fabrication of porous gelatin scaffolds for tissue engineering. Biomaterials 20 (1999): 1339-1344.

Landi, E., Valentini, F., and Tampieri, A. Porous hydroxyapatite/gelatine scaffolds with ice-designed channel-like porosity for biomedical applications. Acta Biomaterialia xx (2008): xxx-xxx.

Lau, C., Cooney, M.J., and Atanassov, P. Conductive macroporous composite chitosan#carbon nanotube scaffolds. Langmuir 24 (2008): 7004-7010.

Lee, S.-H., Pumprueg, S., Moudgil, B., and Sigmund, W. Inactivation of bacterial endospores by photocatalytic nanocomposites. Colloids and Surfaces B: Biointerfaces 40 (2005): 93–98.

Leroy, C.M., Carn, F., Backov, R., Trinquecoste, M., and Delhaes P. Multiwalled-carbon-nanotube-based carbon foams. Letters to the Editor / Carbon 45 (2007): 2307–2320.

Li, J.R., Xu, J.R., Zhang, M.Q., and Rong, M.Z. Carbon black/polystyrene composites as candidates for gas sensing materials. Carbon 41 (2003): 2353-2360.

Lu, Y., Partridge, C., Meyyappan, M., and Li, J. A carbon nanotube array for sensitive gas discrimination using principal component analysis. Journal of Electroanalytical Chemistry 593 (2006): 105-110.

Ma, X., Zhang, X., Li, Y., Xu, H., Li, G., Wang, M., et al. Gas sensing behavior of nano-structured polypyrrole prepared by carbon nanotubes seeding approach. Journal of Nanoparticle Research 10 (2008): 289-296.

Mukai, S.R., Nishihara, H., and Tamon, H. Porous properties of silica gels with controlled morphology synthesized by unidirectional freeze-gelation. Microporous and Mesoporous Materials 63 (2003): 43-51.

Mukai, S.R., Nishihara, H., and Tamon, H. Formation of monolithic silica gel microhoneycombs (SMHs) using pseudosteady state growth of microstructural ice crystals. Chemical Communication (2004): 874-875.

Mukai, S.R., Nishihara, H., Yoshida, T., Taniguchi, K., and Tamon, H. Morphology of resorcinol–formaldehyde gels obtained through ice-templating. Carbon 43 (2005): 1563-1565.

Nabeta, M. and Sano, M. Nanotube foam prepared by gelatin gel as a template. Langmuir 21 (2005): 1706-1708.

Nakagawa, K. Modeling of freezing step during freeze-drying of drugs in vials. AIChE 53(5) (2007): 1362-1372.

Nakagawa, K., Hottot, A., Vessot, S., and Andrieu, J. Influence of controlled nucleation by ultrasounds on ice morphology of frozen formulations for pharmaceutical proteins freeze-drying. Chemical Engineering and Processing 45 (2006): 783–791.

Nakagawa, K., Thongprachan, N., Charinpanitkul, T., and Tanthapanichakoon, W. Nano-material derived macro-porous solid foams: Preparation method and applications. NanoThailand Symposium 2008, Nov 06 to 08, 2008, Thailand, 2008.

Nazarov, R., Jin, H.-J., and Kaplan, D.L. Porous 3-D scaffolds from regenerated silk fibroin. Biomacromolecules 5 (2004): 718-726.

Nishihara, H., Mukai, S.R., Yamashita, D., and Tamon, H. Ordered macroporous silica by ice templating. Chemistry of Materials 17 (2005): 683-689.

Paradise, M. and Goswami, T. Carbon nanotubes – Production and industrial applications. Materials & Design 28 (2007): 1477-1489.

Quang, N.H., Trinh, M.V., Lee, B.-H., and Huh, J.-S. Effect of NH_3 gas on the electrical properties of single-walled carbon nanotube bundles. Sensors and Actuators B 113 (2006): 341-346.

Ren, L., Zeng, Y.-P., and Jiang, D. Preparation of porous TiO_2 by a novel freeze casting. Ceramics International xxx (2008): xxx-xxx.

Romanenko, A.I., Anikeeva, O.B., Kuznetsov, V.L., Buryakov, T.I., Tkachev, E.N., and Usoltseva, A.N. Influence of helium, hydrogen, oxygen, air and methane on conductivity of multiwalled carbon nanotubes. Sensors and Actuators A 138 (2007): 350-354.

Roque-Malherbe, R.M.A. Adsorption and diffusion in nanoporous materials. New York: CRC Press, 2007.

Rouquerol, F., Rouquerol, J., and Sing, K. Adsorption by powders and porous solids: Principle, methodology and applications. New York: Academic Press, 2001.

Sayago, I., Santos, H., Horrillo, M.C., Aleixandre, M., Fernandez, M.J., Terrado, E., et al. Carbon nanotube networks as gas sensors for NO_2 detection. Talanta 77 (2008): 758-764.

Schroder, K.D. Semiconductor Material and Device Characterization. 2nd Edition, New York: John Wiley & Sons, 1998.

Serp, P., Corrias, M., and Kalck, P. Carbon nanotubes and nanofibers in catalysis. Applied Catalysis A: General 253 (2003): 337-358.

Shih, Y.-h. and Li, M.-s. Adsorption of selected volatile organic vapors on multiwall carbon nanotubes. Journal of Hazardous Materials 154 (2008): 21-28.

Srisurichan, A. Multi-wall carbon nanotube-polymethyl methacrylate composite for volatile organic compound sensor. Master's Thesis, Department of Chemical Engineering, Faculty of Engineering, Chulalongkorn University, 2008.

Star, A., Joshi, V., Skarupo, S., Thomas, D., and Gabriel, J.-C.P. Gas sensor array based on metal-decorated carbon nanotubes. The Journal of Physical Chemistry B 110 (2006): 21014-21020.

Suehiro, J., Zhou, G., and Hara, M. Fabrication of a carbon nanotube-based gas sensor using dielectrophoresis and its application for ammonia detection by impedance spectroscopy. Journal of Physics D: Applied Physics 36 (2003): L109-14.

Sun, G., Liu, S., Hua, K., Lv, X., Huang, L., and Wang, Y. Electrochemical chlorine sensor with multi-walled carbon nanotubes as electrocatalysts. Electrochemistry Communications 9 (2007): 2436–2440.

Swarbrick, J. and Boylan, J.C. Encyclopedia of Pharmaceutical Technology. US: Marcel Dekker, Inc., 2002.

Tamon, H., Ishizaka, H., Yamamoto, T., and Suzuki, T. Influence of freeze-drying conditions on the mesoporosity of organic gels as carbon precursors. Carbon 38 (2000): 1099–1105.

Thongprachan, N., Nakagawa, K., Sano, N., Kitamura, M., Charinpanitkul, T., and Tanthapanichakoon, W. Preparation of macro-porous solid foam from CNTs

using ice-crystal templates. 2008 International Conference on Carbon, July 13 to 18, 2008, Japan, 2008.

Ueda, T., Katsuki, S., Takahashi, K., Narges, H.A., Ikegami, T., and Mitsugi, F. Fabrication and characterization of carbon nanotube based high sensitive gas sensors operable at room temperature. Diamond & Related Materials 17 (2008): 1586-1589.

Van Hieu, N., Bich Thuy, L.T., and Duc Chien, N. Highly sensitive thin film NH_3 gas sensor operating at room temperature based on SnO_2/MWCNTs composite. Sensors and Actuators B 129 (2008): 888-895.

Velardi, S.A. and Barresi, A.A. Development of simplified models for the freeze-drying process and investigation of the optimal operating conditions. Chemical Engineering Research and Design 86 (2008): 9-22.

Wang, H.C., Li, Y., and Yang, M.J. Sensors for organic vapor detection based on composites of carbon nanotubes functionalized with polymers. Sensors and Actuators B 124 (2007): 360-367.

Wang, W., Serp, P., Kalck, P., and Faria, J.L. Photocatalytic degradation of phenol on MWNT and titania composite catalysts prepared by a modified sol–gel method. Applied Catalysis B: Environmental 56 (2005): 305–312.

Yunoki, S., Ikoma, T., Monkawa, A., Ohta, K., Kikuchi, M., Sotome, S., etc. Control of pore structure and mechanical property in hydroxyapatite/collagen composite using unidirectional ice growth. Materials Letters 60 (2006): 999-1002.

Zarbin, A.J.G. Quimica de (nano) materials. Quimica Nova 30 (2007): 1469-1479.

Zhang, B., Dong, X., Fu, R., Zhao, B., and Zhang, M. The sensibility of the composites fabricated from polystyrene filling multi-walled carbon nanotubes for mixed vapors. Composites Science and Technology 68 (2008): 1357-1362.

APPENDIX

PUBLICATIONS

International Journal

1. **Thongprachan, N.**, Nakagawa, K., Sano, N., Charinpanitkul, T., and Tanthapanichakoon, W. Preparation of macroporous solid foam from multi-walled carbon nanotubes by freeze-drying technique. Materials Chemistry and Physics 2008; 112: 262–269.

International Proceedings

1. Nakagawa, K., **Thongprachan, N.**, Sano, N., Charinpanitkul, T., and Tanthapanichakoon, W. Application of freeze-drying technique to preparation of nano-material derived macro-porous bulk. 16th International Drying Symposium (IDS 2008), Nov 09 to 12, 2008, India, 2008.
2. Nakagawa, K., **Thongprachan, N.**, Charinpanitkul, T., and Tanthapanichakoon, W. Nano-material derived macro-porous solid foams: Preparation method and applications. NanoThailand Symposium 2008, Nov 06 to 08, 2008, Thailand, 2008.
3. **Thongprachan, N.**, Nakagawa, K., Sano, N., Kitamura, M., Charinpanitkul, T., and Tanthapanichakoon, W. Preparation of macro-porous solid foam from CNTs using ice-crystal templates. International Conference on Carbon 2008, July 13 to 18, 2008, Japan, 2008.

Materials Chemistry and Physics 112 (2008) 262–269

Contents lists available at ScienceDirect

Materials Chemistry and Physics

journal homepage: www.elsevier.com/locate/matchemphys

Preparation of macroporous solid foam from multi-walled carbon nanotubes by freeze-drying technique

N. Thongprachan [a], K. Nakagawa [b,*], N. Sano [c], T. Charinpanitkul [a], W. Tanthapanichakoon [d]

[a] Center of Excellence in Particle Technology, Faculty of Engineering, Chulalongkorn University, Phayathai Road, Pathumwan, Bangkok 10330, Thailand
[b] Department of Mechanical and System Engineering, University of Hyogo, 2167 Shosha, Himeji City, Hyogo 671-2201, Japan
[c] Department of Chemical Engineering, Kyoto University, Katsura, Kyoto 615-8501, Japan
[d] National Nanotechnology Center, National Science and Technology Development Agency, Paholyothin Road, Klong Luang, Pathumthani 12120, Thailand

ARTICLE INFO

Article history:
Received 9 April 2008
Accepted 22 May 2008

Keywords:
MWCNTs
Solidification
Porous materials
Electric conductivity

ABSTRACT

Macroporous solid foams, made of multi-walled carbon nanotubes (MWCNTs), having a high porosity of 97% were produced using a freeze-drying technique. MWCNTs were dispersed in a carboxymethyl cellulose (CMC) sodium salt (surfactant) solution. Placed on a heat exchanger, the solution was frozen and lyophilized to obtain a dry sample. The prepared solid foam specimen had a macroporous structure, and its resulting pore sizes were mainly controlled by the initial formulation and freezing condition. A faster cooling rate led to a higher degree of homogeneity and a smaller macropore network in the bulk matrix, as did a higher surfactant concentration or a higher MWCNT content. The shapes of the macropores were quite similar even when the cooling rate and/or initial formulation were different. Interestingly, the electric resistivity of the solid foams, which depended on the preparation conditions, could rapidly respond to an ambient pressure change. It was found that the prepared macroporous solid foams displayed hybrid characteristics of the original MWCNTs and the resulting bulk matrix with a controlled macropore system. These results suggest that the prepared solid foams have high potential to be used as a gas sensing material.

1. Introduction

Carbon nanotubes (CNTs) have gained world-wide attention because of their fascinating characteristics due to the combination of their electronic, adsorptive, mechanical and thermal properties [1,2]. Owing to CNTs' potential functions, their applications are expected in many fields such as chemical sensors, field emission materials, catalyst support, gas storage and so on [3]. However, being nano-scale in sizes, CNTs are frequently unsuitable and even unsafe to employ in engineering and daily-life applications. In order to solve these handling difficulties, several researchers are interested to prepare functional bulk material from CNTs. Indeed, there are a few reports on the preparation of bulk matrix made of nanomaterials. Nabeta and Sano prepared sponge-like bulk materials from CNTs [4]. They prepared them by freeze-drying acidified CNTs dispersed in gelatin solution. In their samples, porous structures were derived from the self-networking nature of gelatin and appeared after freeze-drying. Leroy et al. also employed the freeze-drying technique to produce solid foams from CNTs, wherein the porous structure was obtained by bubbling during the freezing step [5]. Abarrategi et al. developed CNTs derived scaffolds by freeze-drying chitosan containing dispersed CNTs and showed the applicability of the prepared bulk sample to tissue engineering [6]. These reports have clearly shown evidences that macroporous bulk foams can be produced from CNTs, which were supported by an agent that helps to disperse the CNTs in a starting solution and keeps its bulk structure after freeze-drying. In our point view, it is a great challenge to develop a technique that allows the preparation of controlled pore systems in a bulk sample while simultaneously displaying characteristics of the original CNTs in the resulting bulk matrix.

In the present work, macroporous solid foams were prepared by freeze-drying multi-walled carbon nanotubes (MWCNTs) dispersed in a carboxymethyl cellulose (CMC) sodium salt solution. As reported by several researches, ice crystal is an effective template to design the microscopic structure of freeze-dried materials [7–11]. The freezing protocol and initial formulation are key parameters to control the porous structure because they directly influenced the ice crystal sizes [12,13]. Here the influences of the freezing condition and initial formulation on the macroporous structures of the prepared solid foams and their associated characteristics (i.e. electric resistance) were investigated.

* Corresponding author. Tel.: +81 79 267 4849; fax: +81 79 267 4849.
E-mail address: nakagawa@eng.u-hyogo.ac.jp (K. Nakagawa).

0254-0584/$ – see front matter © 2008 Elsevier B.V. All rights reserved.
doi:10.1016/j.matchemphys.2008.05.067

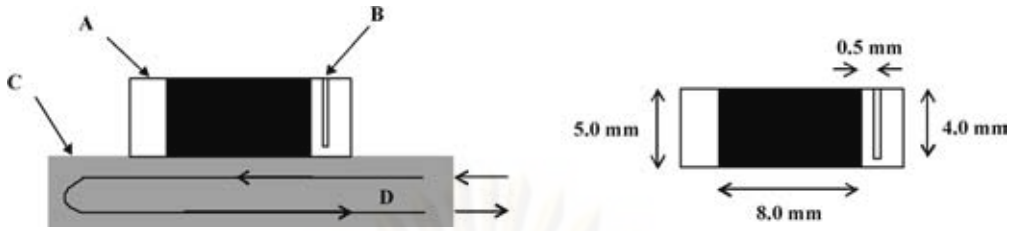

Fig. 1. Main components of the freeze-drying system: (A) samples holder, (B) holes for thermocouples, (C) heat exchanger and (D) cooling fluid.

2. Experimental

2.1. Materials

Commercial MWCNTs (Bayer Materials Science Ltd., 13–16 nm in mean outer diameter, 1 to >10 μm in length, purity >95%, synthesized by chemical vapor decomposition) were used in this work. CMC sodium salt surfactant (Fluka, Sweden) was used as dispersing agent.

2.2. Preparation of solid foams from MWCNTs

Using an ultrasonic homogenizer (UH-300, SMT company, Japan), MWCNTs (50, 100, and 150 mg) were dispersed in 10 mL of aqueous solution of 0.5, 1 or 2 wt.% CMC sodium salt for 30 min at 15 W output. The prepared solution was put into a sample holder equipped with a cooling device (Fig. 1). Cooling fluid (methanol) was continuously circulated through the heat exchanger to control the temperature of the sample. The temperatures were monitored using type K thermocouples connected to a digital multimeter (Keithley 2700, U.S.). The thermocouples were buried in the exterior wall of the sample holder in order to prevent the thermocouples from becoming nucleation points during the freezing step (Fig. 1). The prepared solutions were frozen and sublimated in a freeze-drying system shown in Fig. 2. The sample temperatures were reduced from 5 to −40 °C at a constant cooling rate (−0.5 or −3.0 K min^{-1}) and subsequently, the frozen samples were lyophilized at −20 °C for 4 days.

2.3. Analysis

The morphology of the freeze-dried samples was observed with a SEM (S-2400, Hitachi, Japan). The obtained samples were vertically cut in halves in order to observe a cross-section that corresponds to the direction of freezing. To characterize the porous networks in the bulk samples, SEM images were taken at several positions as described in Fig. 3. The macropore size distributions of the samples were determined by image analysis (ImageJ 1.38v software). About 200 pore samples in each image were counted in the analysis.

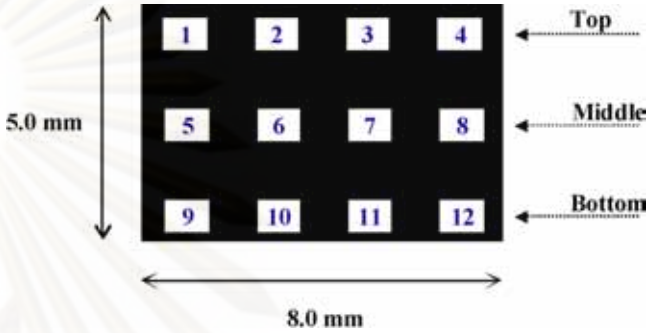

Fig. 3. Positions for observation of solid foam specimens with SEM.

Bulk density of a prepared solid foam was calculated from its weight and volume. Its porosity of bulk sample was determined from the ratio of the volume of pore spaces to the total volume of the bulk sample. Volume of pore spaces was calculated by subtracting the volume of the constituent materials from the total volume of the bulk sample. The volume of the constituent materials was estimated from their apparent densities measured with a pycnometer.

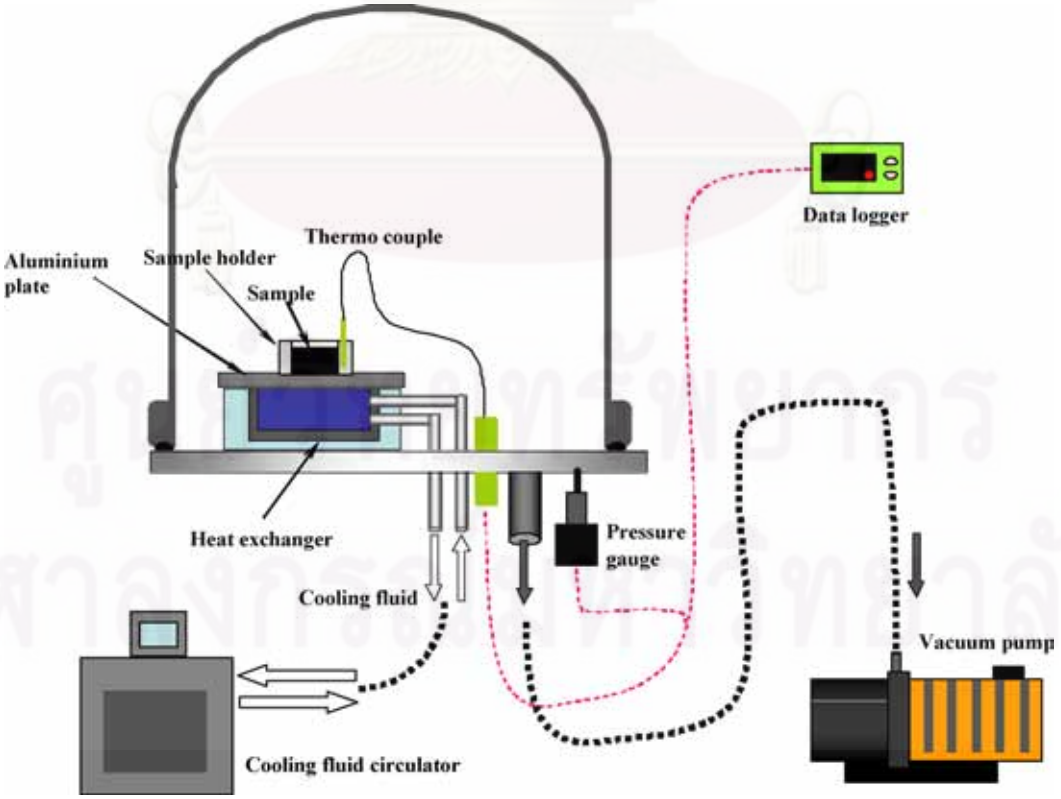

Fig. 2. Schematic diagram of the freeze-drying system.

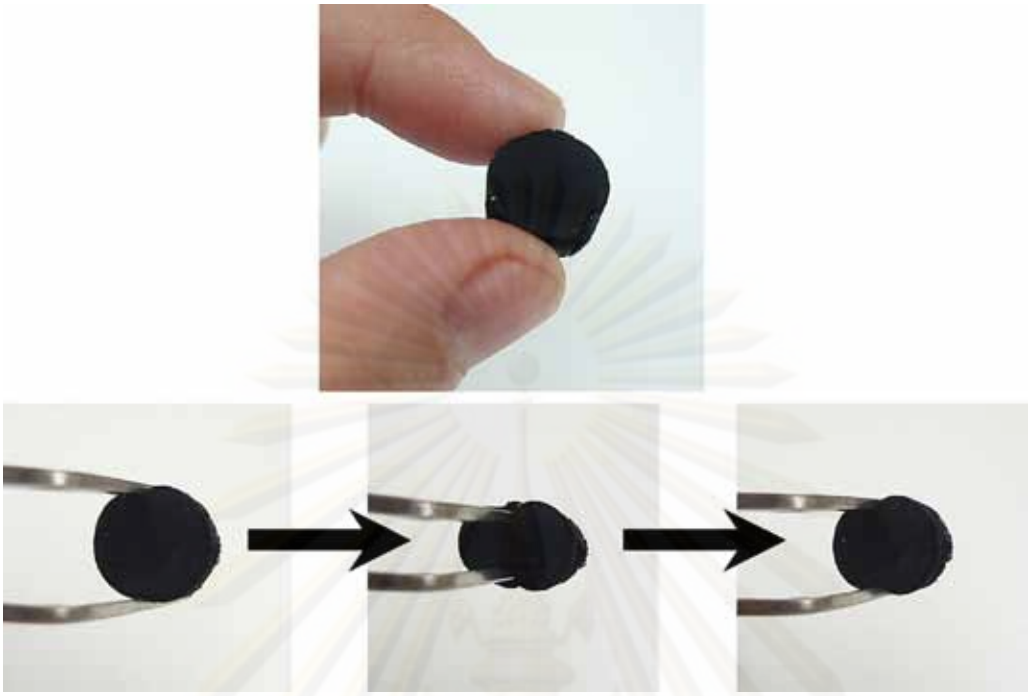

Fig. 4. Elastic feature of the obtained sample.

Table 1
Physical characteristics of freeze-dried samples

Formulation	Cooling rate (K min^{-1})	Bulk density (g cm^{-3})	Porosity (%)	Average pore diameter (μm)
100 mg MWCNTs, 1.0 wt.% CMC sodium salt	−0.5	0.06	97.0	73
100 mg MWCNTs, 1.0 wt.% CMC sodium salt	−3.0	0.05	97.6	71
100 mg MWCNTs, 2.0 wt.% CMC sodium salt	−0.5	0.05	97.1	61
100 mg MWCNTs, 2.0 wt.% CMC sodium salt	−3.0	0.05	97.4	52
150 mg MWCNTs, 1.0 wt.% CMC sodium salt	−0.5	0.05	97.7	74
150 mg MWCNTs, 1.0 wt.% CMC sodium salt	−3.0	0.05	97.4	49

Remark: Apparent density of MWCNTs in this study is 2.5 g cm^{-3}.

2.4. Electric resistivity test

Electric resistivity of the solid foam made of MWCNTs was determined via the four-probe method under controlled pressure. The four probes (each 0.5 mm in diameter, 4.0 mm in length, 1.5 mm apart) were vertically inserted into the sample to be measured. The sample with the inserted probes was put in a vacuum chamber (same as the freeze-dryer in Fig. 2). The pressure in the chamber and the electric resistivity were monitored using a digital multimeter (Keithley 2700, U.S.). The measurements were carried out under ambient temperature, about 20 °C.

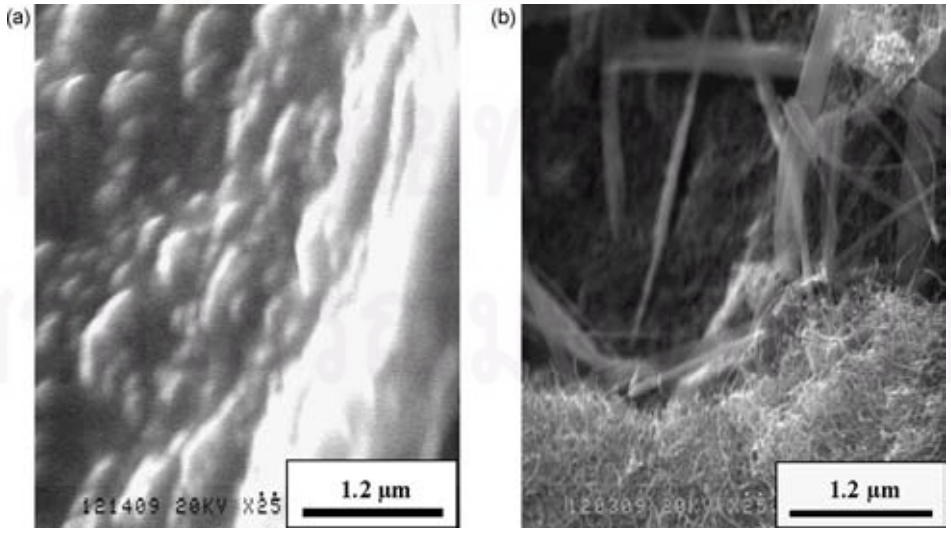

Fig. 5. SEM images of prepared solid foam surfaces: (a) freeze-dried sample and (b) calcined sample.

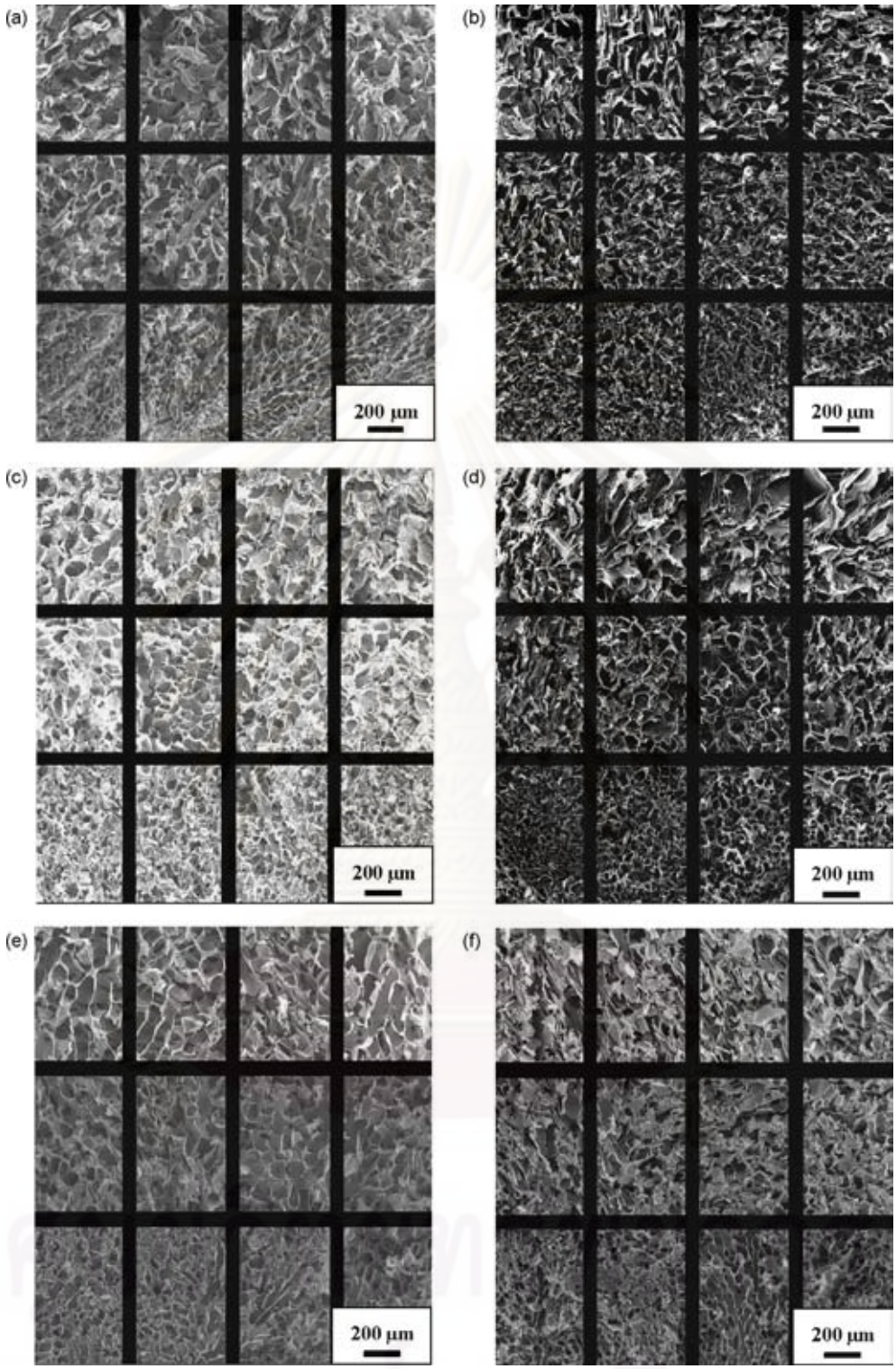

Fig. 6. SEM images of freeze-dried samples obtained under different experimental conditions: (a) 100 mg of MWCNTs in 1.0 wt.% surfactant with cooling rate of −0.5 K min^{-1}, (b) 100 mg of MWCNTs in 2.0 wt.% surfactant with cooling rate of −0.5 K min^{-1}, (c) 100 mg of MWCNTs in 1.0 wt.% surfactant with cooling rate of −3.0 K min^{-1}, (d) 100 mg of MWCNTs in 2.0 wt.% surfactant with cooling rate of −3.0 K min^{-1}, (e) 150 mg of MWCNTs in 1.0 wt.% surfactant with cooling rate of −0.5 K min^{-1} and (f) 150 mg of MWCNTs in 1.0 wt.% surfactant with cooling rate of −3.0 K min^{-1}.

3. Results and discussion

3.1. Solid foam from MWCNTs by freeze-drying technique

The elastic feature of a typical bulk sample was displayed in Fig. 4. The prepared samples in our work exhibited sponge-like nature because of their elasticity and can repeatedly recover their original shapes after being squeezed. Table 1 summarizes the physical characteristics of the freeze-dried samples made with different formulations. It indicates that our preparation method can provide highly porous materials with porosity of about 97% and bulk density of 0.05–0.06 g cm^{-3}.

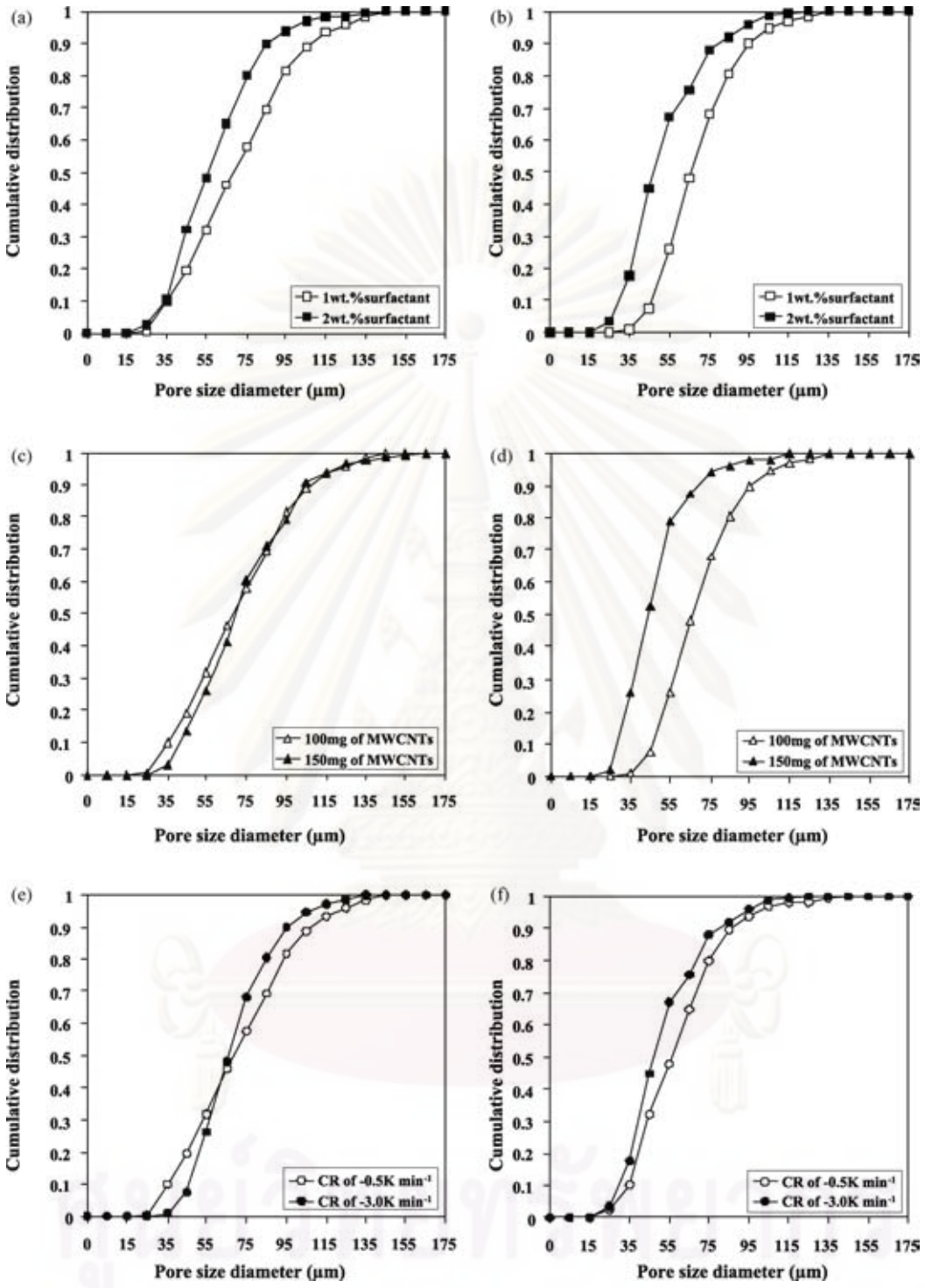

Fig. 7. Cumulative distribution of pore size for freeze-dried samples obtained under different experimental conditions: (a) 100 mg of MWCNTs with cooling rate of −0.5 K min^{-1}, (b) 100 mg of MWCNTs with cooling rate of −3.0 K min^{-1}, (c) 1.0 wt.% surfactant with cooling rate of −0.5 K min^{-1}, (d) 2.0 wt.% surfactant with cooling rate of −3.0 K min^{-1}, (e) 100 mg of MWCNTs in 1.0 wt.% surfactant and (f) 100 mg of MWCNTs in 2.0 wt.% surfactant.

Fig. 5a shows a micrograph of the inner wall surface of a pore in a prepared solid foam specimen. It can be seen that MWCNTs were mainly embedded inside the CMC sodium salt. The freeze-dried sample was next calcined in N_2 flow at 500 °C to remove the residual salt on the pore walls, thereby revealing the inside of these walls. We thus confirmed that the calcined sample still kept its structure after the CMC sodium salt surfactant was removed. One can recognize the MWCNTs on the pore walls of the calcined solid foam as shown in Fig. 5b. It can be concluded that CMC sodium salt surfactant was a key chemical for constructing the porous network and incorporating the MWCNTs into the foam walls. As a result, a calcined sample could maintain its structure though it lost the elastic nature of the original freeze-dried state.

As expected, the samples prepared with low surfactant concentration (0.5 wt.%) and low MWCNT content (50 mg) were rather weak in strength. In fact, the strength of a sample depended on

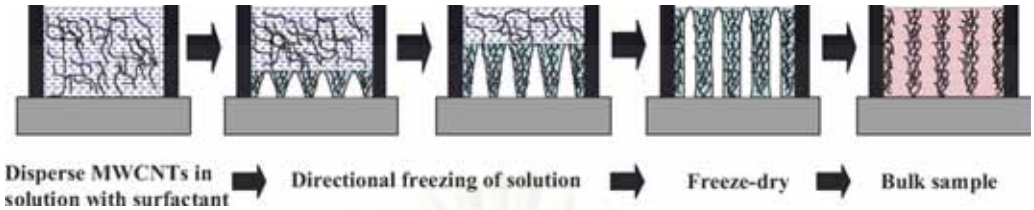

Fig. 8. Sketch of a mechanism for solid foam formation.

the concentration of the surfactant as well as the MWCNT content. Fig. 6 shows micrometer scale images of the freeze-dried bulk samples with different surfactant concentrations and MWCNT contents, and Fig. 7 shows cumulative pore size distributions of the corresponding samples. One can see from Fig. 6a vs. 6b (or Fig. 6c vs. 6d) that a higher surfactant concentration led to a smaller macroporous structure in the bulk matrix. In fact this trend is much clearer when the samples were prepared at a faster cooling rate ($-3.0\,K\,min^{-1}$) (Fig. 7a vs. 7b). Similarly, when the samples were prepared at a higher MWCNT content, smaller pores appeared in the samples (Fig. 6b vs. 6f). This trend became clearer when the samples were prepared at the faster cooling rate ($-3.0\,K\,min^{-1}$), though it cannot be discerned when the samples were prepared at a slow cooling rate ($-0.5\,K\,min^{-1}$).

Fig. 8 illustrates the mechanism that shows how a pore system is prepared on a typical solid foam made of CNTs. At first, ice nuclei initiate freezing in the supercooled solution, and the resulting ice crystals gradually grow up from the bottom to the top of the sample. During the freezing process, the CMC sodium salt surfactant (attached to the MWCNTs) is pushed into the interdendritic spaces by ice dendrites, and consequently, the CMC sodium salt with its embedded MWCNTs is assembled onto the ice crystal surface. After the bulk matrix is completely solidified, the sample is lyophilized to remove the ice crystals from the bulk sample. Finally, a typical macroporous solid foam is obtained.

Deville et al. reported that the initial formulation influenced the ice crystal size because the volume of water directly affects ice crystal growth [12]. It is likely that the ice crystal growth was limited by the volume of water. At a low volume of water, there is lower probability to combine the ice dendrites. This is why a smaller ice crystal size was obtained with a higher surfactant concentration or MWCNT content. Since the pore structures are associated with the ice crystals in a frozen sample, it is reasonable to expect that the design of macropore structures can be realized by the control of ice crystals growth, that is, the freezing condition. We will discuss the influence of the freezing condition on the pore structure of the prepared solid foam in the next section.

3.2. Influence of freezing condition on macro-porosity

It was reported that a nucleation temperature during freezing process influences on ice crystal morphologies [7,8]. Ice crystal morphologies are controlled by the ice crystal growth rate and temperature distribution in a system. As a result, the nucleation temperature and cooling rate are major controlling factors [14]. However, the nucleation process in supercooled solution is known as a random phenomenon due to the spontaneous nature of nucleation. Therefore, a device to artificially break down supercooling should be employed if we want to control the nucleation phenomena. As a matter of fact, the nucleation temperatures of our systems were approximately close to each other, and they varied between -5 and $-8\,^{\circ}C$. It is reasonable to consider that the uniformly dispersed MWCNTs could play a role of the nuclei for initiating ice crystal nucleation. As a result, the system nucleated at essentially the same subcooled temperatures. So, in this work, the morphologies of the samples should mainly be controlled by the cooling rate.

Fig. 9 shows typical examples of the temperature profiles of the solutions during freeze-drying. The average ice crystal growth rate was calculated from the temperature profile of each experimental condition, and summarized in Table 2. As expected, the ice crystal growth rate was higher at a faster cooling rate. Morphological differences of the bulk samples due to different cooling rates can be observed upon comparing Fig. 6a–c (and Fig. 6b–d). It is confirmed that the cooling rate (ice crystal growth rates) clearly affects the ice crystal size (in turn the pore sizes). These images reveal that, though the shapes of the macroporous structures were quite similar, their macropore sizes in the bulk samples were different from each other as illustrated in Fig. 7e vs. 7f. The cumulative distributions indicate that the average macropore size was dependent on the cooling rate,

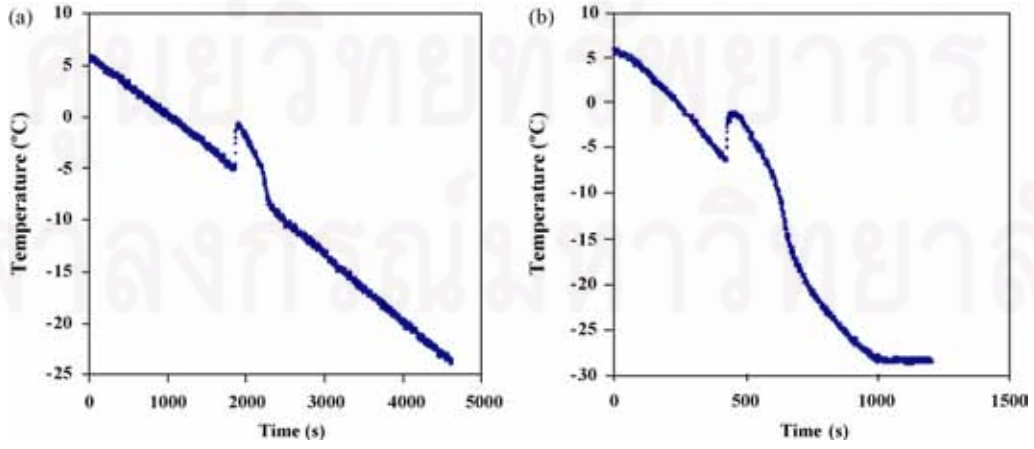

Fig. 9. Freezing curves of freeze-dried samples made of 100 mg of MWCNTs in 1.0 wt.% surfactant under different freezing condition: (a) cooling rate of $-0.5\,K\,min^{-1}$ and (b) cooling rate of $-3.0\,K\,min^{-1}$.

Table 2
Ice crystal growth rates during freezing step

Formulation	Cooling rate ($K\,min^{-1}$)	Ice crystal growth rate ($cm\,min^{-1}$)
100 mg MWCNTs, 1.0 wt.% CMC sodium salt	−0.5	0.08
100 mg MWCNTs, 1.0 wt.% CMC sodium salt	−3.0	0.14
100 mg MWCNTs, 2.0 wt.% CMC sodium salt	−0.5	0.10
100 mg MWCNTs, 2.0 wt.% CMC sodium salt	−3.0	0.12
150 mg MWCNTs, 1.0 wt.% CMC sodium salt	−0.5	0.09
150 mg MWCNTs, 1.0 wt.% CMC sodium salt	−3.0	0.13

that is, a faster cooling rate led to better homogeneity and a smaller macropore network in the bulk matrix of MWCNTs. In fact these results suggest that the macroporous system in a solid foam is simply controlled by the freezing condition (in case the formulation is fixed). In other words, porous structure design, i.e. the average size and shape of a bulk matrix could be achieved via a proper cooling program.

3.3. Electric resistivity of solid foam from MWCNTs

As described in the previous sections, we could produce solid foam from MWCNTs dispersed in a CMC sodium salt solution and could reasonably control its macropores by the freezing condition. In this section, we will discuss about another specific character of the prepared solid foam—its electric conductivity. It is known that the CNT is a superb material to adsorb gas molecules [15]. Romanenko et al. reported that the change in electric conductivity of CNTs was connected to the process of gas adsorption–desorption on the nanotube surface [16]. Electron transfer was promoted when certain gas molecules were adsorbed on the CNT wall. In other words, the electric conductivity is dependent on the interaction between the adsorbed molecules and CNT wall. Conversely, it was reported that the electric resistance of the CNTs responded sensitively to the adsorption of various gases [17,18]. It can be deduced from these reports that our solid foam preparation would present a very fascinating technique if these characteristics remain in the bulk samples.

It is noteworthy that the bulk samples prepared in this work show electric resistivity in the range of $1–10\,k\Omega\,m^{-1}$. This fact is one of the evidences that these samples retain part of the MWCNT characteristics. As for potential application of the solid foams, the foams are expected to display characteristics of the original MWCNTs in combination with the characteristic as the bulk sample. Fig. 10 shows typical examples of the relationship between the electric resistivity of the solid foam and the chamber pressure. It is obvious that the resistivity responds rapidly to the rise and drop to the pressure. It is straightforward to attribute this change in electric resistivity to the adsorption and desorption of air on the foam walls composed of CNTs.

In fact that the absolute resistivity value decreased as the MWCNT content increased (Fig. 10a–c). Moreover, it is interesting that the specific value of resistivity difference, ΔR (corresponding to 0.1 MPa pressure difference) also showed a similar trend (Fig. 10a–c). It is reasonable to deduce from these results that the contacts between the CNTs in the bulk walls are influenced by the CNT concentration, and the difference in the contacts appeared as a difference in the electric resistance of the bulk sample. It should be noted that this characteristic of the electric conductivity is determined by the preparation condition of the solid foam. For example, if we want to employ the solid foam as a pressure sensing material, we can control its sensitivity by selecting a proper preparation condition, which in turn influences the degree of homogeneity and macropore size of the bulk network.

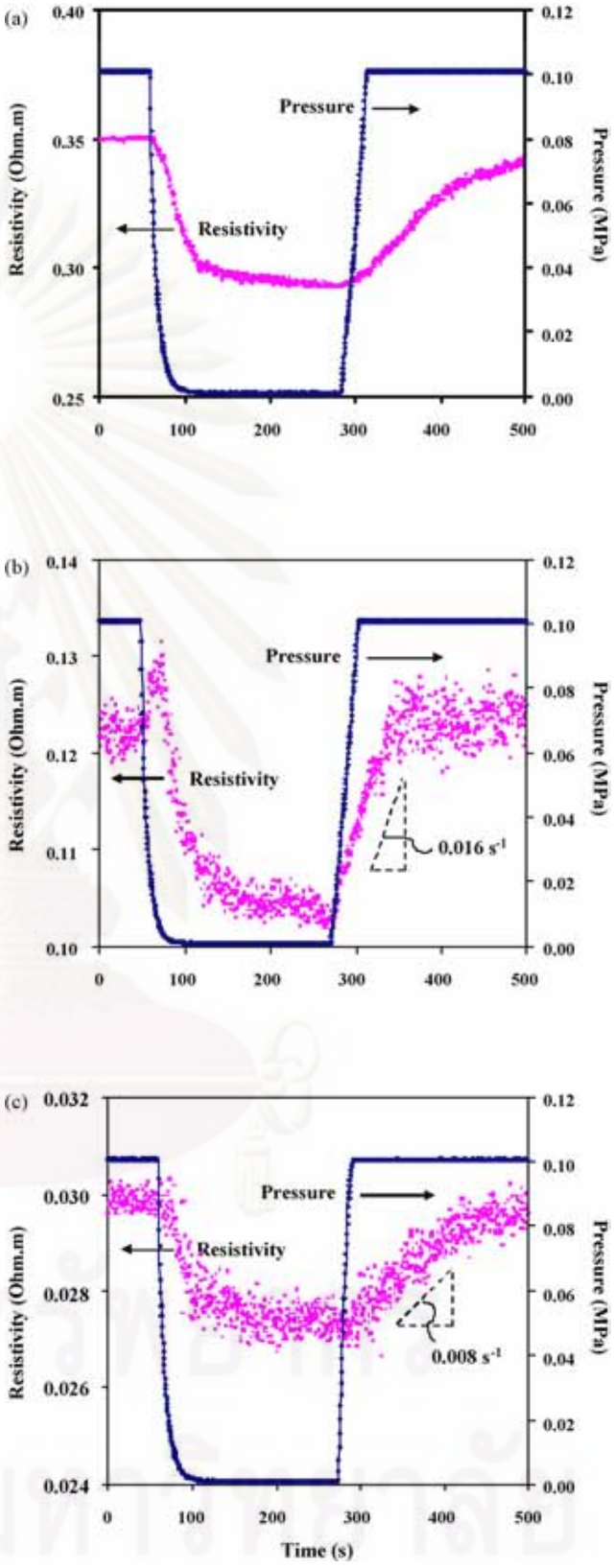

Fig. 10. Relationship between electric resistivity and ambient pressure of freeze-dried samples in 1.0 wt.% surfactant under different experimental conditions: (a) 50 mg of MWCNTs with cooling rate of $-3.0\,K\,min^{-1}$, (b) 100 mg of MWCNTs with cooling rate of $-3.0\,K\,min^{-1}$ and (c) 150 mg of MWCNTs with cooling rate of $-3.0\,K\,min^{-1}$.

As discussed in a previous section, a sample prepared with a higher MWCNT content had smaller macropore sizes. The average macropore size of a sample made from 150 mg of MWCNTs (per 10 mL original solution) was 49 μm, whereas a sample made from 100 mg of MWCNTs had average macropore size of 71 μm. When we scrutinize the normalized uptake rate of resistivity ($1/\Delta R(dR/dt)[s^{-1}]$) during pressure drop and rise with time (Fig. 10b and c), we find that the sample containing a lower amount of MWCNTs shows two times a higher normalized uptake rate. It is considered that gas molecules were more rapidly transported, adsorbed and desorbed within larger macropores. In short, we can say that the properly designed macroporous solid foam containing MWCNTs shows high potential for use as pressure sensor, gas detector and so on.

4. Conclusion

Macroporous solid foams, made of MWCNTs, having a high porosity of 97% were prepared using a freeze-drying technique with the aid of CMC sodium salt surfactant. The following conclusions were obtained.

It was confirmed that the CMC sodium salt surfactant assembled the porous networks in the bulk sample and incorporated MWCNTs on the foam walls. The average macropore size of the solid foam was affected by the concentration of CMC sodium salt surfactant, the MWCNT content, and the cooling rate during the freezing step. The higher surfactant concentration and content of MWCNTs led to smaller macropores. It was found that this relationship was governed by the ice crystal growth rate during freezing. As for the influence of the freezing condition, a faster cooling rate led to a higher degree of homogeneity and a smaller macropore network in the bulk matrix of the MWCNTs. Moreover, we found that the prepared solid foams have high potential as gas sensing materials. The electric resistivity of a bulk sample responded rapidly and sensitively to a change in the ambient pressure. This characteristic was dependent on the preparation conditions.

Acknowledgements

Bayer Material Science Ltd., Germany, provided the MWCNT samples. N.T. acknowledges TGIST (Thailand Graduate Institute of Science and Technology) of NSTDA (National Science and Technology Development Agency) and HUMAP (Hyogo University Mobility in Asia and the Pacific) of University of Hyogo for financial support. Partial support from the Centennial Fund of Chulalongkorn University for researcher exchange is also acknowledged.

References

[1] A.I. Romanenko, O.B. Anikeeva, V.L. Kuznetsov, T.I. Buryakov, E.N. Tkachev, A.N. Usoltseva, Sens. Actuator A 138 (2007) 350.
[2] P. Serp, M. Corrias, P. Kalck, Appl. Catal. A: Gen. 253 (2003) 337.
[3] M. Paradise, T. Goswami, Mater. Des. 28 (2007) 1477.
[4] M. Nabeta, M. Sano, Langmuir 21 (2005) 1706.
[5] C.M. Leroy, F. Carn, R. Backov, M. Trinquecoste, P. Delhaes, Carbon 45 (2007) 2307.
[6] A. Abarrategi, M.C. Gutierrez, C. Moreno-Vicente, M.J. Hortiguela, V. Ramos, J.L. Lopez-Lacomba, M.L. Ferrer, F. Monte, Biomaterials 29 (2008) 94.
[7] K. Nakagawa, A. Hottot, S. Vessot, J. Andrieu, Chem. Eng. Process. 45 (2006) 783.
[8] A. Hottot, S. Vessot, J. Andrieu, Chem. Eng. Process. 46 (2007) 666.
[9] W. Abdelwahed, G. Degobert, H. Fessi, Int. J. Pharm. 324 (2006) 74.
[10] S.R. Mukai, H. Nishihara, T. Yoshida, K. Taniguchi, H. Tamon, Carbon 43 (2005) 1563.
[11] S.R. Mukai, H. Nishihara, H. Tamon, Chem. Commun. 7 (2004) 874.
[12] S. Deville, E. Saiz, A.P. Tomsia, Acta Mater. 55 (2007) 1965.
[13] T.A. Jennings, Lyophilization: Introduction and Basic Principles, Interpharm Press Inc., US, 1999, pp. 262–280.
[14] K. Nakagawa, AIChE J. 53 (2007) 1362.
[15] G. Sun, S. Liu, K. Hua, X. Lv, L. Huang, Y. Wang, Electrochem. Commun. 9 (2007) 2436.
[16] J. Suehiro, N. Sano, G. Zhou, H. Imakiire, K. Imasaka, M. Hara, J. Electrostat. 64 (2006) 408.
[17] J. Suehiro, G. Zhou, M. Hara, J. Phys. D: Appl. Phys. 36 (2003) L109.
[18] N.H. Quang, M.V. Trinh, B.-H. Lee, J.-S. Huh, Sens. Actuator B 113 (2006) 341.

16th International Drying Symposium (IDS 2008)
Hyderabad, India 9-12 November 2008

APPLICATION OF FREEZE-DRYING TECHNIQUE TO PREPARATION OF NANO-MATERIAL DERIVED MACRO-POROUS BULK

Kyuya Nakagawa[*1], Napawon Thongprachan[2], Noriaki Sano[3], Tawatchai Charinpanitkul[2] and Wiwut Tanthapanichakoon[4]

[1]Department of Mechanical and System Engineering, University of Hyogo, 2167 Shosha, Himeji, Hyogo 671-2201, Japan
[2]Center of Excellence in Particle Technology, Faculty of Engineering, Chulalongkorn University, Phayathai Pathumwan, Bangkok, Thailand
[1]Department of Chemical Engineering, Kyoto University, Katsura, Kyoto 615-8510, Japan
[4]National Nanotechnology Center, National Science and Technology Development Agency, Thailand Science Park, Patumtani, Thailand

**Tel.:+81 (0)79 267 4849, E-mail: nakagawa@eng.u-hyogo.ac.jp*

Abstract: Macro-porous bulk matrix was prepared from multi-walled carbon nanotubes (MWCNTs) using conventional freeze-drying technique with the aid of carboxymethyl cellulose (CMC) sodium salt surfactant. Prepared bulk material had a sponge like structure with a porosity of 97 %. It was confirmed that the CMC sodium salt surfactant assembled the porous networks in the bulk sample and incorporated MWCNTs on the foam walls. The average macropore size of the solid foam was affected by the concentration of CMC sodium salt surfactant, the MWCNT content, and the cooling rate during the freezing step. The relationship between pore structures and preparation conditions was confirmed to be governed by the ice crystal growth rate during freezing. It was found that prepared bulk showed unique drying kinetics due to the structural formation of the matrix.

Keywords: freeze-drying, carbon nanotube, ice crystal structure, macropore

INTRODUCTION

Nano-materials attract great interests in various scientific fields due to the specific characters of nano-materials themselves that cannot be seen on their bulk matrixes. For example, carbon nanotube (CNT) has gained world wide attention because of their catalytic activities due to the combination of their electronic, adsorptive, mechanical and thermal properties, see Serp et al. (2003), Paradise et al. (2007) and Romanenko et al. (2007). However, being nano-scale in sizes, CNTs are frequently unsuitable and even unsafe to employ in engineering and daily-life applications. In order to solve these handling difficulties, several researchers are interested to prepare functional bulk material from CNTs, indeed, there are a few reports on the preparation of bulk matrix made of nanomaterials. Nabeta et al. (2005) prepared sponge-like bulk materials from CNTs. They prepared them by freeze-drying acidified CNTs dispersed in gelatin solution. In their samples, porous structures were derived from the self-networking nature of gelatin and appeared after freeze-drying. Leroy et al. (2007) also employed the freeze-drying technique to produce solid foams from CNTs, wherein the porous structure was obtained by bubbling during the freezing step. Abarrategi et al. (2008) developed CNTs derived scaffolds by freeze-drying chitosan containing dispersed CNTs and showed the applicability of the prepared bulk sample to tissue engineering. These reports have clearly shown evidences that macroporous bulk foams can be produced from CNTs, which were supported by an agent that helps to disperse the CNTs in a starting solution and keeps its bulk structure after freeze-drying. In our point view, it is a great challenge to develop a technique that allows the preparation of controlled pore systems in a bulk sample while simultaneously displaying characteristics of the original CNTs in the resulting bulk matrix. Thongprachan et al. (2008) proposed a method to prepare macroporous solid foams by a conventional freeze-drying technique. Firstly, solution with dispersed nano-materials (multi-walled carbon nano-tube) was prepared, and then, it was frozen under a proper condition. After the sample was completely solidified at low temperature, it was freeze-dried under vacuume condition. As a consequence, we

could obtain macro-porous sponge like bulk samples. A principle of this method is that ice crystals have a role of templates during the freezing step, thus, they make macropores after the sublimation step. The freezing protocol and initial formulation are key parameters to control the porous structure because they directly influenced the ice crystal sizes, as reported by Mukai et al. 2004 and Deville et al. 2007. This paper discuss the influences of the freezing condition and initial formulation on the macroporous structures of the prepared solid foams. Drying kinetics during sublimation steps were also examined to consider a structural insight of the obtained dried samples.

MATERIALS AND METHOD

Materials

Commercial multi-walled carbon nano-tube (MWCNT) (Bayer Materials Science Ltd., 13-16 nm in mean outer diameter, 1 to 10 μm in length, purity over 95%, synthesized by chemical vapour decomposition) was used in this work. Carboxy methyl cellulose (CMC) sodium salt surfactant (Fluka, Sweden) was used as a dispersing agent.

Method

Fixed amount of MWCNTs (50, 100, 150 mg) was dispersed in 10 mL of 0.5, 1 or 2 wt.% of surfactant solution by applying the 15 watts of ultrasound (UH-300, SMT company, Japan) for 30 minutes. Then the prepared solution was put into sample holder (8.0 mm in diameter and 5.0 mm in length) equipped with cooling device (Fig. 1). Cooling fluid was circulated through the heat exchanger continuously for controlling the temperature of sample. The temperatures were monitored using type K thermocouples connected to a digital multimeter (Keithley 2700, U.S.). The thermocouples were buried in the exterior wall of the sample holder in order to prevent the thermocouples from becoming nucleation points during the freezing step (Fig. 1).

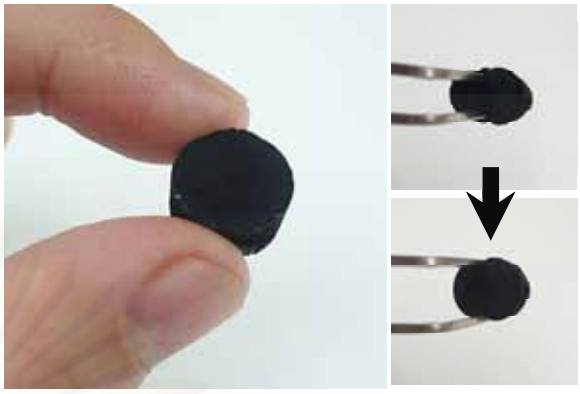

Fig. 2. Prepared sample bulk

The equipment of cooling system was set up in a vacuum chamber. Prepared solutions were frozen from 5 °C to -40 °C at a constant cooling rate (-0.5, -3.0 K/min), and finally the frozen samples were sublimated at -20 °C, 10-25 Pa. In this study, heat transfer and phase transitions were occurred from the bottom to top of samples because of the setting manner of the heat exchanger. Prepared samples were listed in Table 1.

Table 1 Preparation conditions

Sample	CNT [mg/10ml-sol]	CMC [wt%]	Cooling Rate [°C/min]
F101	100	1	-3.0
S101	100	1	-0.5
F102	100	2	-3.0
S102	100	2	-0.5
F151	150	1	-3.0
S151	150	1	-0.5

Analysis

The morphology of the freeze-dried samples was observed with a SEM (S-2400, Hitachi, Japan). The

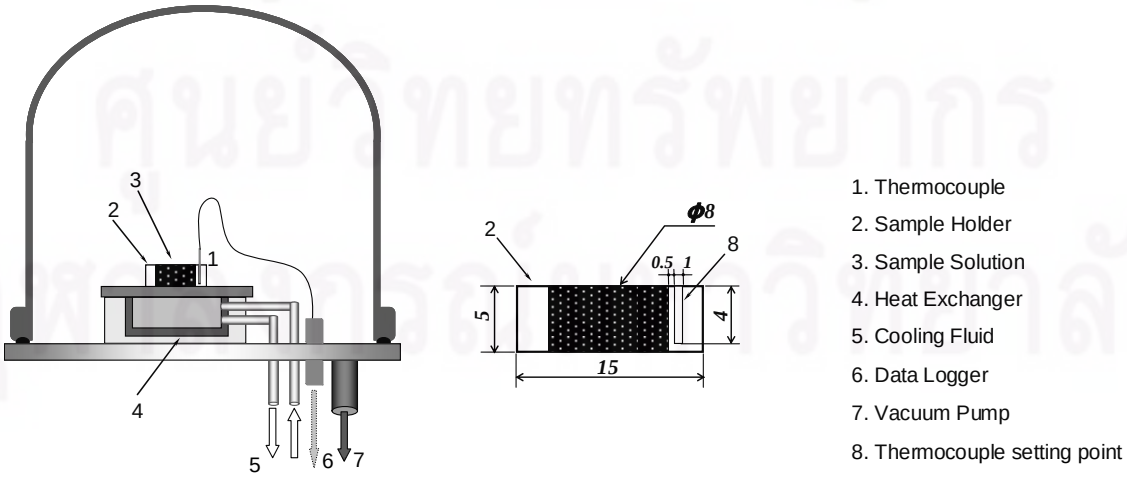

Fig. 1. Experimental Scheme

obtained samples were vertically cut in halves in order to observe a cross section that corresponds to the direction of freezing. To characterize the porous networks in the bulk samples, SEM images were taken at the several positions (top, middle, bottom) to represent the pore structure in bulk samples. The macropore size distributions of the samples were determined by image analysis (ImageJ 1.38v software). About 200 pore samples in each image were counted in the analysis.

RESULTS AND DISCUSSION

Prepared Bulk Sample

One can see the elastic feature of a typical bulk sample in Fig. 2. The prepared samples in our work exhibited sponge-like nature because of their elasticity and can repeatedly recover their original shapes after being squeezed. It was confirmed that the present bulk samples were provided with porosity of about 97 % and bulk density of 0.05 to 0.06 g/cm^3. Mean macropore sizes of the freeze-dried samples made with different formulations and conditions were listed in Table 2.

Fig. 3 shows SEM images of the inner wall surface of a pore in a prepared solid foam specimen. It can be seen that CNTs were mainly embedded inside the CMC sodium salt. The freeze-dried sample was next calcined in N_2 flow at 500 °C to remove the residual salt on the pore walls, thereby revealing the inside of these walls. We thus confirmed that the calcined sample still kept its structure after the CMC sodium salt surfactant was removed. One can recognize the CNTs on the pore walls of the calcined solid foam as shown in Fig. 3B. It can be concluded that CMC sodium salt surfactant was a key chemical for constructing the porous network and incorporating the CNTs into the foam walls. As a result, a calcined sample could maintain its structure though it lost the elastic nature of the original freeze-dried state.

Table 2. Ice crystal growth rate and mean pore size

	Ice crystal growth rate	Mean pore sizes
F101	0.14 (cm/min)	71 (μm)
S101	0.08	73
F102	0.12	52
S102	0.10	61
F151	0.13	49
S151	0.09	74

Porous Properties of Prepared Bulk

It was reported that a nucleation temperature during freezing process influences on ice crystal morphologies, Nakagawa et al. (2006) and Hottot et al. (2007). Ice crystal morphologies are controlled by the ice crystal growth rate and temperature distribution in a system. As a result, the nucleation temperature and cooling rate are major controlling factors, Nakagawa et al. (2007). However, the nucleation process in supercooled solution is known as a random phenomenon due to the spontaneous nature of nucleation. Therefore, a device to artificially break down supercooling should be employed if we want to control the nucleation phenomena. As a matter of fact, the nucleation temperatures of our systems were approximately close to each other, and they varied between -5 to -8 °C. It is reasonable to consider that the uniformly dispersed CNTs could play a role of the nuclei for initiating ice crystal nucleation. As a result, the system nucleated at essentially the same subcooled temperatures. So, in this work, the morphologies of the samples should mainly be controlled by the cooling rate.

The average ice crystal growth rate was calculated from the temperature profile of each experimental condition, and summarized in Table 2. As expected, the ice crystal growth rate was higher at a faster cooling rate. Morphological differences of the bulk

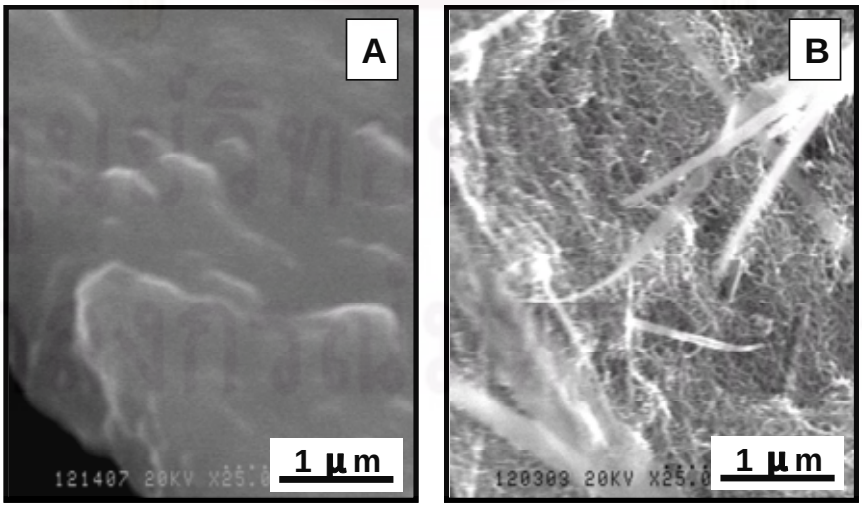

Fig. 3. SEM images of sample wall surface; (A) freeze-dried sample wall, (B) heat-treated sample wall.

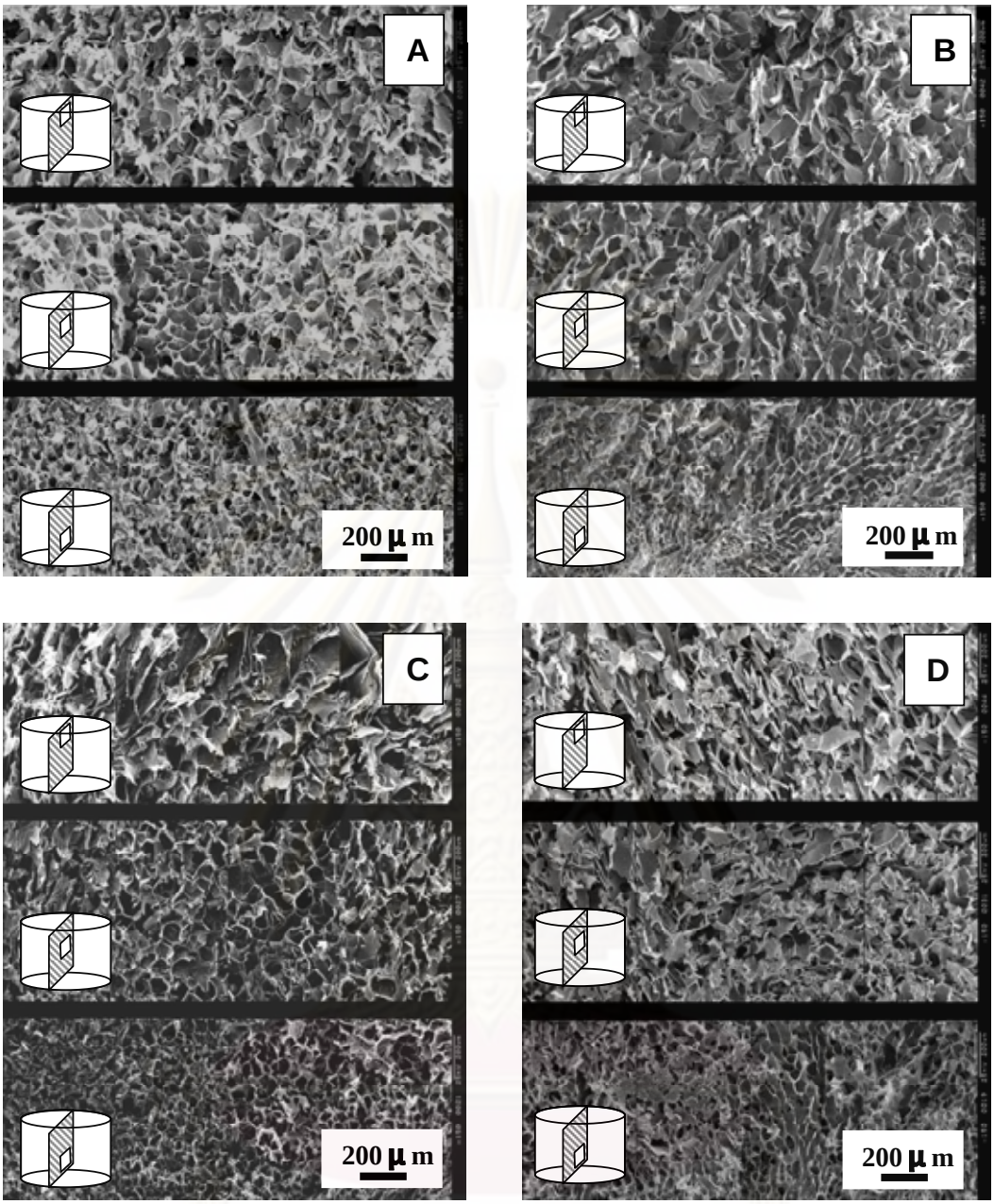

Fig. 4. Macroporous structures of prepared bulk; (A) F101, (B) S101, (C) F102, (D) F151.

samples due to different cooling rates can be observed upon comparing Fig. 4. It is confirmed that the cooling rate (ice crystal growth rates) clearly affects the ice crystal size (in turn the pore sizes). These images reveal that, though the shapes of the macroporous structures were quite similar, their macropore sizes in the bulk samples were different from each other. Fig. 5 indicate that the macropore size istribution was dependent on the cooling rate, that is, a faster cooling rate led to better homogeneity and a smaller macropore network in the bulk matrix of MWCNTs. In fact these results suggest that the macroporous system in a solid foam is simply controlled by the freezing condition (in case the formulation is fixed). In other words, porous structure design, i.e. the average size and shape of a bulk matrix could be achieved via a selected cooling program.

However, it is not only the freezing conditions that impact on those pore structures. We cannot ignore the influence of the components of initial formulation, that is, CNT and CMC concentration. Deville et al. (2007) reported that the initial formulation influenced the ice crystal size because the volume of water directly affects ice crystal growth. It is likely that the ice crystal growth was limited by the volume of water. At a low volume of water, there is lower probability to combine the ice dendrites. This is why a smaller ice crystal size was obtained with a higher

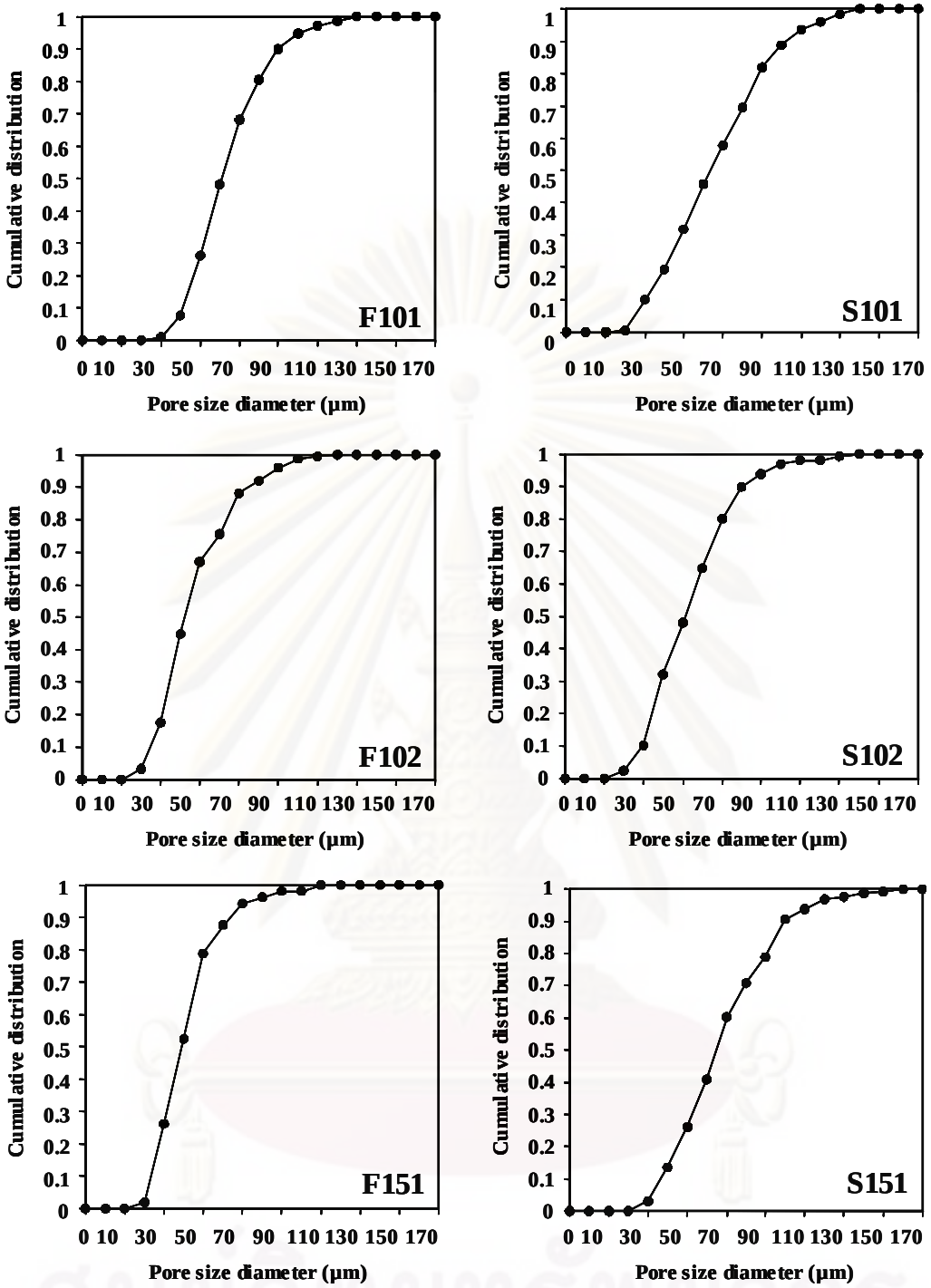

Fig. 5. Macropore size distributions.

surfactant concentration or MWCNT content. It is confirmed from Fig. 5 and Table 2 that the higher surfactant concentration and content of MWCNTs led to smaller macropores, however, this relationship was confirmed to be governed by the ice crystal growth rate during freezing. It is reasonable to expect that the design of macropore structures can be realized by the control of the freezing condition under the consideration of the amount of compositions.

Sublimation Procedure of Solid Foam

As described in the previous sections, a sponge like solid foam was prepared in this work by freeze-drying process. MWCNTs were associated with CMC sodium salts to form macroporous structures in their bulk matrix. Considering that CNT is a porous material itself, it is expected that the solid foam would not be dried in a simple manner. Fig. 6 illustrates drying kinetics during primary drying step of the freeze-drying, sublimated at -20°C, 25Pa. One

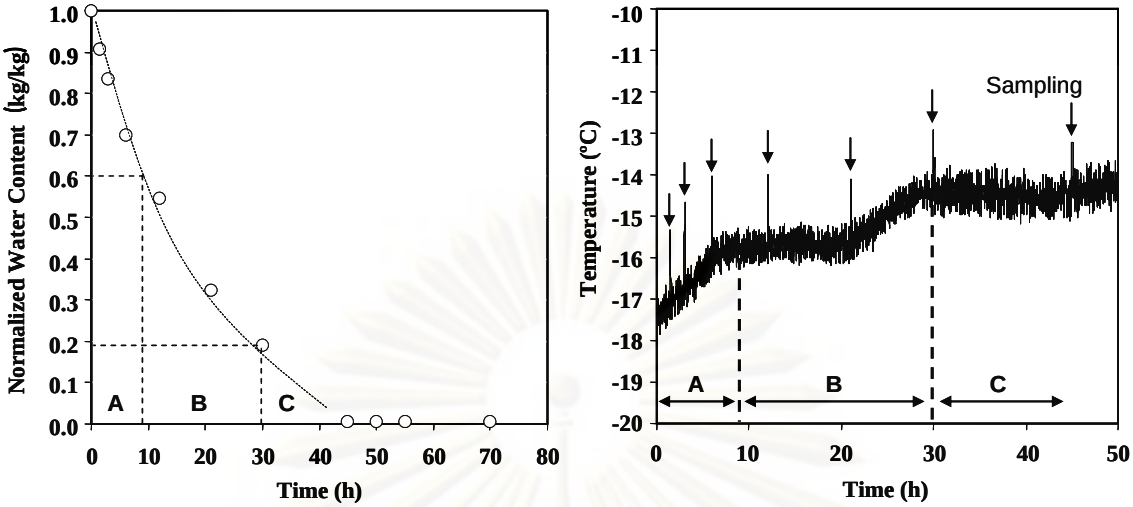

Fig. 6. Drying kinetics during sublimation step (sample S101).

can see that the primary drying duration seems quite long as a material with mean pore size ca 70 μm. It is interesting that the temperature profile during the primary drying shows two shoulders, e.g. at the point around 9 hr and 30 hr. It is suggested from this profile that, in the present solid foam, the sublimations progressed in separated two steps, that is, sublimation of macro-ice-crystals and sublimation of nano-ice-crystals. Fig. 7 shows the schematic sketch of the mechanism during the freezing and the primary drying. Firstly, ice nuclei initiate freezing in the supercooled CNTs dispersed solution, and the resulting ice crystals gradually grow up from the bottom to the top of the sample. During the freezing process, the CMC sodium salt surfactant (attached to the CNTs) is pushed into the interdendritic spaces by ice dendrites, and consequently, the CMC with its embedded CNTs is assembled onto the ice crystal surface. After the bulk matrix is completely solidified, the sample is freeze-dried to remove the ice crystals from the frozen bulk sample. At the first step of primary drying (duration A in Fig. 6), the ice crystals that correspond to macropores (macro-ice-crystals) are preferentially sublimated. Subsequently, ice crystals embedded together with CNTs (nano-ice-crystals) are sublimated (duration B). The difference of the sublimation rates from the macro-ice-crystals and nano-ice-crystals results to arise the unique temperature profile like in Fig. 6. After adsorbed waters were desorbed from bulk matrix (duration C), we can finally obtain a dried bulk material.

It is expected that the knowledge obtained in this work would be a strong support for future development of nano-material utilization technologies.

CONCLUSIONS

In this work, a macroporous solid foams, made of multi-walled carbon nanotubes, having a high porosity of 97 % were prepared using a freeze-drying technique with the aid of carboxymethyl cellulose sodium salt surfactant, and the following conclusions were obtained.

It was confirmed that the CMC sodium salt surfactant assembled the porous networks in the bulk sample and incorporated MWCNTs on the foam walls. The average macropore size of the solid foam was affected by the concentration of CMC sodium salt surfactant, the MWCNT content, and the cooling rate during the freezing step. The higher surfactant concentration and content of MWCNTs led to smaller macropores. It was found that this relationship was governed by the ice crystal growth rate during freezing. As for the influence of the freezing condition, a faster cooling rate led to a higher degree of homogeneity and a smaller macropore network in the bulk matrix of the CNTs. The drying kinetics of the prepared bulk was unique due to the structural formation as a solid foam.

REFERENCES

Abarrategi A.,M.C. Gutierrez, C. Moreno-Vicente, M.J. Hortiguela, V. Ramos, J.L. Lopez-Lacomba (2008), Multiwall carbon nanotube scaffolds for tissue engineering purposes, Biomaterials, Vol. 29, pp. 94-102.

Deville S., E. Saiz, A.P. Tomsia (2007), Ice-templated porous alumina structures, Acta Materialia, Vol.55, pp. 1965-1974.

Hottot A., S. Vessot, J. Andrieu (2007), Freeze drying of pharmaceuticals in vials: Influence of freezing protocol and sample configuration on ice morphology and freeze-dried cake texture, Chemical Engineering and Processing, Vol.46, pp. 666-674.

Leroy C.M., F. Carn, R. Backov, M. Trinquecoste, P. Delhaes (2007), Multiwalled-carbon-nanotube-

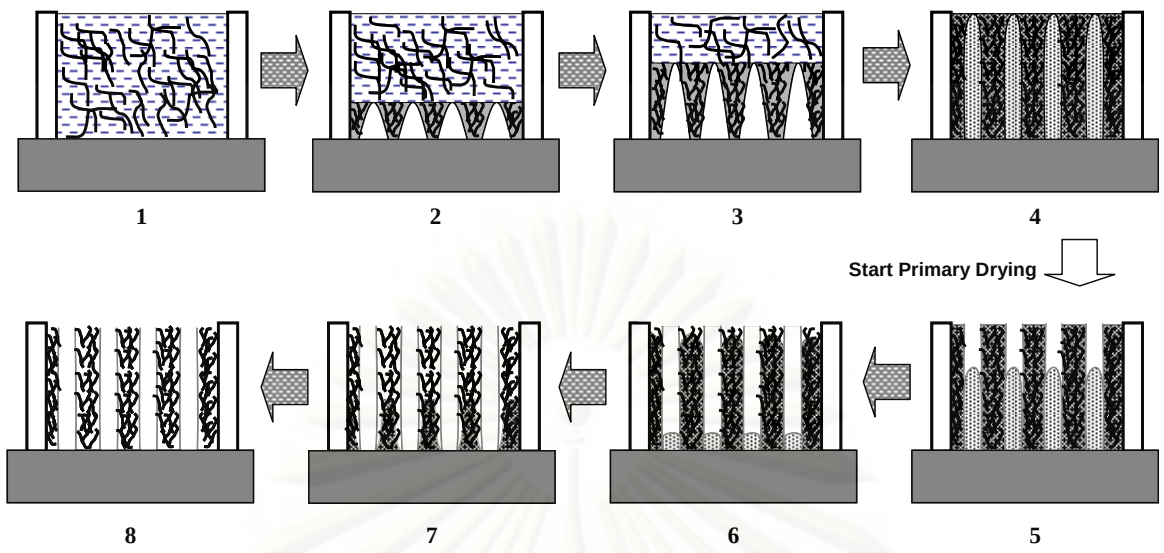

1: CNT dispersing solution
2, 3: Ice crystal nucleation and growth
4: Complete solidification
5: Sublimation of macro-ice-crystals
6: Sublimation of macro- and nano-ice-crystals
7: Sublimation of nano-ice-crystals
8: Complete sublimation

Fig. 7. Freezing and primary drying progress (sketch)

based carbon foams, Carbon, Vol. 45, pp2307-2320.

Mukai S.R., H. Nishihara, H. Tamon, Formation of monolithic silica gel microhoneycombs (SMHs) using pseudosteady state growth of microstructural ice crystals, Chemical Communication, pp. 874-876.

Nabeta M., M. Sano (2005), Nanotube Foam Prepared by Gelatin Gel as a template, Langmuir, Vol. 21, pp.1706-1708.

Nakagawa K., A. Hottot, S. Vessot, J. Andrieu (2006), Influence of controlled nucleation by ultrasounds on ice morphology of frozen formulations for pharmaceutical proteins freeze-drying, Chemical Engineering and Processing, Vol.45, pp. 783-791.

Nakagawa K., A. Hottot, S. Vessot, J. Andrieu (2007), Modeling of freezing step during freeze-drying of drug in vials, AIChE Journal, Vol.53, pp. 1362-1372.

Paradise M., T. Goswami (2007), Carbon nanotubes – Production and industrial applications, Materials & Design, Vol. 28, pp.1477-1489.

Romanenko A.I., OB Anikeeva, V.L. Kuznetsov, T.I. Buryakov, E.N. Tkachev, A.N.Usoltseva (2007), Influence of helium, hydrogen, oxygen, air and methane on conductivity of multiwalled carbon nanotubes, Sensors and Actuators A, Vol. 138, pp. 350-354.

Serp P., M. Corrias, P. Kalck (2003), Carbon nanotubes and nanofibers in catalysis, Applied Catalysis A: General, Vol. 253, pp.337-358.

Thongprachan N., K. Nakagawa, N. Sano, T. Charinpanitkul, W. Tanthapanichakoon (2008), Preparation of macroporous solid foam from muti-walled carbon nanotubes by freeze-drying technique, Materials Chemistry and Physics, *in press*.

NANO-MATERIAL DERIVED MACRO-POROUS SOLID FOAMS: Preparation Method and Applications

K. Nakagawa[*1], N. Thongprachan[2], T. Charinpanitkul[2] and W. Tanthapanichakoon[3]

[1]*Department of Mechanical and System Engineering, University of Hyogo, 2167 Shosha, Himeji, Hyogo 671-2201, Japan*

[2]*Center of Excellence in Particle Technology, Faculty of Engineering, Chulalongkorn University, Phayathai Pathumwan, Bangkok, Thailand*

[3]*National Nanotechnology Center, National Science and Technology Development Agency Thailand Science Park, Patumtani, Thailand*

** Corresponding to Kyuya Nakagawa; [*]Tel.:+81 (0)79 267 4849, E-mail: nakagawa@eng.u-hyogo.ac.jp*

Abstract

Nano-materials attract great interests in various scientific fields due to the specific characters of nano-materials themselves that cannot be seen on their bulk matrices. We can see a lot of evidences of functions of nano-materials in various scientific fields. However, being nano-scale in sizes, nano-materials are sometimes unsuitable and even unsafe to employ in engineering and daily-life applications. Thus, we suggest a methodology for preparing nano-materials derived bulk matrix by applying freeze-drying technique. Our challenge is the preparation of the bulk materials with the function of original nano-materials.

Firstly, a solution with dispersed nano-materials was prepared with an aid of dispersing agent (surfactant), and then, it was frozen under a selected condition. After the sample was solidified completely at temperature lower than the eutectic point of the cryo-concentrate, it was lyophilized under vacuum condition. Finally, we could obtain a dried macro-porous bulk sample, that is a solid foam. A principle of this method is that ice crystals have a role of templates during freezing step, consequently, they make macropores after the sublimation step. Thus, the porosity is mainly controlled by freezing protocol, and also by drying condition if there is large shrinkage. We have succeeded to apply this method to obtain macro-porous solid foam from several nano-materials (CNT, TiO_2 nano-particle etc.). It should be noted that these bulk samples prepared via present method have specific characters (e.g. electric conductivities, photo catalytic effect etc.), that they are derived from original nano-materials, thus, it is expected that the present methodology possibly accelerates nano-material applications. This lecture would like to present recent progress of the macro-porous solid foams preparation and the investigations of the solid foam functions.

Fig. 1 Prepared solid foams from CNT.

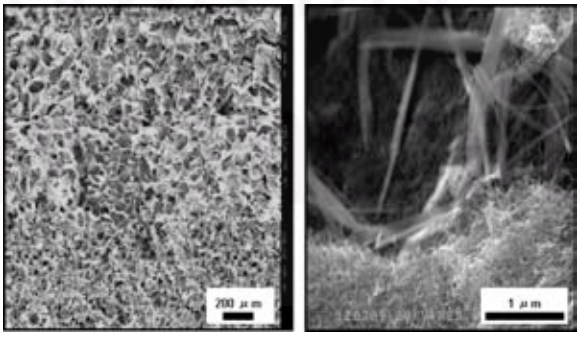

Fig. 2 SEM images of macroporous solid foam.

PREPARATION OF MACRO-POROUS SOLID FOAM FROM CNTs USING ICE-CRYSTAL TEMPLATES

Napawon Thongprachan[1], Kyuya Nakagawa[2,], Noriaki Sano[2], Mitsutaka Kitamura[2], Tawatchai Charinpanitkul[1] and Wiwut Tanthapanichakoon[3]*

[1]Center of Excellence in Particle Technology, Faculty of Engineering, Chulalongkorn University, Phayathai Rd., Pathumwan, Bangkok 10330, Thailand
[2]Department of Mechanical and System Engineering, University of Hyogo, 2167 Shosha, Himeji City, Hyogo 671-2201, Japan
[3]National Nanotechnology Center, National Science and Technology Development Agency, Paholyothin Rd., Klong Luang, Pathumthani 12120, Thailand

**Corresponding E-mail: nakagawa@eng.u-hyogo.ac.jp*

Abstract

Ice-crystal templates were effectively employed to produce macroporous solid foam from multi-walled carbon nanotubes (MWCNTs) via freeze-drying technique. Dispersed MWCNTs in carboxymethyl cellulose (CMC) sodium salt (surfactant) solution or chitosan solution were frozen at constant cooling rate, and lyophilized to obtain dry sample. It was found that the prepared solid foams were highly macroporous which porous networks in bulk matrix were constructed by dispersing agent (CMC sodium salt, chitosan) after freeze-drying. SEM observations of the bulk samples made from CMC sodium salt surfactant and chitosan solution revealed that they had well-organized macroporous structures, and pore morphology of both bulk matrices were quite similar with each other. It was found that the macropore sizes were controlled by initial formulation and freezing condition. The bulk samples produced at the higher surfactant and MWCNTs concentration condition had smaller macropores. Moreover, the bulk samples prepared at a faster cooling rate had homogeneous and smaller macropores. It is suggested that the proposed method for solid foam preparation is useful to produce controlled macropore structures on a bulk sample.

Introduction

Nowadays, it is well known that carbon nanotubes (CNTs) are very potential materials due to the combination of their electronic, adsorptive, mechanical and thermal properties (Romanenko et al., 2007; Serp et al., 2003). However, being nano-scale in sizes, CNTs are frequently unsuitable and even unsafe to employ in engineering and daily-life applications. In order to solve these handling difficulties, several researchers are interested to prepare functional bulk material from CNTs. Indeed, there are a few reports on the preparation of bulk matrix from CNTs. Nabeta et al. produced sponge-like bulk solid from CNTs by dispersing them in gelatin solution and freeze-drying (Nabeta et al., 2005). They reported that gel structure of gelatin helped to organize the porous structure in bulk matrix of the samples after freeze-drying. Leroy et al. prepared solid foams from CNTs by using sodium dodecyl sulfate (SDS) or carboxymethyl cellulose (CMC) sodium salt surfactants as dispersing agent (Leroy et al., 2007). The porous structure was controlled by bubbling during freeze-drying process. Abarrategi et al. produced CNTs derived scaffolds by freeze-drying dispersed CNTs in chitosan solution (Abarrategi et al., 2008). These reports have evidenced that macroporous bulk foams can be produced from CNTs. In our point view, it is a great challenge to develop a technique that allows the preparation of controlled pore systems in a bulk sample.

In this work, macroporous solid foams from multi-walled carbon nanotubes (MWCNTs) were prepared via freeze-drying technique supported by carboxymethyl cellulose (CMC) sodium salt surfactant and chitosan as dispersing agent. As reported by several researches, ice crystal is an effective template to design the structure of freeze-dried materials (Nakagawa et al., 2006; Hottot et al., 2007; Abdelwahed et al., 2006; Mukai et al., 2005; Mukai et al., 2004). Both freezing protocol and initial formulation would be key parameters to control the porous structure because they directly influenced the ice crystal sizes

(Deville et al., 2007; Jennings, 1999). Thus, in the present paper, the influences of initial formulation and freezing condition on the macropore structures of solid foams from MWCNTs were also presented.

Experimental

Materials

Commercial MWCNTs (Bayer Materials Science Ltd., 13-16 nm in mean outer diameter, 1 to >10 μm in length, purity > 95%, synthesized by chemical vapor decomposition) were used in this work. CMC sodium salt surfactant (Fluka, Sweden) and chitosan (TCI, Japan) were used as dispersing agent. Distillated water was used throughout this work.

Preparation of solid foam from MWCNTs

Fixed amount of MWCNTs (50, 100, 150 mg) was dispersed in 10 mL of 0.5, 1 or 2 wt.% of CMC sodium salt solution by applying the 15 watts of ultrasound (UH-300, SMT company, Japan) for 30 minutes. While, chitosan was also employed as dispersing agent, 100 mg of MWCNTs was dispersed in 15 mL of 1 wt.% of chitosan solution of acetic acid (0.05 M) by applying the 15 watts of ultrasound for 30 minutes, subsequently stirring for 1 hour.

Then the prepared solution was put into sample holder (8.0 mm in diameter and 5.0 mm in length) equipped with cooling device (**Figure 1**). Cooling fluid (methanol) was circulated through the heat exchanger continuously for controlling the temperature of sample. The temperatures were monitored using type K thermocouples connected to a digital multimeter (Keithley 2700, U.S.). The thermocouples were buried in the exterior wall of the sample holder in order to prevent the thermocouples from becoming nucleation points during the freezing step (**Figure 1**). The equipment of cooling system was set up in a vacuum chamber. Prepared solutions were frozen from 5 ^{o}C to -40 ^{o}C at a constant cooling rate (-0.5, -3.0 K min^{-1}), and finally the frozen samples were sublimated at -20 ^{o}C for 4 days. In this study, heat transfer and phase transitions were occurred from the bottom to the top of the samples because of the setting manner of heat exchanger and samples.

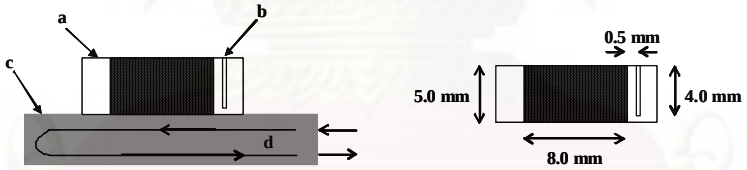

Figure 1. Cooling system: (a) samples holder, (b) holes for thermocouples, (c) heat exchanger and (d) cooling fluid.

Analysis

The morphology of the freeze-dried samples was observed with a SEM (S-2400, Hitachi, Japan). The obtained samples were vertically cut in halves in order to observe a cross section that corresponds to the direction of freezing. To characterize the porous networks in the bulk samples, SEM images were taken at the several positions (top, middle, bottom) to represent the pore structure in bulk samples. The macropore size distributions of the samples were determined by image analysis (ImageJ 1.38v software). About 200 pore samples in each image were counted in the analysis.

Results and discussion

Solid foam from MWCNTs by ice crystal templates

The elastic feature of obtained bulk sample was displayed in **Figure 2**. The prepared samples in our work exhibited sponge-like nature because of their elasticity and can repeatedly recover their original

shapes after being squeezed. This trend was also confirmed both in case of CMC sodium salt and chitosan were employed as dispersing agent.

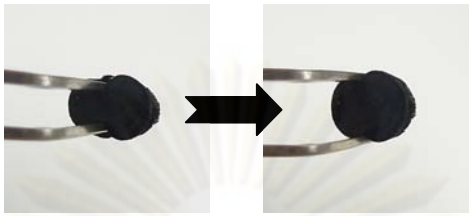

Figure 2. Elastic feature of the prepared solid foam.

The surface of pore wall in bulk sample was shown in **Figure 3A**. One can see from these SEM images that MWCNTs were covered by CMC sodium salt surfactant. To eliminate these surfactants on pore walls, freeze-dried samples were calcined in N_2 flow at 500 ^oC for 3 hours. After heat treatment, MWCNTs can be seen on pore walls **(Figure 3B)**. Calcined bulk samples could keep their original shapes, however, their elastic natures were lost after the heat treatment. It was suggested that CMC sodium salt surfactant was not only dispersing agent of MWCNTs but it also helped to produce the porous network, supported MWCNTs into pore walls and controlled the strength of bulk samples.

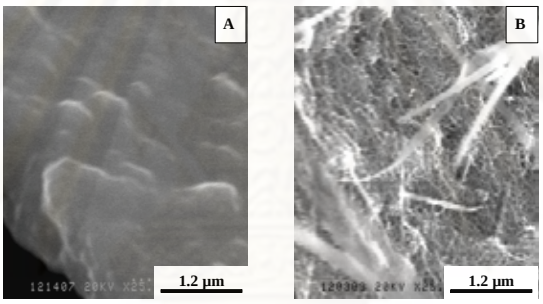

Figure 3. Surface observation on pore walls (sample prepared from CMC sodium salt solution): (A) freeze-dried sample and (B) calcined sample.

Figure 4 shows the macropore images of freeze-dried bulk samples prepared from different dispersing agents (CMC sodium salt, chitosan). One can see that the prepared solid foam had well-organized macropore structures, and the pore morphology of bulk sample made of CMC sodium salt was similar to the pore shape of sample made of chitosan. Moreover, it was concluded that the pore networks in bulk matrix were organized by dispersing agents after freeze-drying. The experimental parameters for controlling macropore sizes will be discussed in the next section.

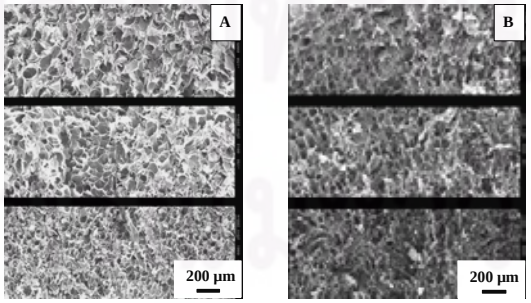

Figure 4. Macropores of freeze-dried samples made of different dispersing agents with cooling rate of -3.0 K min^{-1}: (A) 100 mg of MWCNTs in 1.0 wt.% of CMC sodium salt solution and (B) 100 mg of MWCNTs in 1.0 wt.% of chitosan solution.

Influences of initial formulation and freezing condition on macro-porosity

In this section, we limit the discussions only on the samples prepared from MWCNTs-CMC sodium salt dispersing agent. The obtained samples prepared at low concentration of CMC sodium salt surfactant (0.5 wt.%) and MWCNTs content (50 mg) were fragile, while the samples prepared at higher surfactant and MWCNTs concentrations had higher strength. It was suggested that the concentration of the components affected the strength of obtained samples. **Figure 5** shows cumulative pore size distributions of the freeze-dried bulk samples with different surfactant concentrations and MWCNT contents. One can see that a higher surfactant concentration led to a smaller macroporous structure in the bulk matrix. Similarly, when the samples were prepared at a higher MWCNT content, smaller pores appeared in the samples. This trend became clearer when the samples were prepared at the faster cooling rate (-3.0 K min^{-1}), though it cannot be discerned when the samples were prepared at a slow cooling rate (-0.5 K min^{-1}). Deville et al. reported that the initial formulation influenced on the ice crystal size due to volume of water directly relates to ice crystal growth (Deville et al., 2007). Ice crystal growth was limited by the volume of water when it was frozen. At low volume of water, a possibility to combine dendrites of ice become lower, consequently, a smaller ice crystal size was obtained with higher surfactant concentration and amount of MWCNTs in our preparation condition.

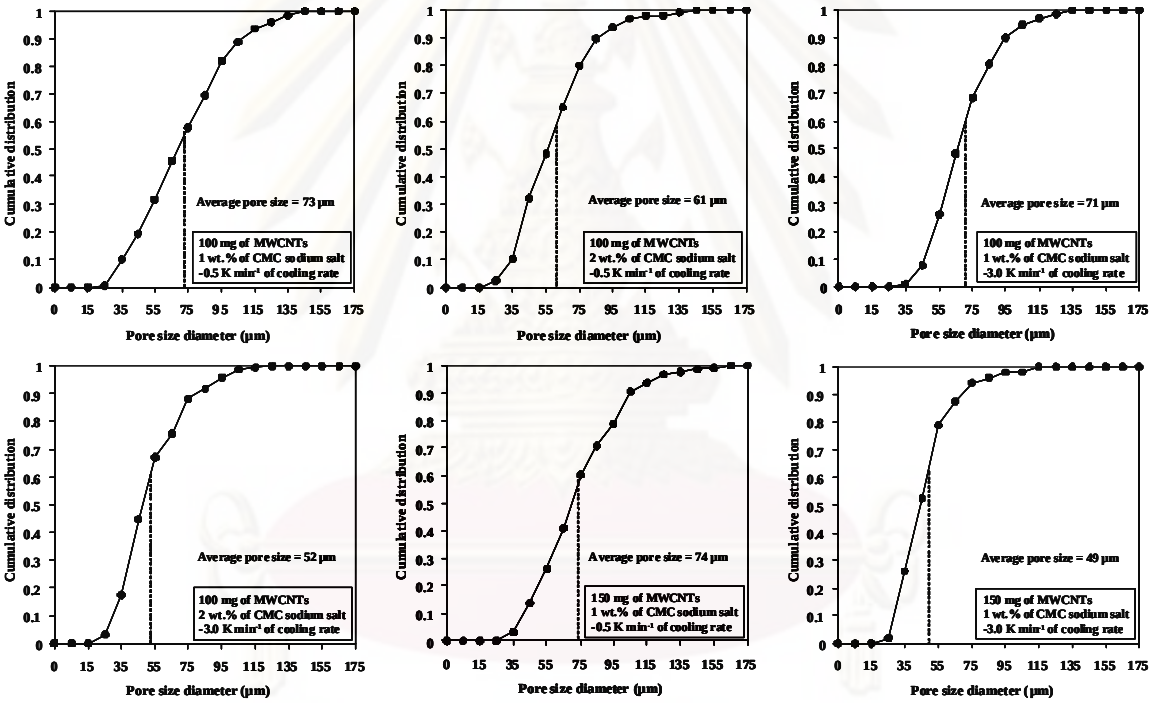

Figure 5. Cumulative pore size distributions of freeze-dried samples.

Moreover, freezing condition is another parameter to control the macropore size of bulk sample. It was reported that the nucleation temperature during freezing step greatly influences on ice crystal morphologies (Nakagawa et al., 2006; Hottot et al., 2007). Ice crystal morphologies are controlled by ice crystal growth rates and temperature distribution in a frozen system, thus, nucleation temperatures and cooling rates are major controlling factors (Nakagawa et al., 2007). Nevertheless, it is well known that a nucleation from supercooled solution is the random phenomenon because of spontaneous nature of nucleation. In our system, nucleation temperatures were approximately similar, that is, they varied between -5 to -8 ^{o}C. It is reasonable to consider that the uniformly dispersed MWCNTs could play a role of the nuclei for initiating ice crystal nucleation. As a result, the system nucleated at essentially the same subcooled temperatures. So, in this work, the morphologies of the samples should mainly be controlled by the cooling rate. The pore size distributions of freeze-dried samples with different cooling rates indicate that the macropore sizes were dependent on the cooling rate, that is, a faster cooling rate led to

homogeneity and smaller macroporous networks in the bulk matrix of MWCNTs. In fact these results suggest that the macroporous system in solid foams is simply controlled by the freezing condition (in case the formulation is fixed). In other words, porous structure design, i.e. the average size and shape of a bulk matrix could be achieved via a proper cooling program.

Conclusion

In this work, a macroporous solid foam from MWCNTs was prepared via freeze-drying technique. CMC sodium salt surfactant or chitosan (dispersing agent) helped to assemble the porous networks of bulk sample and also supported MWCNTs on pore walls. The samples made from CMC sodium salt surfactant and chitosan provided the similar pore morphology in bulk matrix. The macropore sizes in solid foam were dependent on the concentration of surfactant, MWCNTs content, and cooling rate during freezing step. A higher surfactant concentration and amount of MWCNTs led to smaller macropores. A faster cooling rate also led to homogeneity and smaller macropore networks in the bulk matrix of MWCNTs.

Acknowledgement

Bayer Material Science Ltd., Germany, provided the MWCNT samples. N.T. acknowledges TGIST (Thailand Graduate Institute of Science and Technology) of NSTDA (National Science and Technology Development Agency) and HUMAP (Hyogo University Mobility in Asia and the Pacific) of University of Hyogo for financial support. Partial support from the Centennial Fund of Chulalongkorn University for researcher exchange is also acknowledged.

References

1) Romanenko AI, Anikeeva OB, Kuznetsov VL, Buryakov TI, Tkachev EN, Usoltseva AN. *Sensors and Actuators A* 2007;138:350-354.
2) Serp P, Corrias M, Kalck P. *Applied Catalysis A: General* 2003;253:337-358.
3) Nabeta M, Sano M. *Langmuir* 2005;21:1706-1708.
4) Leroy CM, Carn F, Backov R, Trinquecoste M, Delhaes P. *Carbon* 2007;45:2307-2320.
5) Abarrategi A, Gutierrez MC, Moreno-Vicente C, Hortiguela MJ, Ramos V, Lopez-Lacomba JL, et al. *Biomaterials* 2008;29:94-102.
6) Nakagawa K, Hottot A, Vessot S, Andrieu J. *Chemical Engineering and Processing* 2006;45:783-791.
7) Hottot A, Vessot S, Andrieu J. *Chemical Engineering and Processing* 2007;46:666-674.
8) Abdelwahed W, Degobert G, Fessi H. *International Journal of Pharmaceutics* 2006;324:74-82.
9) Mukai SR, Nishihara H, Yoshida T, Taniguchi K, Tamon H. *Carbon* 2005;43:1563-1565.
10) Mukai SR, Nishihara H, Tamon H. *Chemical Communication* 2004:874-876.
11) Deville S, Saiz E, Tomsia AP. *Acta Materialia* 2007;55:1965-1974.
12) Jennings TA. Lyophilization: Introduction and Basic Principles. CRC Press LLC 1999:262-280.
13) Nakagawa K. *AIChE Journal* 2007;53:1362-1372.

VITA

Ms. Napawon Thongprachan was born on July 4, 1982 in Bangkok, Thailand. In 2004, she was graduated from Mahidol University with first-class honor in Bachelor's Degree of Chemical Engineering. Her senior project was focused on the PMMA membrane synthesis via wet phase separation technique. In her junior year, she gained useful experience at an air separation plant of TIG company as a trainee engineer who studied, monitored and analyzed the performance of the process using a Toolkit program. She gained admission to study for a Master degree in Chemical Engineering at Chulalongkorn University, and graduated in 2006 with a thesis entitled "A novel rotary drum filtering reactor for photocatalytic decomposition of phenol in slurry containing titanium dioxide (TiO_2) nanoparticles". Then she decided to pursue her doctoral study in Department of Chemical Engineering, Chulalongkorn University, and graduated in April 2009 with a dissertation entitled "Development and characterization of highly macroporous carbon nanotube foams by freeze-drying method". During her doctoral study she won full-expense scholarship from TGIST (Thailand Graduate Institute of Science and Technology), NSTDA (National Science and Technology Development Agency).